

In presenting the dissertation as a partial fulfillment of the requirements for an advanced degree from the Georgia Institute of Technology, I agree that the Library of the Institution shall make it available for inspection and circulation in accordance with its regulations governing materials of this type. I agree that permission to copy from, or to publish from, this dissertation may be granted by the professor under whose direction it was written, or, in his absence, by the Dean of the Graduate Division when such copying or publication is solely for scholarly purposes and does not involve potential financial gain. It is understood that any copying from, or publication of, this dissertation which involves potential financial gain will not be allowed without written permission.

---



THE DETERMINATION OF EFFECTIVE DELAYED  
NEUTRON AND PHOTONEUTRON KINETICS PARAMETERS  
IN A HIGHLY ENRICHED HEAVY-WATER REACTOR

A THESIS

Presented to

The Faculty of the Graduate Division

by

Walter Waverly Graham, III

In Partial Fulfillment

of the Requirements for the Degree

Doctor of Philosophy in the School of Nuclear Engineering

Georgia Institute of Technology

August, 1965



Approved:

Chairman

Date approved by Chairman: Aug 16, 1965

## ACKNOWLEDGMENTS

It is a pleasure to acknowledge the assistance of at least some of the many people who have had an interest in the work described in this thesis. Dr. W. B. Harrison has provided generous support and, along with the other faculty members of the School of Nuclear Engineering, a considerable measure of encouragement. Dr. D. S. Harmer, my thesis advisor, and Dr. C. E. Cohn of the Argonne National Laboratory, my thesis consultant, have provided invaluable technical advice and direction. I am grateful to Dr. G. G. Eichholz and Dr. C. J. Roberts, who served as members of my reading committee, and who very kindly provided helpful suggestions, both during the course of the experimental work and the drafting of this manuscript. To Mr. R. E. Meek and his team of electronics technicians I am indebted for their diligence on my behalf. I would like to thank Mr. J. C. Gundlach of Reactor Controls, Inc. for his inspired response to my detector needs and Mr. F. W. Shue for genius in the machine shop of the Georgia Institute of Technology Nuclear Research Center. To my good friend, Mr. R. J. Johnson, I wish to express my sincere gratitude for hours of unselfish advice and assistance. He was also instrumental in the development of the methods described in Appendix B for assessing reactor power history. Mrs. Lydia Fisher has done an outstanding job of editing and typing this manuscript.

The research represented here has been supported by Atomic Energy Commission Special Fellowships in Nuclear Science and Engineering, administered by the Oak Ridge Institute of Nuclear Studies, by the Ford

Foundation Loan Fund, and by Atomic Energy Commission Research Contract No. AT(38-1)-403. I also acknowledge gratefully support by funds from the Georgia Tech School of Nuclear Engineering and the Nuclear Sciences Division of the Engineering Experiment Station.

Finally, to my wife, Ann, and to our children, Kerry and Holly, I want to express my appreciation for love and understanding when work took priority over conversation and story-books.

## TABLE OF CONTENTS

	Page
ACKNOWLEDGMENTS. . . . .	ii
LIST OF TABLES . . . . .	vi
LIST OF ILLUSTRATIONS. . . . .	vii
SUMMARY. . . . .	x
NOMENCLATURE . . . . .	xii
Chapter	
I. INTRODUCTION . . . . .	1
Background	
Purpose of the Research	
II. INSTRUMENTATION AND EQUIPMENT. . . . .	16
The Georgia Tech Research Reactor	
Detection and Data Recording Systems	
III. PROCEDURES . . . . .	38
Detector Positioning	
Dead Time Determination	
Delayed Neutron Precursor Concentration Buildup	
Rod Drop Zero Time Determination	
Data Reduction and Fitting	
IV. RESULTS. . . . .	54
V. CONCLUSIONS. . . . .	71
VI. RECOMMENDATIONS. . . . .	77
APPENDICES . . . . .	79
A. EXPERIMENTAL RESULTS . . . . .	80
B. PROCEDURE BLDUP. . . . .	87
C. RP-129 AND ROD DROP. . . . .	98

## TABLE OF CONTENTS (Concluded)

APPENDIX	Page
D. PROCEDURE DATED. . . . .	117
E. VARIABLE METRIC MINIMIZATION WITH INTEGRAL FUNCTION PROCEDURE. . . . .	122
F. PROCEDURE RSLTS. . . . .	143
G. SCHEMATIC DIAGRAMS OF ELECTRONIC UNITS . . . . .	153
BIBLIOGRAPHY . . . . .	163
VITA . . . . .	166

## LIST OF TABLES

	Page
1. Test A(s) 13-Group Parameters with Correction Terms. . . .	58
2. Test A(s) Parameters . . . . .	62
3. Comparison of 13-Group Parameters - Tests A and B. . . . .	63
4. Comparison of 13-Group Parameters of the Present Work with Literature Values . . . . .	66

## LIST OF ILLUSTRATIONS

Figure		Page
1.	Process Development Pile -- Reactivity and Reciprocal Doubling Time Relationships for Various Kinetics Parameter Sets . . . . .	14
2.	Georgia Tech Research Reactor -- Horizontal Section at the Core Mid-plane. . . . .	17
3.	Georgia Tech Research Reactor -- Fuel Element Cutaway View . . . . .	18
4.	Georgia Tech Research Reactor -- Vertical Section. . . . .	20
5.	Georgia Tech Research Reactor -- Vessel Interior Before Fuel Element Loading. . . . .	21
6.	Block Diagram of Neutron Detection Systems . . . . .	23
7.	Cross Section Diagram of Fission Chamber . . . . .	24
8.	Fission Chamber, Radiation Shield, and Preamplifier. . . . .	25
9.	Performance Characteristics of Fission Chamber Both in and out of the Reactor as a Function of Preamplifier Gain . . . . .	29
10.	Scintillation Detector -- Active Element . . . . .	30
11.	Detector Incorporating Neutron Scintillator, Photo-multiplier Tube, and Preamplifier. . . . .	32
12.	Detection and Data Recording Equipment at Reactor Face . . . . .	37
13.	Detector Positioning Devices . . . . .	39
14.	Detectors Positioned in Through-Tubes. . . . .	40
15.	Detector-Analyzer System Response with Reactor on a Positive Asymptotic Period . . . . .	42
16.	Logical Flow Chart of Information in Process . . . . .	44
17.	Shim Safety Control Rod Calibration from the Banked-Critical Position to Full-in . . . . .	47

## LIST OF ILLUSTRATIONS (Continued)

Figure		Page
18.	Shim Safety Control Rod Position as a Function of Time Following a Drop from the Banked-Critical Position . . . . .	48
19.	Shim Safety Control Rod -- Negative Reactivity Insertion as a Function of Time Following a Drop from the Banked-Critical Position. . . . .	49
20.	Figure-of-Merit for Test A(s) Parameters as a Function of Number of Delayed Neutron Groups Used in the Fitting. . . . .	57
21.	Log n Power Recording for the Georgia Tech Research Reactor At-Power Periods Immediately Preceding the Start of Test A. . . . .	60
22.	Georgia Tech Research Reactor -- Regulating Rod Calibration as Determined from Experimental Data by Using Both Previously Available Parameters and Those Determined in the Present Work. . . . .	73
23.	Positive Reactivity as a Function of the Reciprocal of Asymptotic Period Calculated by Using Previously Available and Present Work Parameters. . . . .	75
24a.	Representation of Test A(s) Data and Calculated 13-Group Fit from 0.1 - 4000 Seconds. . . . .	81
24b.	Representation of Test A(s) Data and Calculated 13-Group Fit from 4000 - 250,000 Seconds. . . . .	82
25a.	Representation of Test B(f) Data and Calculated 13-Group Fit from 0.1 - 1000 Seconds. . . . .	83
25b.	Representation of Test B(f) Data and Calculated 13-Group Fit from 1000 - 275,000 Seconds. . . . .	84
26.	Test A(s) Residuals for Each Data Point in the 13-Group Fit. . . . .	85
27.	Test B(f) Residuals for Each Data Point in the 13-Group Fit. . . . .	86
28.	Standardized Approximations for Reactor Power-History Record . . . . .	90
29.	Schematic Block Diagram of Multiscaler Sequencing Logic. .	154



## LIST OF ILLUSTRATIONS (Concluded)

Figure		Page
30.	Schematic Diagram of Scintillation Detector High Voltage Divider and Preamplifier . . . . .	155
31.	Schematic Diagram of Fission Chamber Preamplifier. . . . .	156
32.	Schematic Diagram of Analyzer and Clock Control Circuit. .	157
33.	Schematic Diagram of Decade Divider Trigger Section. . . .	158
34.	Schematic Diagram of 1 kc Oscillator . . . . .	159
35.	Schematic Diagram of Decade Divider First Section. . . . .	160
36.	Schematic Diagram of Decade Divider Intermediate Section. . . . .	161
37.	Schematic Diagram of Decade Divider Final Section. . . . .	162

## SUMMARY

This research was undertaken in order to determine experimentally effective values of the delayed neutron and photoneutron relative abundances,  $\beta_{i,\text{eff}}/\Sigma \beta_{i,\text{eff}}$ , and the decay constants,  $\lambda_i$ , which are applicable to a highly enriched heavy-water nuclear reactor. These parameters are required for precise calculations of the kinetic behavior of the reactor. They have not previously been determined in a reactor of this specific type. Neutron flux decay data following a rod drop in the Georgia Tech Research Reactor were collected over periods in excess of three days. The reactor had not operated above 200 watts; most of its operation had been at 1 watt. Scintillation and fission chamber detection systems were used. The data have been fitted to the expression

$$n(t_j \rightarrow t_j + \Delta t_j) = \sum_{i=1}^M \int_{t_j}^{t_j + \Delta t_j} a_i' e^{-\lambda_i' t} dt$$

by the weighted least-squares criterion, using the Variable Metric Minimization method. Corrections have been made in order to account for delayed neutron precursor concentrations at the time of the rod drop, the finite time required to drop the rods, and for post-drop sub-critical neutron multiplication. Various values of M, the total number of groups permitted in the summation, have been tried, and the best fit was found for  $M = 13$ . One of the thirteen groups is attributed to background. Thus, twelve

delayed neutron groups are indicated for the Georgia Tech Research Reactor. Comparisons are made with previously obtained values of relative group abundances and decay constants available in the literature.

## NOMENCLATURE

$a_i$	fraction of count rate after the prompt drop attributable to the $i^{\text{th}}$ delayed neutron group
$a'_i$	count rate after the prompt drop attributable to the $i^{\text{th}}$ delayed neutron group (counts/sec)
$B$	total number of counting intervals
$C_i$	concentration of the $i^{\text{th}}$ delayed neutron group precursor (atoms/cm <sup>3</sup> )
$F$	sum of squares of weighted differences between collected and calculated counts for all intervals
$k_{\text{eff}}$	effective neutron reproduction factor
$k_p$	neutron reproduction factor component attributable to prompt neutrons
$\ell^*$	prompt neutron lifetime (sec)
$M$	total number of delayed neutron groups
$n$	reactor neutron concentration (neutrons/cm <sup>3</sup> )
$P$	reactor poisoning, the ratio of the number of thermal neutrons absorbed by the poison to those absorbed in the fuel
$Q_i$	equilibrium fraction of the $i^{\text{th}}$ delayed neutron precursor
$R_i$	relative abundance of the $i^{\text{th}}$ delayed neutron group
$s_i$	$i^{\text{th}}$ root of the inhour equation (sec <sup>-1</sup> )
$t$	time (sec)
$T$	instantaneous reactivity insertion time
$T_D$	reactor flux doubling time (sec)
$V$	weighted variance of fit, a statistical figure-of-merit for curve fitting which equals $\sum_{j=1}^B \chi_j^2 / (B - 2M)$
$y$	experimentally observed neutron count

## NOMENCLATURE (Concluded)

$\alpha$	general constant of exponential change ( $\text{sec}^{-1}$ )
$\beta$	fraction of neutrons from a fission which are delayed
$\beta_i$	fraction of neutrons from a fission which are attributable to the $i^{\text{th}}$ delayed neutron group
$\Delta k$	fractional change in the neutron reproduction factor
$\Delta t$	time interval
$\lambda_i$	decay constant of the $i^{\text{th}}$ delayed neutron precursor ( $\text{sec}^{-1}$ )
$\sigma$	standard deviation of data
$\Sigma_a$	macroscopic absorption cross section ( $\text{cm}^{-1}$ )
$\phi$	reactor neutron flux (neutrons/ $\text{cm}^2$ sec)
$\chi$	weighted difference between experimentally observed quantity and the calculated value for that quantity

## CHAPTER I

### INTRODUCTION

#### Background

Nuclear fission was discovered in 1939. In this process a fissionable isotope such as U-235 captures a neutron and within about  $10^{-14}$  seconds<sup>1</sup> breaks up into two heavy fragments while emitting about 2 or 3 neutrons and about 5 gamma rays. The two heavy products of the fission process decay at characteristic rates until they reach stable isobars. The fraction of each isobar produced in fission is called the "yield." This yield varies from extremely small values up to about 0.06 per fission. The nuclide from which a given decay or isomeric transition product is produced is called that product's "precursor" or "parent."

The production of a self-sustaining chain reaction in 1942 depended upon the fissioning nucleus yielding a sufficient number of neutrons so that, on the average, one of those fission neutrons would go on to produce a subsequent fission. More than 99 percent of the neutrons originating in the fission process are emitted at the instant that the fission occurs. For this reason they are called "prompt" neutrons. But in the same year that fission was discovered, another category of fission-produced neutrons, "delayed" neutrons, was found by Roberts, Meyer and Wang.<sup>2</sup> Delayed neutrons are products of the fission event, but they appear after the moment of fission at a time that is long compared with the extremely short time scale over which prompt neutrons appear.

It has been generally concluded that the emission of delayed neutrons arises from the decay of excited fission-product nuclides, including some isotopes of bromine and iodine.<sup>3</sup> The process is evidently influenced by the shell structure of certain of these radioisotopes. For example, Kr-87, a known delayed-neutron emitter, contains 51 neutrons, one more than the number required to produce a closed "nuclear shell" structure. The binding energy of this extra neutron is 5.5 MeV.<sup>4</sup> The parent of Kr-87, Br-87, contains too many neutrons for stability and is a beta emitter. If the Kr-87 is formed with an excitation energy greater than this 5.5 MeV binding energy, it will emit the odd neutron and become Kr-86. Since this neutron is emitted as a result of a fission event which, on the average, occurred some seconds earlier, it is referred to as a "delayed neutron," distinguishing it from "prompt neutrons" which appear at the instant of fission. The beta decay of Br-87 does not always yield a daughter nucleus which is in the highly excited state required for delayed neutron emission. As a matter of fact, in at least 90 percent of the transitions,<sup>4</sup> Kr-87 decays by beta emission to Rb-87 which then decays to stable Sr-87 by another beta decay. If the highly excited state of the delayed neutron emitter, Kr-87, is obtained, however, then the neutron emission occurs immediately after the formation of the Kr-87, and the observed half-life of such a process in a reactor is that of the parent beta emitter.

In heavy-water- and beryllium-moderated reactors, another category of delayed neutrons may result from a fission event in a less direct manner. High-energy gamma rays may interact with deuterium or beryllium nuclei to emit neutrons. The threshold for such photoneutron production is 2.23 MeV for H-2 and 1.67 MeV for Be-9.<sup>5</sup> While photoneutron produc-


tion by prompt gamma rays occurs continuously in the operating reactor, these photoneutrons are indistinguishable from the prompt neutrons produced directly in the fission process. However, photoneutrons are particularly significant for kinetics considerations when they are produced by delayed gamma rays from fission products. The period of a delayed photoneutron (i.e. the mean time between a fission event and the subsequent absorption of the delayed neutron attributable to that fission event) is determined by precursor beta decay. Photoneutron periods are generally much longer than delayed-neutron periods.<sup>6</sup>

Delayed neutrons of both types are important to the control of a nuclear reactor. It has been mentioned that a self-sustaining chain reaction requires, on the average, that each fissioning nucleus produce enough neutrons so that one of these neutrons may itself cause a subsequent fission. That is, in order for the neutron population to remain constant, each neutron which is lost in a fission must be replaced by another which will cause a later fission. This replacement neutron may be either prompt or delayed. If the reactor is just critical or not-too-far super-critical, it requires the small fraction of delayed neutrons as replacements in order to maintain the neutron population, in the critical case, or to cause it to increase in the not-too-far super-critical case. Under these circumstances, the reactor is said to be "delayed critical," meaning that if the delayed neutron contribution were not present, the reactor would no longer be critical. When the super-critical reactor configuration is such that criticality does not depend on the presence of delayed neutrons, then the reactor is said to be "prompt critical."

The kinetic or time behavior of the reactor is determined by the



production rate and loss rate of neutrons and the time between neutron generations i.e. the time from the appearance of a neutron until the event in which it produces its successor. In spite of their small abundance, delayed neutrons control the time between neutron generations because of their long periods. There are different periods and thus half-lives associated with different "groups" of delayed neutrons. These depend upon the half-lives of the delayed neutron precursors. The significance of this effect is well illustrated in a numerical example presented by Glasstone and Edlund.<sup>7</sup>

Thus, since the role of delayed neutrons in setting the pace for reactor kinetic behavior is an established qualitative fact, it is appropriate that their role be examined in a quantitative manner. 

Neutron population change in a reactor is frequently described by the space-independent zero-energy kinetics equations.<sup>7</sup> These equations describe the observable neutron density in a reactor before and after a change in control rod position or reactor configuration which affects the neutron reproduction factor,  $k_{\text{eff}}$ . The first equation,

$$\frac{dn}{dt} = \left[ k_{\text{eff}}(1 - \beta) - 1 \right] \frac{n}{\ell^*} + \sum_{i=1}^M \lambda_i C_i \quad (1)$$

describes the change in neutron level,  $n$ , as a function of time following a step insertion of reactivity. In this equation

$n$  = reactor neutron concentration

$t$  = time

$k_{\text{eff}}$  = effective neutron reproduction factor

$\beta$  = fraction of neutrons from a fission which are delayed

$\ell^* =$  prompt neutron lifetime

$M =$  total number of delayed neutron groups

$\lambda_i =$  decay constant of the  $i^{\text{th}}$  delayed neutron precursor

$C_i =$  concentration of the  $i^{\text{th}}$  delayed neutron group precursor

Since a change in the number of fission events also changes the number of fission product nuclides produced, such a step change in reactivity also alters the supply of delayed neutrons. This can be expressed by describing the change in concentration of the neutron precursors as

$$\frac{dC_i}{dt} = \frac{k_{\text{eff}} \beta_i n}{\ell^*} - \lambda_i C_i \quad (2)$$

where  $\beta_i$  is that fraction of neutrons from a fission which is attributable to the  $i^{\text{th}}$  delayed neutron group. The solution of these equations for neutron density as a function of time following a step insertion of negative reactivity is given in considerable detail by Cohn and Toppel<sup>8</sup> and results in the expression

$$n(t) = n(0) \sum_i a_i e^{-\lambda'_i t}$$

where  $n(t)$  is the neutron flux at any time,  $t$ ,  $n(0)$  is the neutron density just before the step insertion was made,  $a_i$  is the fraction of post-shutdown neutron density which is attributable to the  $i^{\text{th}}$  delayed neutron group, and  $\lambda'_i$  is the apparent decay constant of the  $i^{\text{th}}$  delayed group. This parameter,  $\lambda'_i$ , differs from the  $\lambda_i$  defined above only because of the sub-critical

multiplication of delayed neutrons due to new fissions which occur after shutdown. The more sub-critical the reactor is, the smaller the difference between  $\lambda_i$  and  $\lambda'_i$ .

An accurate interpretation of the dynamic performance of a highly enriched heavy water reactor, like the Georgia Tech Research Reactor, requires an accurate input of the parameters, delayed neutron group fractions,  $\beta_i$ ; delayed neutron group decay constants,  $\lambda_i$ ; and prompt neutron lifetime,  $\ell^*$ , into these kinetics equations. Delayed neutron and delayed photoneutron parameters are available in the literature.<sup>9,10,11</sup> Because many of these data were obtained with small irradiated samples of uranium which do not necessarily represent an actual in-reactor situation adequately, they may not be entirely satisfactory for application to a specific reactor.

These small-sample experiments employ a piece of irradiated uranium to provide the delayed neutrons and high-energy gamma rays which can produce delayed photoneutrons. This sample is moved rapidly from the irradiation facility (a reactor or neutron generator) to a counting assembly, which incorporates heavy water, shielding material, and detectors. In a typical experiment, data are collected for several hours and stored for analysis. The experiment may be run with heavy water in place and then absent, in order to separate the photoneutron contribution. Alternatively, a bismuth shield may be placed around the sample to suppress the photoneutron-producing gamma rays.

Data obtained by the small-sample method have typically produced the accepted literature values for general kinetics applications. This technique was used in a number of "standard" delayed neutron experiments reported in 1947 - 1958.<sup>9,12,13</sup> By "standard" here we mean the delayed

neutrons which appear directly from the nucleus of a fission product atom as opposed to photoneutrons which are produced in an indirect manner. Accepted for many years were the parameters of Hughes, Dabbs, Cahn, and Hall.<sup>9</sup> More recently a comprehensive study of delayed neutrons has been carried out at Los Alamos by Keepin, Wimett, and Zeigler.<sup>12</sup> Their technique is typical of the small-sample method. A few grams of U-235 were irradiated in a neutron flux of the highest possible intensity for a period, the length of which depended upon whether short or long delayed neutron groups were to be emphasized. The use of a small sample minimized the multiplication of neutrons within the fissionable material itself. The combination of small sample and high flux produced satisfactory counting statistics without the necessity for large corrections for sub-critical multiplication. A pneumatic system transferred the irradiated uranium from the reactor to a counting tank equipped with detectors. The decay of delayed neutron activity was monitored by a crystal-controlled multichannel time delay analyzer with variable channel widths. The analysis of these data was accomplished by an iterative weighted least squares program on a digital computer. The best fit was obtained for six groups.

Small-sample methods have also been employed in the study of photoneutrons resulting from delayed fission product gamma rays above the 2.23 MeV threshold for interaction with heavy water. This reaction is described as:  $\gamma + D \rightarrow n + p$ . Spatz, Hughes, and Cahn<sup>14</sup> and Bernstein et al.<sup>10</sup> have used this method. Bernstein's work remains the apparent standard, although more recent work has been proceeding at Princeton<sup>15</sup> to obtain new measurements. Bernstein's apparatus was similar in concept to the Los Alamos equipment described above. The detection tank was a 19-inch diameter hollow

aluminum sphere which could be filled with  $D_2O$ . The sphere was immersed in a large tank of oil. The tank was a four-foot cube. A pneumatic rabbit containing the enriched uranium oxide sample could be transferred from the center of the reactor to the center of the sphere in about 0.25 second. The sphere could be filled with heavy water or drained, thus permitting separation of standard delayed neutron and photoneutron contributions. The neutrons were observed with fission chambers located at various radial positions in the oil bath. These detectors had a resolving time of 20 microseconds. The data were recorded by photographing the scaling circuit interpolation bulbs with an open shutter oscilloscope camera. A 0.1 second time signal was recorded on the film. As the film moved past the neon interpolation bulbs, each bulb produced a dashed line on the film for the time it was lit. Data were taken for approximately 70 hours. In this work some rather detailed corrections were required to account for the gamma-ray attenuation in the irradiation capsule of the pneumatic rabbit system and to extrapolate the data to an infinite  $D_2O$  volume. The accuracy of the results may suffer from this since the gamma energies are not now precisely known and were even less well determined at the time of this experiment in 1947.

In the Bernstein work, photoneutron group abundances were related to the yield of the 22-second delayed neutron group reported by Hughes,<sup>9</sup> and thus may be used to give group constants for kinetics calculations which are based on the best current estimate of that 22-second group yield. This is, in fact, what Finn did in comparing experimental and predicted reactivity values for the Savannah River Process Development Pile reactor.<sup>16</sup> An additional long-lived precursor, obtained from absolute radiochemical measure-

ments has been reported by Ergen<sup>17</sup> and this group is frequently included in recommended group constants for kinetics calculations.<sup>11</sup>

Because of the experimental method employed and the corrections applied to obtain these group constants, they do not take into account the gamma-ray attenuation tending to diminish the number of gamma rays which are above the energy threshold when they attain access to the heavy water of a given D<sub>2</sub>O reactor. Neither do they incorporate the potentially higher effectiveness of delayed neutrons in producing subsequent neutron generations due to their lower mean energy spectrum.<sup>18</sup> In order to assess the adjusted values which apply to a specific reactor, delayed neutron parameters have been determined by analyzing the post-shutdown flux in that reactor.

At the Canadian low-power ZEEP reactor, Johns and Sargent<sup>19</sup> analyzed the decaying flux over a 37 hour period. Their abundance values were related to that value obtained for a prominent group whose period corresponded to one found by Hughes et al.<sup>9</sup> In their work, carried out in 1946-1947 and published in 1953, three proportional counters of different sensitivities were used. Each was placed at a different location in the reactor. To obtain the flux as a function of time over the periods of operation and shutdown, an inter-calibration of relative sensitivity of the counters was accomplished. All relative neutron fluxes were then expressed in terms of that of the most sensitive neutron counter. Counts, in units of 128, were recorded on moving paper by pen recorders. No assessment of system resolving time per se is given, but the statement is made that surprisingly large counting losses were probably caused by an unnecessarily long dead time in the discriminators. However, it is also



noted that, for the counting data on which most of the decay analysis depends, the losses were five percent or less. The ZEEP reactor was operated at power levels up to 50 watts for periods of 10, 50, and 230 minutes before shutdown and the resulting parameters were corrected from these periods of operation to represent infinite operation.

Tunncliffe<sup>20</sup> performed a similar experiment in 1952, collecting data with ionization chambers in the NRX reactor over a 24 hour period. In his analysis, however, Tunncliffe assumed the validity of the decay constants of the six standard delayed neutron groups as determined by Hughes et al.<sup>9</sup> and fitted just the photoneutron values by a least squares method. In the weighting of data points, the standard deviation,  $\sigma$ , was obtained by attributing a reading accuracy to the chart records of one percent of the full scale deflection and neglecting any systematic errors from range to range of the D.C. amplifiers.

At the Swiss Federal Institute for Reactor Studies, Würenlingen, data on DIORIT have been taken,<sup>21</sup> but as yet no results have been published. DIORIT, ZEEP, and NRX are all natural-uranium fueled and, therefore, are not typical of highly enriched research reactors either in dimension or gamma-ray attenuation. There is the additional complicating factor of an appreciable fast fission contribution in these reactors with the resulting delayed neutrons from a different fissionable species, U-238. The ratio of fast to total fissions in DIORIT amounts to about five percent.<sup>21</sup>

All of the work which has been described in the preceding pages has dealt with U-235. Summaries of detailed neutron experiments for many fissionable species have been prepared by Keepin.<sup>22, 23</sup>

The technique of analyzing the post-shutdown flux in an actual reactor has not been applied to a highly enriched heavy-water reactor, such as the Georgia Tech Research Reactor. Consequently, the appropriate parameters required in the various mathematical treatments of reactor kinetics for this type reactor have not been determined. The flux decay analysis procedure has the advantage of deriving parameters from experimental operation of precisely the same reactor type for which the results will be utilized, thus assuring their applicability. In practice, one fits the data collected

following a rod drop to a sum of terms,  $\sum_{i=1}^M a_i e^{-\lambda_i' t}$ , representing a linear superposition of the exponential decay periods of the delayed neutron activity present at the time of shutdown. The results may be examined in order to determine how many delayed neutron groups,  $M$ , are required to represent this flux decay process. The intermediate parameters obtained from the data fitting analysis must be adjusted to correct for the sub-critical neutron multiplication (or more specifically, the production of new fission products which is initiated by delayed neutron induced fission) and for non-equilibrium of precursors. This is required in order to remove from the parameters any dependence on power history and degree of sub-criticality. These corrections are obviously necessary to ensure the general utility of the results; they are also prerequisites to comparing them with literature values which have been obtained using small irradiated uranium samples with a negligible sub-critical multiplication and no appreciable irradiation history. Such a comparison is useful in itself, since it sheds light on the mechanisms operating within the nuclear reactor which cause the differences between the small-sample values,  $\beta_i$ , and the effective values,  $\beta_{i \text{ eff}}$ .



The differences in these parameters may be attributed to several causes. First, since the energy spectra of delayed neutrons and delayed photoneutrons are known to be lower in average value than those of prompt neutrons, the delayed neutrons require less time to slow to thermal energy, hence experience less capture and leakage in the process. According to the data of Batchelor and Hyder,<sup>18</sup> the average energy of the six standard delayed neutron groups is 430 keV. The photoneutron spectrum is dependent on the spectrum of gamma rays producing the reaction; in a reactor, most known precursor gamma rays possess energies less than three MeV and hence would produce neutron energies less than about 0.8 MeV in a  $D_2O$  reactor. This may be compared with the 2 MeV average energy of U-235 fission neutrons.<sup>24</sup> This gives delayed neutrons a greater importance as far as their ability to initiate subsequent generations of neutrons, and this greater "worth" results in an effective abundance fraction which, for some reactors, has been 25 percent<sup>25</sup> greater than the fraction which one might expect from data obtained with a small sample. It is evident that the magnitude of this energy-dependent worth is a reactor-dependent quantity since slowing down and leakage vary among reactor types. }

Competing with the enhancement effect just mentioned is another effect which is a strong function of the configuration of fuel elements used. Since photoneutrons in heavy water are the result of an interaction of a gamma ray possessing more than the 2.23 MeV threshold energy with the deuterium of the heavy water, and these energetic gamma rays originate in the fuel, any interaction which a gamma ray undergoes between its formation and its arrival in the heavy water region tends to result in its removal or reduction in energy below threshold value. These events cause a

smaller effective abundance fraction for delayed photoneutrons than one might observe in the small-sample method where very little attenuation occurs in the uranium sample and cladding. In the Process Development File at the Savannah River Plant, gamma-ray interactions with materials other than  $D_2O$  result in a reduction of the intensity of the high-energy gamma rays by 78 - 82 percent of the initial level.<sup>16</sup> In the Zero Energy Experimental File at Chalk River, the comparable value was calculated to be 74 percent.<sup>19</sup> At DIORIT the value 64 percent is used.<sup>21</sup> In the Massachusetts Institute of Technology Reactor, the removal or reduction was calculated to be 31 percent.<sup>26</sup>

As a result of these factors, the effective abundance fractions for a given reactor may be significantly different from those which apply to another reactor or those which might be obtained from small samples. A good illustration of the effect which choice of kinetics parameters may have on such practical considerations as reactor control rod calibrations or other reactivity assessments appears in Finn's work.<sup>16</sup> His plot of reactivity versus reciprocal doubling time is reproduced in Figure 1. It demonstrates the large discrepancy which exists for a particular reactor, PDP, between the experimentally observed relationship and those calculated using the indicated parameters and parameters adjusted for gamma transmission. Variations of this magnitude indicate the desirability of assessing the delayed neutron and photoneutron kinetics parameters for each specific reactor type.

#### Purpose of the Research

It was the purpose of the research described in this thesis to:

1. Establish the number of delayed-neutron and photoneutron groups which are required to describe accurately the kinetics behavior of the

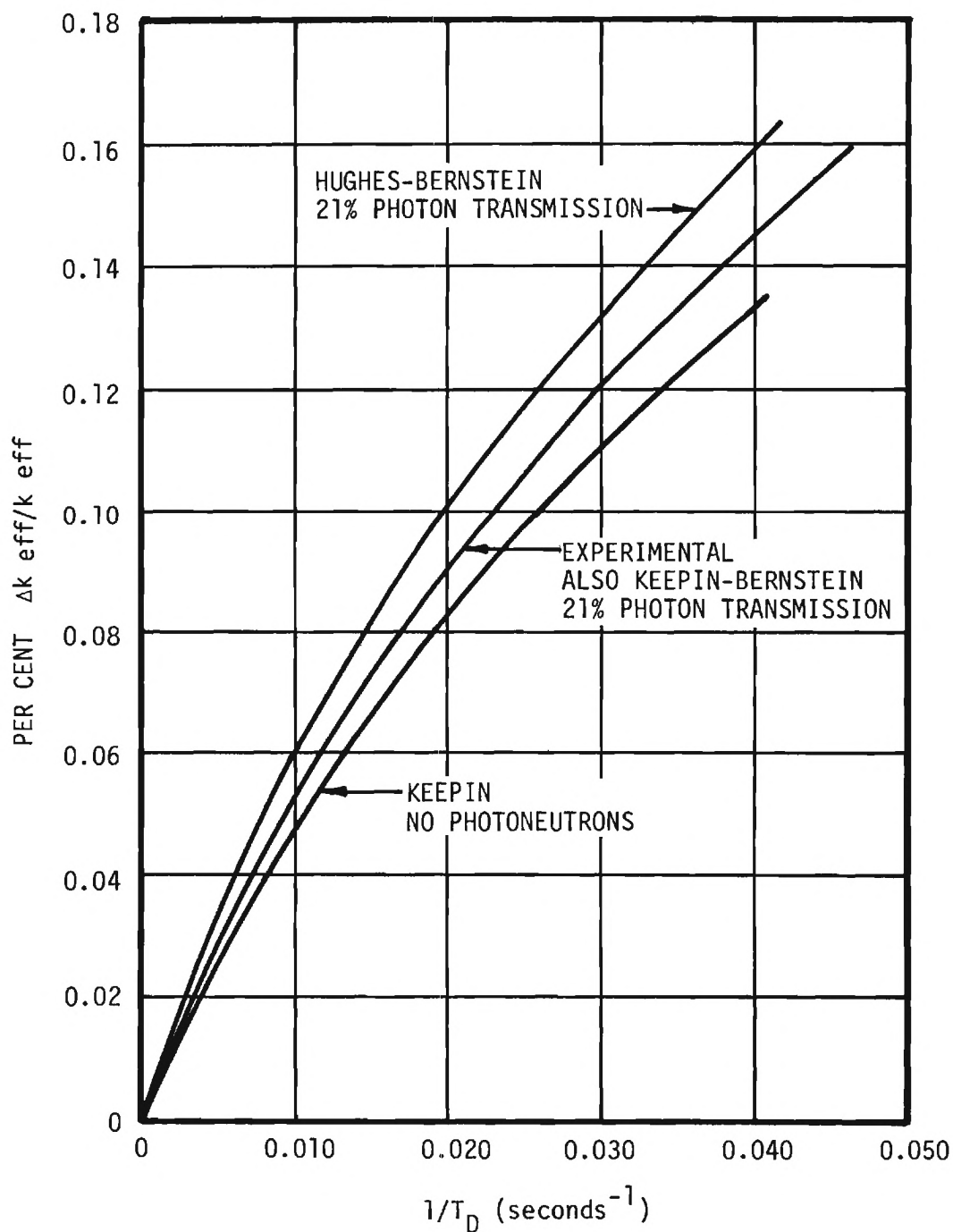


Figure 1. Process Development File -- Reactivity and Reciprocal Doubling Time Relationships for Various Kinetics Parameter Sets (after Finn<sup>16</sup>)

Georgia Tech Research Reactor.

2. Determine the relative abundance,  $\beta_i \text{eff} / \beta_{\text{eff}}$ , of each resolved delayed neutron and photoneutron group.
3. Determine the decay constant,  $\lambda_i$ , of each resolved delayed neutron and photoneutron group.
4. Compare the results obtained above with current literature values.

The delayed neutron and photoneutron kinetics parameters which are the product of this research will permit more precise kinetics calculations for highly enriched heavy-water reactors in general. In addition, some of the techniques that have been developed to facilitate the accomplishment of the purposes stated above may find uses in reactor calculations which are not restricted to a specific reactor type.

## CHAPTER II

### INSTRUMENTATION AND EQUIPMENT

#### The Georgia Tech Research Reactor

The Georgia Tech Research Reactor is a heterogeneous, heavy-water-moderated and cooled research reactor located at the Frank H. Neely Nuclear Research Center on the campus of the Georgia Institute of Technology. This reactor is fueled with highly enriched (greater than 93 percent U-235) plates of an aluminum-uranium alloy that is aluminum clad. The reactor is designed for one megawatt operation with an associated thermal neutron flux in excess of  $10^{13}$  n/cm<sup>2</sup> sec. At the time of the research reported here, low power testing and calibration were in progress and the power level was limited to 200 watts in order to facilitate handling of irradiated fuel elements during flux mapping and other reactor physics measurements.

While the fully loaded reactor core might contain as many as 19 fuel elements spaced six inches apart in a triangular array about two feet in diameter and two feet in height, the data for the present research were obtained on a 13-element core. Figure 2, a horizontal section of the Georgia Tech Research Reactor (hereafter to be referred to as GTRR), illustrates the positions of experimental facilities and fuel elements.<sup>27</sup> The 13-element core occupied locations V2, V4 - V7, V9 - V11, V13 - V16, and V18. The fuel element is illustrated in Figure 3.<sup>27</sup> Each standard element contains ten curved fuel plates 0.060 inch thick and 23.5 inches long. The aluminum cladding is 0.020 inch thick on the sides and 0.205 inch over the

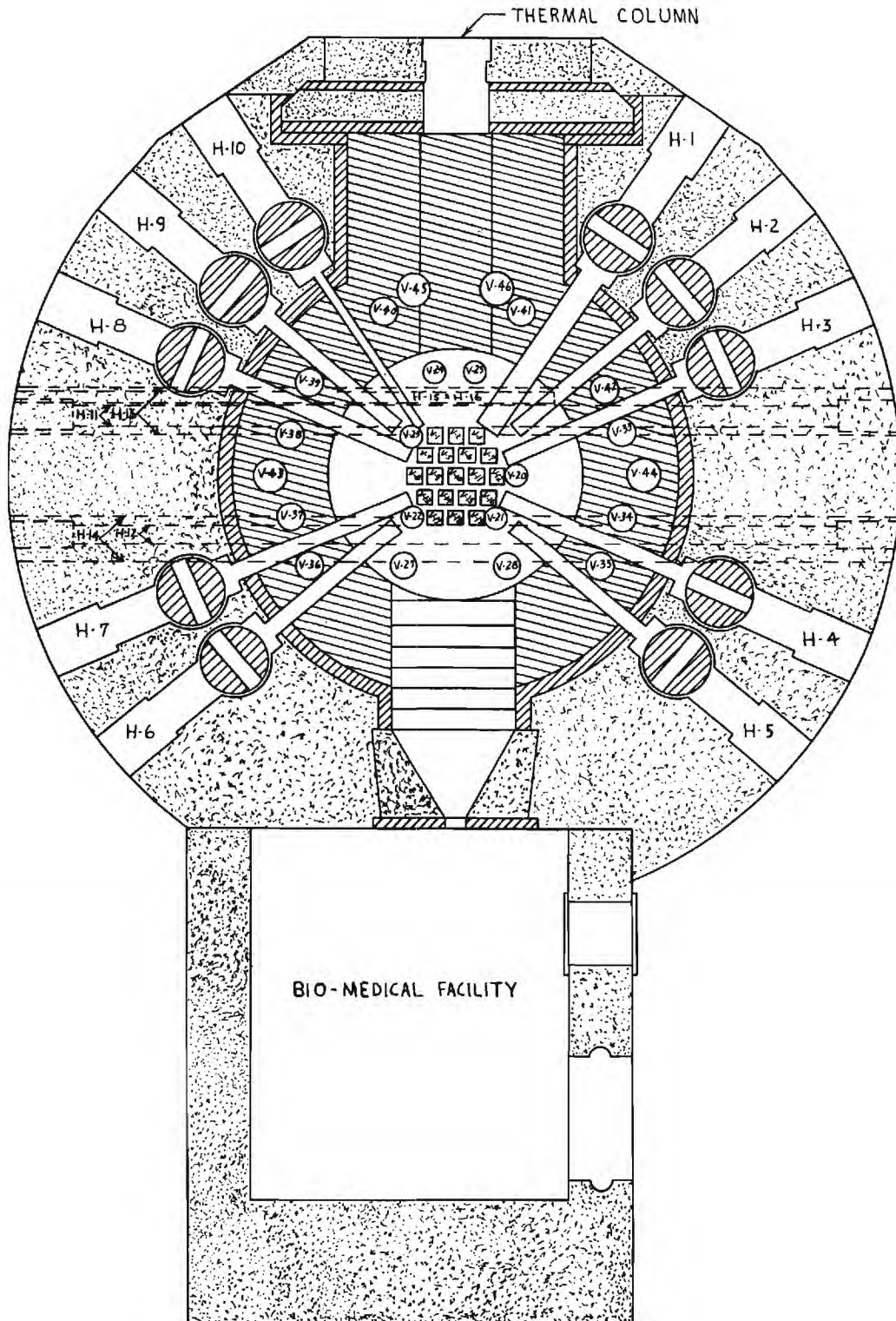


Figure 2. Georgia Tech Research Reactor -- Horizontal Section at the Core Mid-plane

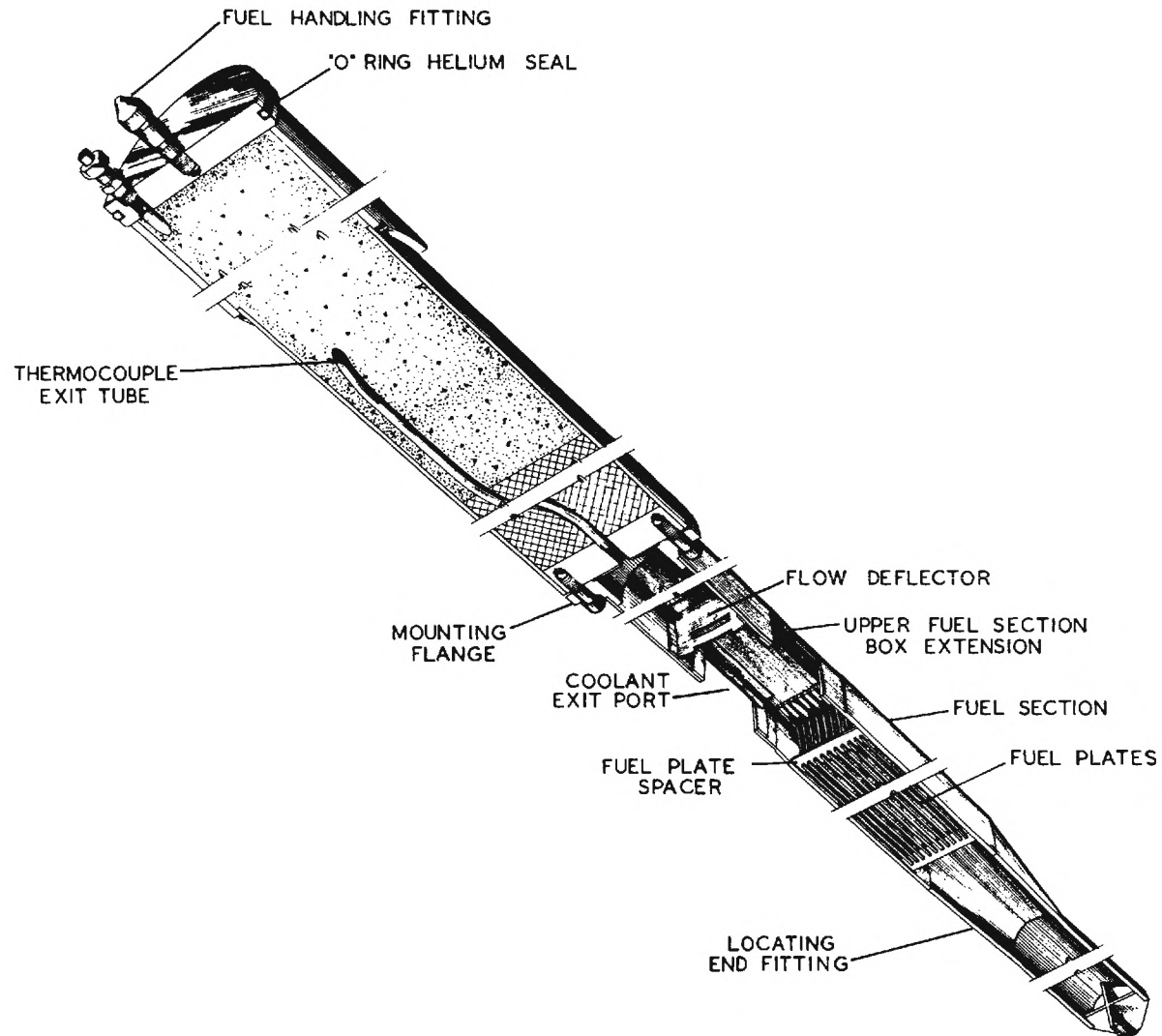


Figure 3. Georgia Tech Research Reactor -- Fuel Element Cutaway View



edges. Coolant passes in the 0.183 inch space between adjacent fuel plates. Each fuel element contains 142 grams of U-235.

The core is contained within a 6-foot diameter aluminum vessel and is immersed in heavy water so as to provide a two-foot thick layer of  $D_2O$  reflector. Figure 4, a vertical section,<sup>27</sup> illustrates the placement of the reactor vessel within the graphite reflector and the concrete biological shield. This figure is also marked to indicate the location of horizontal through-tubes designated H11 and H12. These experimental facilities, which pass tangent to the core, were used for the placement of the neutron detectors of this experiment.

Figure 5 is a photograph of the reactor vessel interior prior to fuel element loading. This picture gives a good view of the semaphore blade type shim safety rods. These blades consist of cadmium metal 0.040 inch thick, clad inside and outside with type 6061 aluminum alloy. They weigh about 20 lb. each and are 5.5 inches wide by 1 inch thick. The cadmium section is 45.5 inches long with the total length being 60 inches. The full travel of these safety blades is  $55^\circ$ . Also visible in Figure 5 are the aluminum thimbles in which the through-tubes H11 and H12 pass.

#### Detection and Data Recording Systems

In applying the method of reactor flux decay analysis for obtaining kinetics parameters, it is essential that reliable neutron detectors be employed in data collection. Accuracy of the parameters which result from the analysis is enhanced if the measurements of neutron flux level in the reactor over various time intervals are made at the highest possible count rates, since this contributes to the statistical precision of the data.



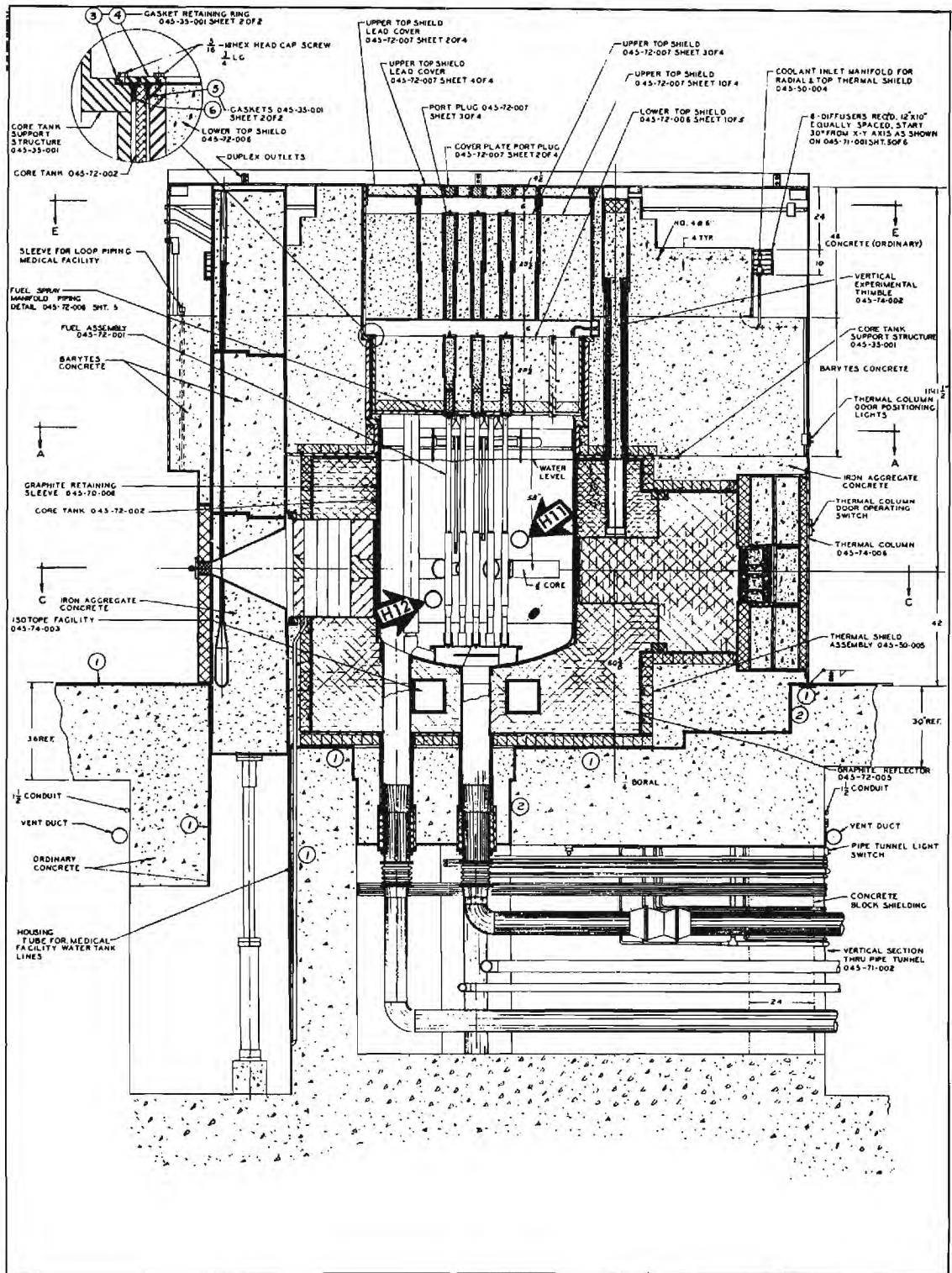


Figure 4. Georgia Tech Research Reactor -- Vertical Section

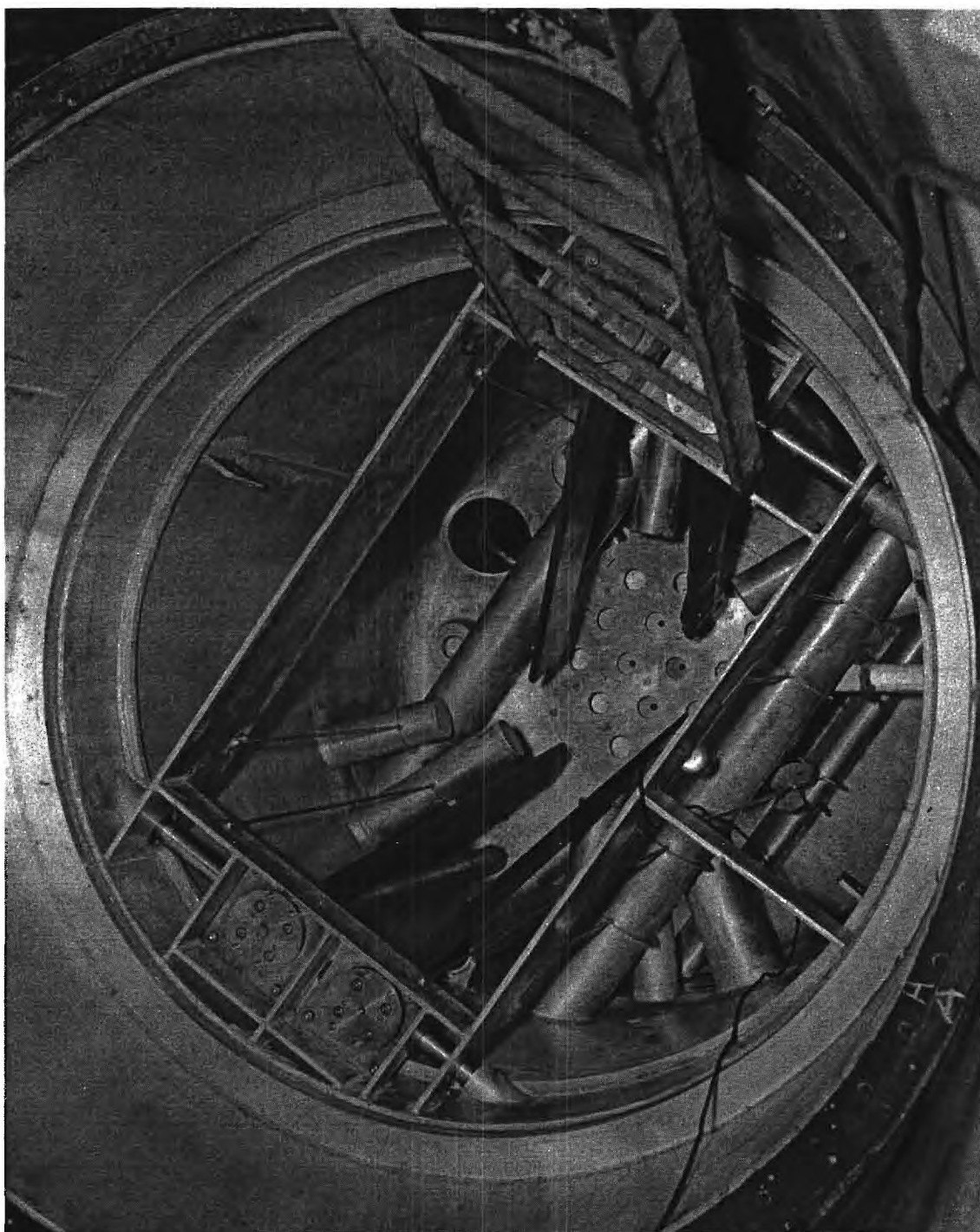


Figure 5. Georgia Tech Research Reactor Vessel Interior  
Before Fuel Element Loading

In the present work, the flux was monitored over a several-day period. Therefore, we required detection systems which were stable at both the initially high count rates immediately after the reactor shutdown by rod drop and at the final low count rates. As the count rate diminished in the course of the experiment, the data were obtained and stored with decreasing frequency. The interval over which pulses from the detectors were accumulated before storing for subsequent recording varied from 0.1 second to 100 seconds.

Two different types of detection systems were used in this work in order to provide a check on the consistency of results. The concept of the first, which uses a fission chamber detector, was suggested by Behringer.<sup>21</sup> This system was supplied by Reactor Controls, Inc. in accordance with our specifications. The second system was developed by the Instruments Group of the Nuclear Research Center. It incorporates a scintillation element. This particular approach of providing two different detector types was chosen since both types appeared to offer attractive possibilities for short resolving times well under a microsecond, and yet both were developmental in nature. Figure 6 is a block diagram of the major components of these two detection systems.

#### Fission Chamber System

The fission chamber, designated as Reactor Controls, Inc. Series RC-26-2451A-1T, has been specially designed for very high counting rates and for high neutron fluxes and gamma-ray fluxes. It is illustrated in Figures 7 and 8. The detector is one inch in diameter with a neutron sensitive length of four inches. The fission chamber has a neutron sensitivity of 0.05 to 0.07 counts/nv. Its construction is all aluminum except

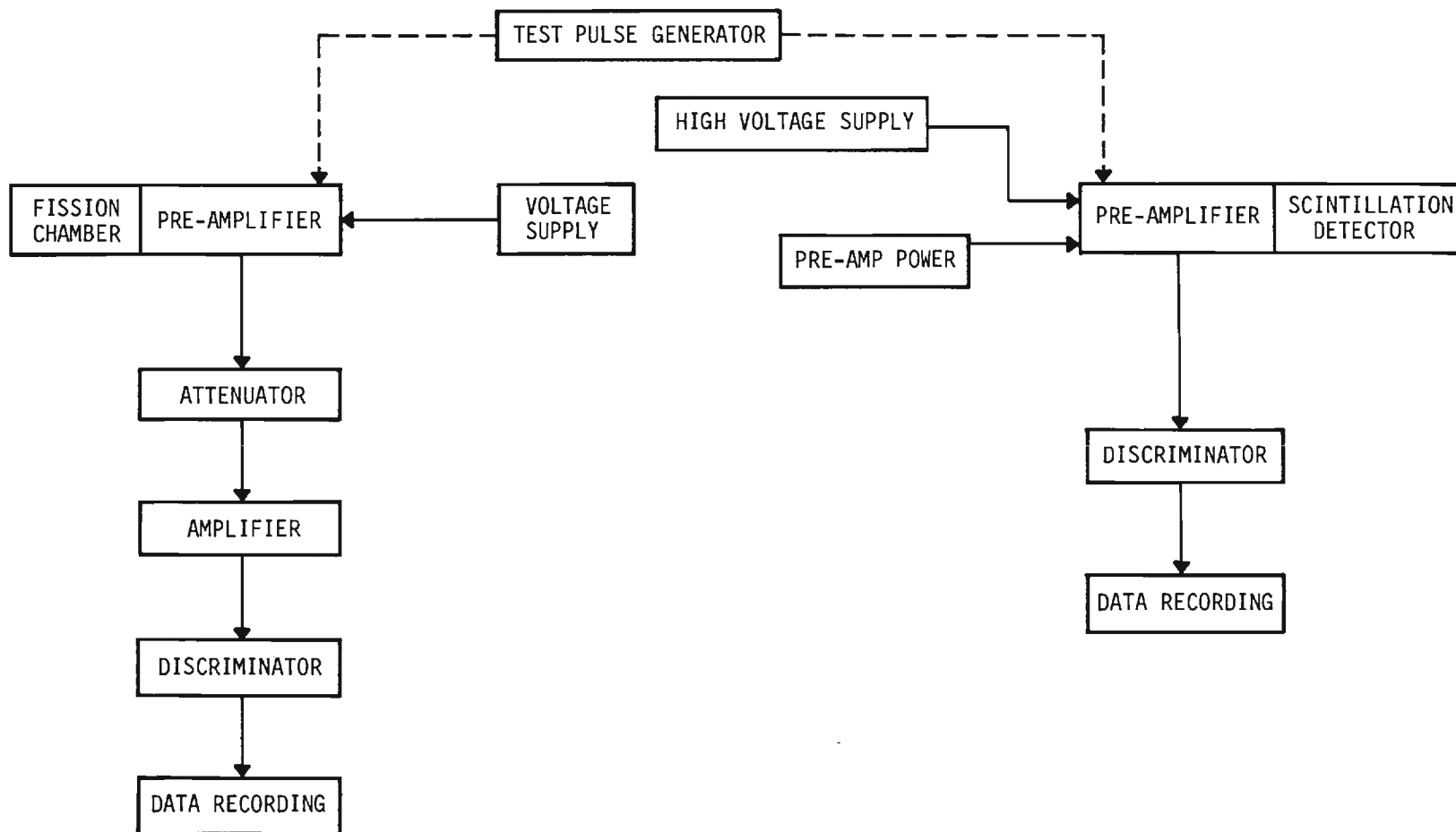


Figure 6. Block Diagram of Neutron Detection Systems

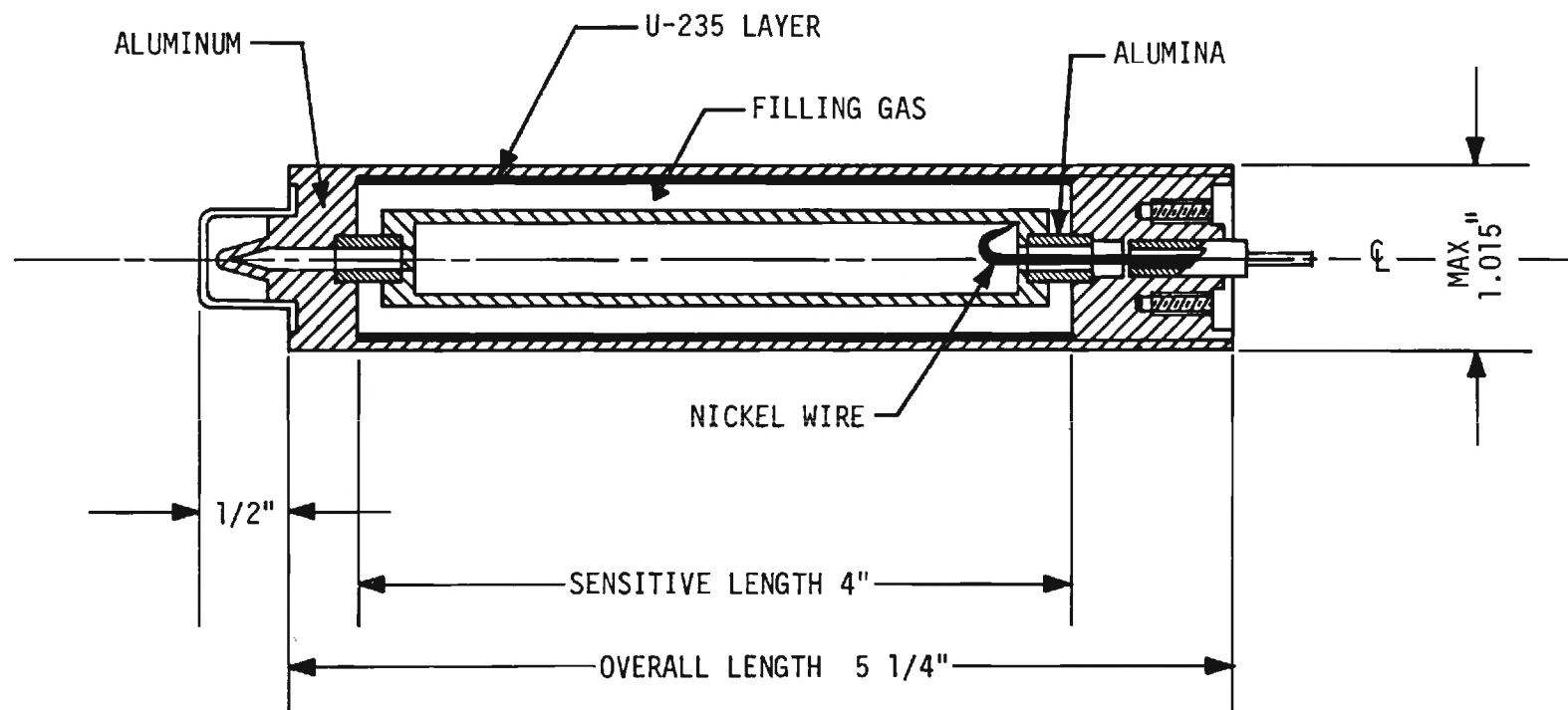


Figure 7. Cross Section Diagram of Fission Chamber

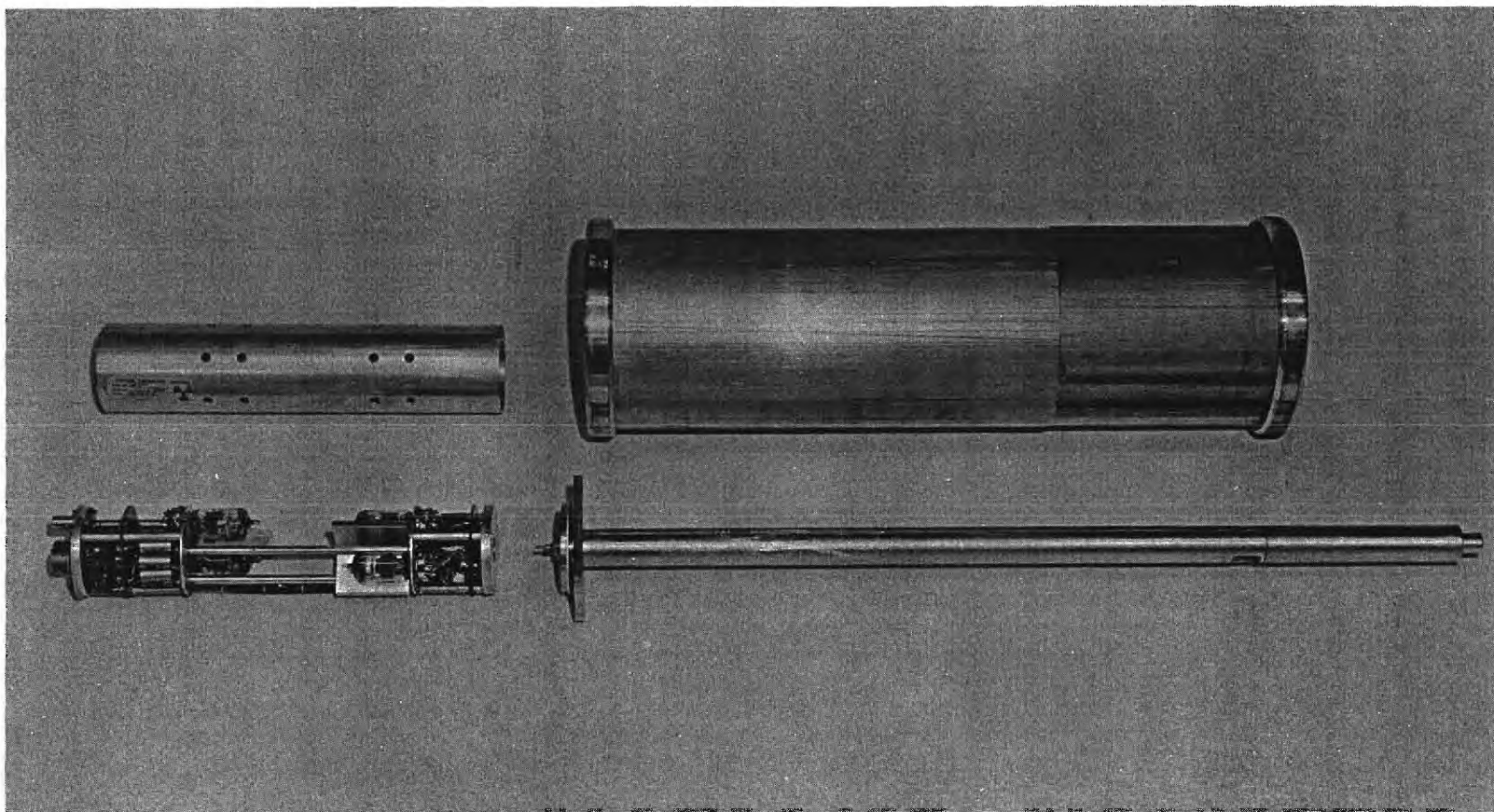


Figure 8. Fission Chamber, Radiation Shield, and Preamplifier



for an alumina ceramic-to-metal seal.

In order to reduce the neutron and gamma radiation at the preamplifier while maintaining the detector in a high neutron flux, such as may be obtained in a radial beam port or through-tube of the GTRR, a 20-inch long solid aluminum plug provides shielding between the detector and the preamplifier. The plug fills the inside diameter of the beam hole to minimize streaming. A 1-inch diameter hole through the large-diameter shield plug accepts a 1-inch diameter shield plug. The detector is mounted on this 1-inch diameter, 19-inch long aluminum shielding plug, and this in turn mounts on the preamplifier. Signal connection from the detector to the preamplifier is made by a 1/16 inch diameter nickel rod mounted on spaced ceramic beads inside a 1/4 inch diameter hole through the 1-inch diameter shielding plug.

The preamplifier was designed by Reactor Controls, Inc. for random nuclear pulse amplification with double differentiation pulse shaping. Double pulse resolution is 240 nanoseconds. The preamplifier has an overall gain, exclusive of pulse shaping stages, of greater than 600, with a rise time of less than 20 nanoseconds. Gain is stabilized by precision resistors in the feedback loops around all sections of the preamplifier.

The input stage is a very low noise cascode circuit designed for random pulse inputs from 50 microvolts to 2 millivolts, negative peak. Provision is made for supplying + 500 volts to the fission chamber signal electrode. First differentiation is accomplished by RC circuitry between amplifier sections.

The cathode follower output of the preamplifier drives a 95 ohm balanced line cable at signal levels up to 1 volt peak. This high level

output is desirable for use with long cable lengths without pickup of significant noise. Second differentiation is accomplished at the main amplifier location after the long cable length. A schematic diagram of the preamplifier may be found in Appendix G.

The preamplifier is packaged in a 2-1/2 inch diameter cylinder, 12 inches long. Fission chamber input is at one end, power and signal cables are located at the opposite end. All components have a low temperature coefficient and, except for the connectors and cables, are capable of operation at temperatures up to 250° F.

An attenuator panel receives a 95 ohm balanced line input and converts it to a 50 ohm single-ended line. The signal is passed through a toggle switch attenuator, adjustable over 42.5 db by 0.5 db steps, and is then RC-differentiated at the output at 50 ohms impedance. The differentiated signal is amplified by a gain-of-ten amplifier having a rise time capability of 2 nanoseconds.

A pulse amplitude discriminator produces a 0.5 V amplitude standard pulse at 50 ohms impedance for each input pulse with amplitude greater than 0.10 V. The pulse amplitude discriminator is capable of less than 10 nanoseconds double-pulse resolution. Both the amplifier and discriminator described above are modules manufactured by Chronetics, Inc.

The preamplifier is powered by a Kepco Model KR-2 regulated power supply set at 212 V. The supply is modified to provide decoupling between preamplifier stages by three RC filters and to provide the fission chamber polarizing voltage regulated by six 85A2 regulator tubes in series. A separate 6.3 V supply provides D.C. filament power to the preamplifier tubes. A connector is provided for the seven-wire cable going to the pre-



amplifier. The power supply is typically located within 15 feet of the preamplifier to reduce filament voltage loss and noise pickup.

The fission chamber system as a whole may, of course, be made sensitive to the alpha rays which are emitted by the fissile uranium coating of the chamber, by sufficient amplification. This provides a convenient test source. But the system possesses an effective alpha discrimination capability without appreciable loss of neutron sensitivity. This discrimination capability may be observed in Figure 9. In Curve A, the detector was tested in the reactor up to a relative gain setting of 61. When the detector was removed from the reactor, there were no counts at this gain setting, and, as indicated in Curve B, it was necessary to increase the relative gain to about 67 before it was possible to observe the lower energy alpha source present within the active material of the fission chamber itself. Thus, it may be concluded from Figure 9 that the gain necessary to obtain a nearly flat neutron flux response is well below that required to detect even a minimum background contribution from alpha-produced pulses.

#### Scintillation Detection System

The active scintillating element used in these detectors was a Nuclear Enterprises, Ltd., Model NE-421 slow-neutron sensitive button of one inch diameter, shown in Figure 10. It employs a lithium compound whose Li content is enriched to 96 percent Li-6 dispersed in a ZnS matrix 0.025 inch thick. The detector design is a modification by Nuclear Enterprises of the type reported by Stedman.<sup>28</sup> The manufacturer specifies that this element provides 50 percent detection efficiency for thermal neutrons (0.01 eV or less) and gamma discrimination to the extent that thermal neutrons may be effectively measured in the presence of gamma radiation as high as

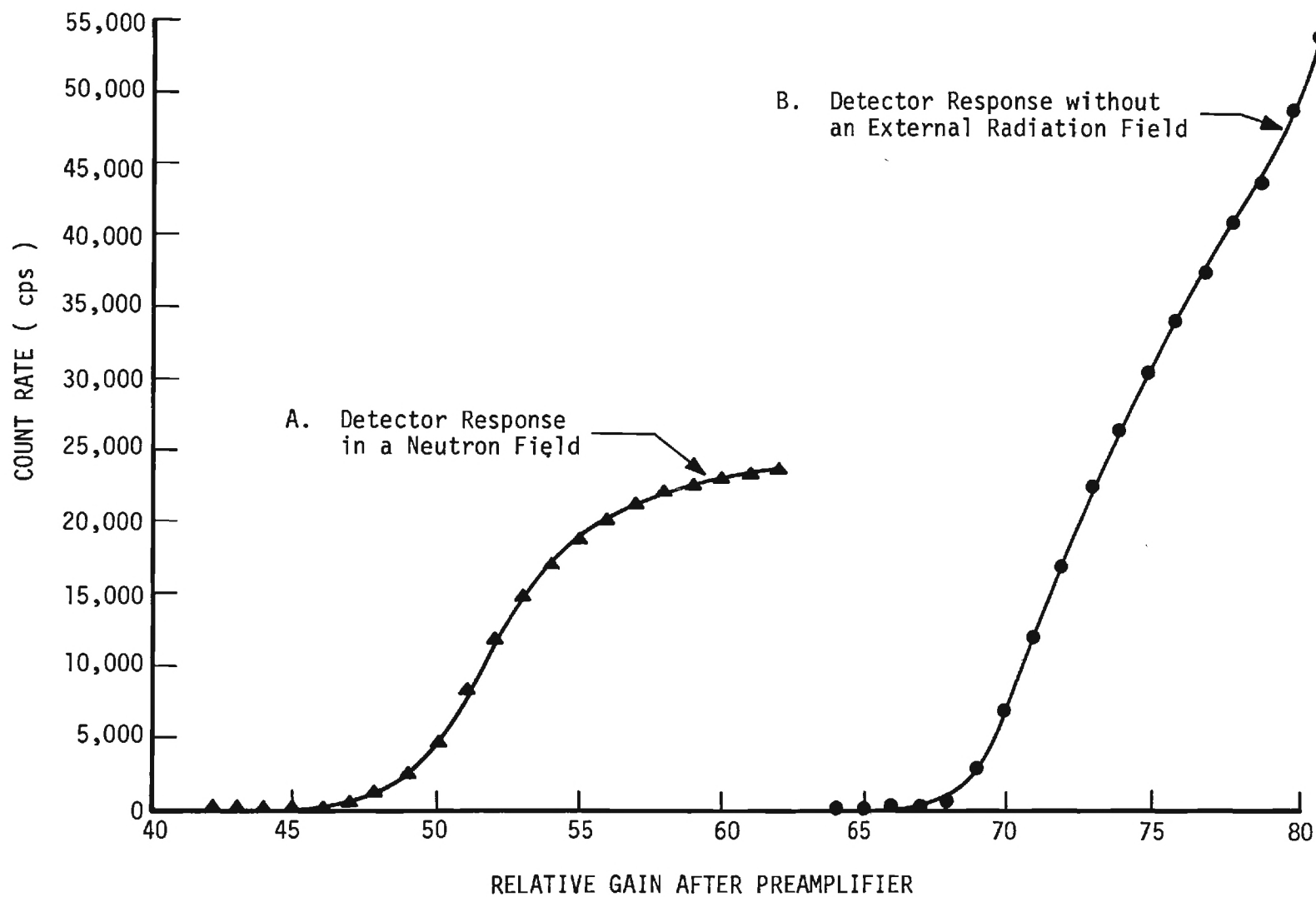


Figure 9. Performance Characteristics of Fission Chamber Both in and out of the Reactor as a Function of Preamplifier Gain

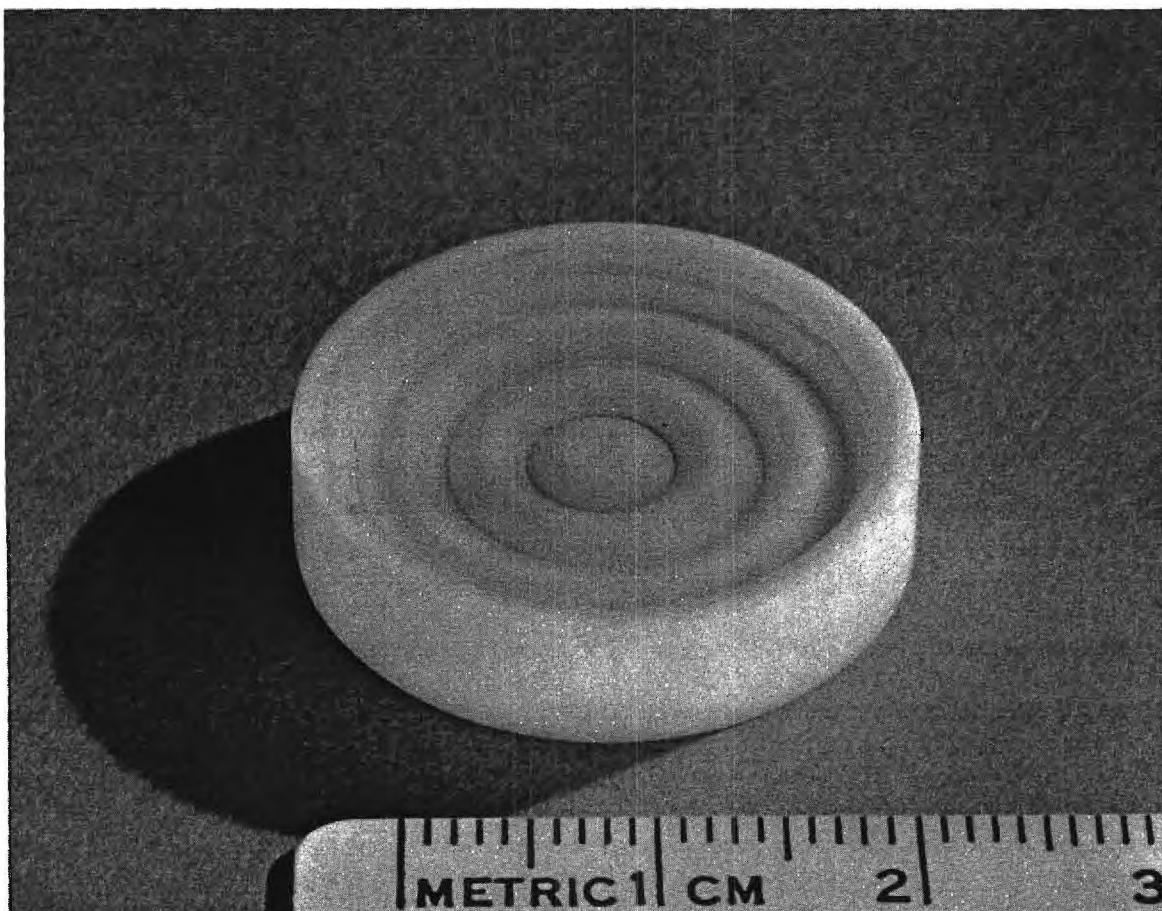


Figure 10. Scintillation Detector Active Element

$10^7$  gamma rays per neutron.

The high voltage was supplied to the photomultiplier tube by an NJE Corporation Regulated High Voltage D.C. Power Supply, Model No. S-327. This unit has an output range of 500 - 5000 volts, 0 - 10 mA. According to the manufacturer's specifications, it has a maximum ripple of 5 V, a static regulation of  $\pm 100$  mV (obtained with constant input voltage and load changes from a nominal half load to no load or full load, respectively), or  $\pm 0.01$  percent (obtained with constant load current and input changes from a specified nominal A.C. Voltage to + 10 percent voltage or - 10 percent voltage, respectively), and stability of 0.03 percent per hour or 0.06 percent for an eight hour period.

The photomultiplier tube employed in the scintillation detector was an Amperex XP1010 tube with ten stages and a cesium-antimony semi-transparent flat cathode of 32 mm diameter. This tube was selected for its low background; the manufacturer specifies a room temperature dark current of  $10^{-15}$  A/cm<sup>2</sup>. The photomultiplier tube was obtained from the Harshaw Chemical Company in an integral assembly incorporating the Nuclear Enterprises NE-421 scintillation detector and mu-metal magnetic field screening cylinder in a light-tight jacket.

The voltage divider string is built up in a standing resistor design as illustrated in Figure 11. This type of construction, along with the detector casing ventilation, permits heat removal by natural convection. At the operating level of 1150 volts, the photomultiplier draws 2.8 milliamperes of current. The high current drain of this voltage divider string is an intentional result of the design of the string with relatively low values of resistance. This was done in order to minimize any effect which

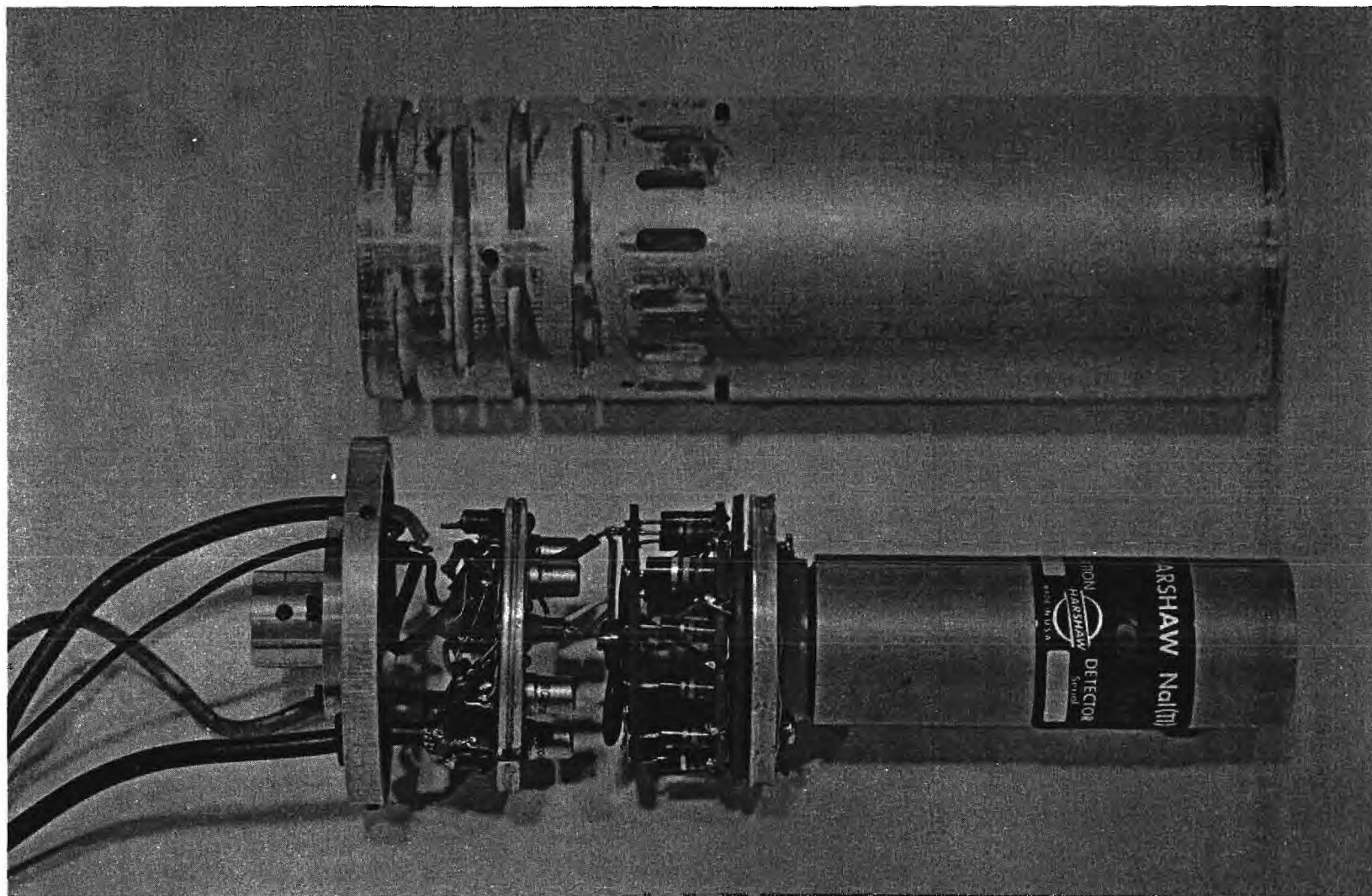


Figure 11. Detector Incorporating Neutron Scintillator, Photomultiplier Tube, and Preamplifier



a rapid change in count rate might have on the gain of the assembly.

The preamplifier used in the scintillation detector was designed and built by the Nuclear Research Center Instruments Group, directed by R. E. Meek. This preamplifier provides double RC differentiation and two stages of amplification. The input stage from the photomultiplier tube is a cathode-coupled amplifier from the photomultiplier tube with cathode-follower input and grounded-grid-amplifier output to the second stage. The first stage has a gain of 15. The second stage is a White cathode-follower with a fractional gain of 0.9. A schematic diagram of this preamplifier circuit is included in Appendix G.

Heat dissipation within the preamplifier assembly was enhanced by mounting the Nuovistor tubes in a 1/4 inch aluminum chassis which was in turn attached directly to the sides of the aluminum detector enclosure. The output pulse width of this preamplifier has been observed by oscilloscope to be 0.4 microsecond with actual input pulses from the phototube. The pulse risetime is 40 nanoseconds. The preamplifier has a test pulse input connection.

#### Data Recording System

Technical Measurement Corporation 400-channel pulse height analyzers were operated in the multiscaler mode in order to provide continuous accumulation of data on two parallel detection channels. Three multiscalers were required; one Model 401 and two Model 404 units were available.\* These units were modified by the Nuclear Research Center Instruments Group in order that they might operate as two megacycle scalars. The electronic modifications

---

\*One TMC analyzer was supplied on loan through the courtesy of the TMC-Ellison Division, Atlanta, in connection with the neutron generator project.

required to provide dwell times beyond the inherent capability of the TMC instruments, and to furnish experiment start pulses and signal routing were all assembled external to the multiscaler units themselves so as to preserve their general utility as pulse height analyzers. Appendix G includes a block diagram of the portion of this modification which accomplished multiscaler sequencing, if required, as well as other schematic diagrams of the electronic circuitry used to amplify the capabilities of the TMC analyzers.

The data recording equipment is capable of automatically sequencing from one analyzer to the next, although this feature was not used in the tests reported in this thesis. Sequencing of multiscalers is based on a signal appearing at the readout light of the unit which has filled its required number of channels. In this mode of operation, data readout is accomplished automatically in order to prepare the analyzer to receive more data. Since the analyzer has been programmed for automatic readout of data by positioning the front panel control switch on "automatic," a readout indicator light appears at the instant the last of the 400 channels is gated off by the "dwell advance" clock. The "automatic" programmed operation would normally result in the analyzer returning to the accumulation of data after completing readout. Since this is not desired, it is necessary to inhibit this step. This is accomplished by routing the same pulse which turns on the readout light to the "accumulate control" section and using it to appropriately modify the state of the control elements. Simultaneously, the readout pulse appears at the "accumulate control" section of the succeeding multiscaler and permits it to initiate the "accumulate" action. This consists of giving a command to the multiscaler to accept counts in its first channel when it receives the first dwell advance pulse. It receives that

dwel advance pulse about one millisecond later, since the "start-accumulate" command also goes to the clock via a built-in delay that is provided to ensure full channel width in time. The timing of subsequent channel advance pulses depends upon the dwell time per channel which has been selected on the control panel. This timing may be provided by either the same or separate circuits for each multiscaler and is derived from a base clock having a 100 kc crystal oscillator as its prime mover. This oscillator is divided down by two stages of five each and one stage of four so that the base clock output frequency is accurately 1.0 kc. The clocks associated with each multiscaler are themselves unijunction transistor oscillators which further divide the one kc base clock input by factors of ten in order to obtain dwell advance pulses every 0.01, 0.1, 1, 10, 100, and 1,000 seconds. With adjustment of variable resistor component values, still other dwell times may be obtained. The accuracy of the resulting dwell advance pulses is typically better than one part in 10,000, as measured by a Hewlett-Packard Model 5233L electronic counter. Channel advance time, i.e. time from the end of storage in one channel to the beginning of storage in the next, is 34  $\mu$ sec. While unijunction transistor oscillators have adequately provided the timing required in this experiment, they are not recommended for this application which demands consistent performance during a several-day experiment. Our experience has indicated that there are component-matching and tuning requirements which make the initial and post-repair calibrations extremely tedious.

Another method of starting multiscaler accumulation is by use of an external signal, or start pulse. In these experiments, all three analyzers were started either manually before rod drop or automatically at the time



shim safety rod #3 engaged its lower limit microswitch. A 110 V signal is available at the control rod drive position when this occurs, and it is brought to the control panel and shaped so as to be suitable for actuating the "accumulate control" section of the appropriate multiscalers.

The actual signal inputs from the detection system pulse height discriminators are brought to the control panel via BNC connectors and wired to multipole switches for routing to the appropriate multiscaler inputs. The control panel and other systems may be seen in Figure 12.

Data readout from the multiscaler memory was accomplished by punching paper tape. Two Tally Model 420 Tape Perforators were used. These units punch at a rate of 60 characters per second and produce six channel tape in a 1-2-4-8-X-0 code. Parallel-to-serial conversion of data from the multiscaler memories is accomplished with TMC Model 520 Punch Control units. These provide a capability for manual input of coded punches on the tape. This feature was used preceding each readout in order to identify the test number and sequence for the associated data. With the multiscaler "reset" toggle switch set on "automatic," the memory may be automatically cleared during the readout to paper tape.



Figure 12. Detection and Data Recording Equipment at Reactor Face

## CHAPTER III

### PROCEDURES

#### Detector Positioning

The detectors described in the last chapter were positioned in instrument hole H21A for preliminary data taking and in the through-tubes H11 and H12 for the final data taking. The through-tubes were selected because they afford a position near the core from which the decaying flux may be monitored with the relatively high count rates which are desirable for good statistics. At the same time, the detector position is readily adjustable within the through-tube.

The nuclear safety requirements for the through-tubes<sup>29</sup> are somewhat more stringent than they are for experimental facilities which do not penetrate the core tank. Experiments, or detectors, inserted in this position must be so constructed or equipped that they will remain fixed when subjected to a three psi pressure differential, such as might occur in the case of a leak of heavy-water into the through-tube. Figures 13 and 14 illustrate the arrangement of components which provide the detector positioning and fixing requirements.

In the flux decay data reported herein, the detectors were typically positioned near their maximum count rate position. This was desirable since the reactor had been operating at low power (less than 200 watts, and usually at only one to five watts) and residual fluxes were relatively low. In future experiments, which will be run after higher power operation, it is

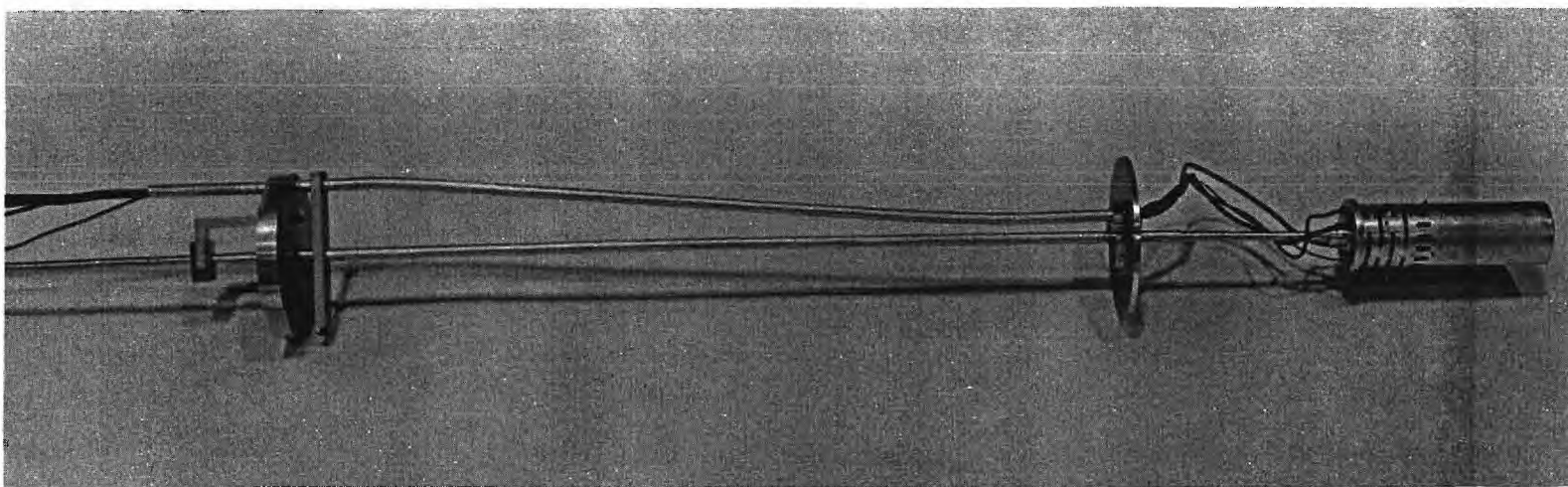
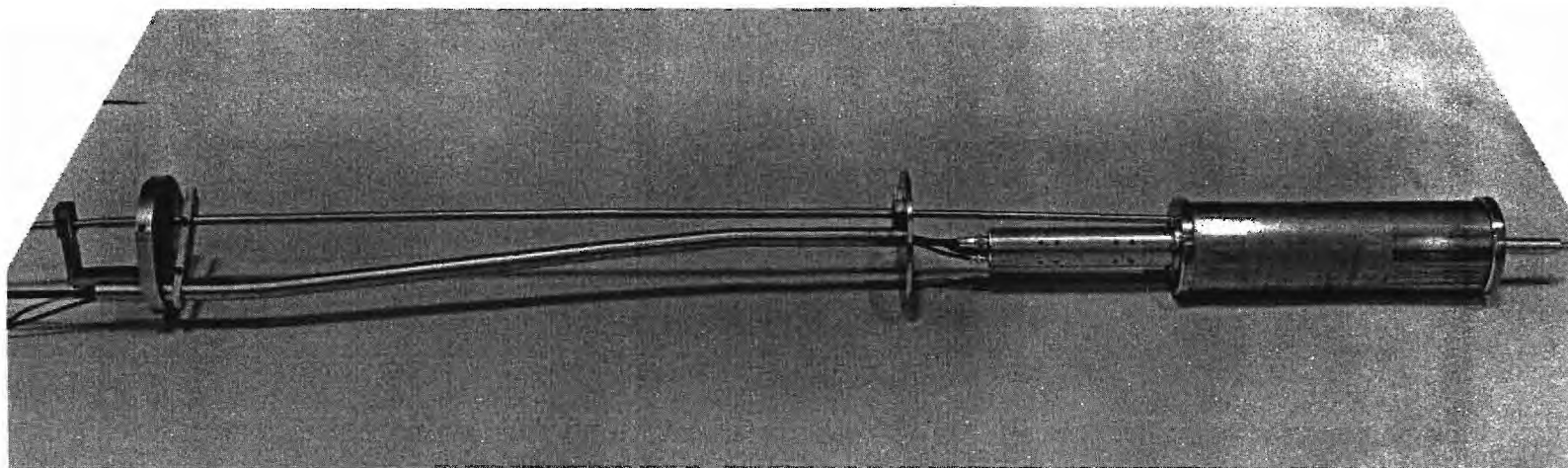


Figure 13. Detector Positioning Devices

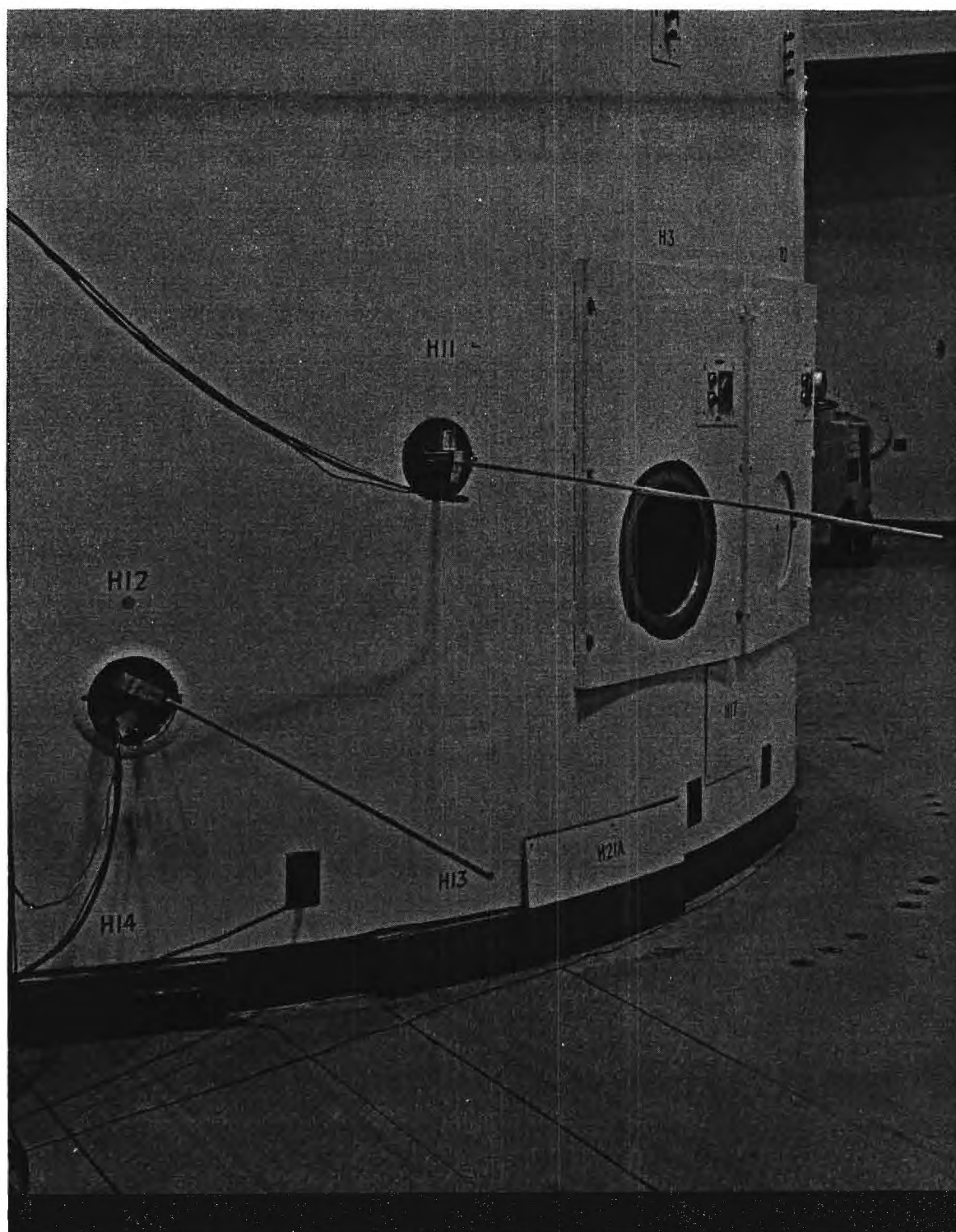


Figure 14. Detectors Positioned in Through-Tubes



expected that the adjustable feature of the detector positioning equipment will be more fully utilized.

Before the safety rods were dropped, commencing the data taking, the neutron start-up source was removed from its position in the core in order to eliminate this background contribution. Any remaining background contribution, such as spontaneous fission or photoneutrons produced by naturally occurring high energy gamma rays, appears in the flux decay analysis as a component with a negligible decay constant value.

#### Dead Time Determination

The dead times of the detectors employed were assessed from interpretation of the Tektronix Type 545A oscilloscope presentation of signal pulses. This procedure yielded a dead time of 400 nanoseconds for the scintillation detector and 240 nanoseconds for the fission chamber. The dead times of detector-analyzer systems were determined in an operational test in which the reactor, initially critical at low power, was put on a positive asymptotic period of about 56 seconds and the system response recorded as the flux increased. The results of this test for the fission chamber system are illustrated in Figure 15. When the reactor had settled out on an asymptotic period, the detector-analyzer system was used to record the response of the detector, which was monitoring the power rise. Counts were recorded at one second per channel, producing the count rate values represented in Figure 15. These counts were plotted. A straight line on semi-logarithmic paper was drawn through the low count rate points for which negligible counting loss was experienced. Then this line was extended to the higher count rate region. Assuming this straight line to represent the ideal or "no-lost-counts" response to reactor behavior, the comparison with recorded

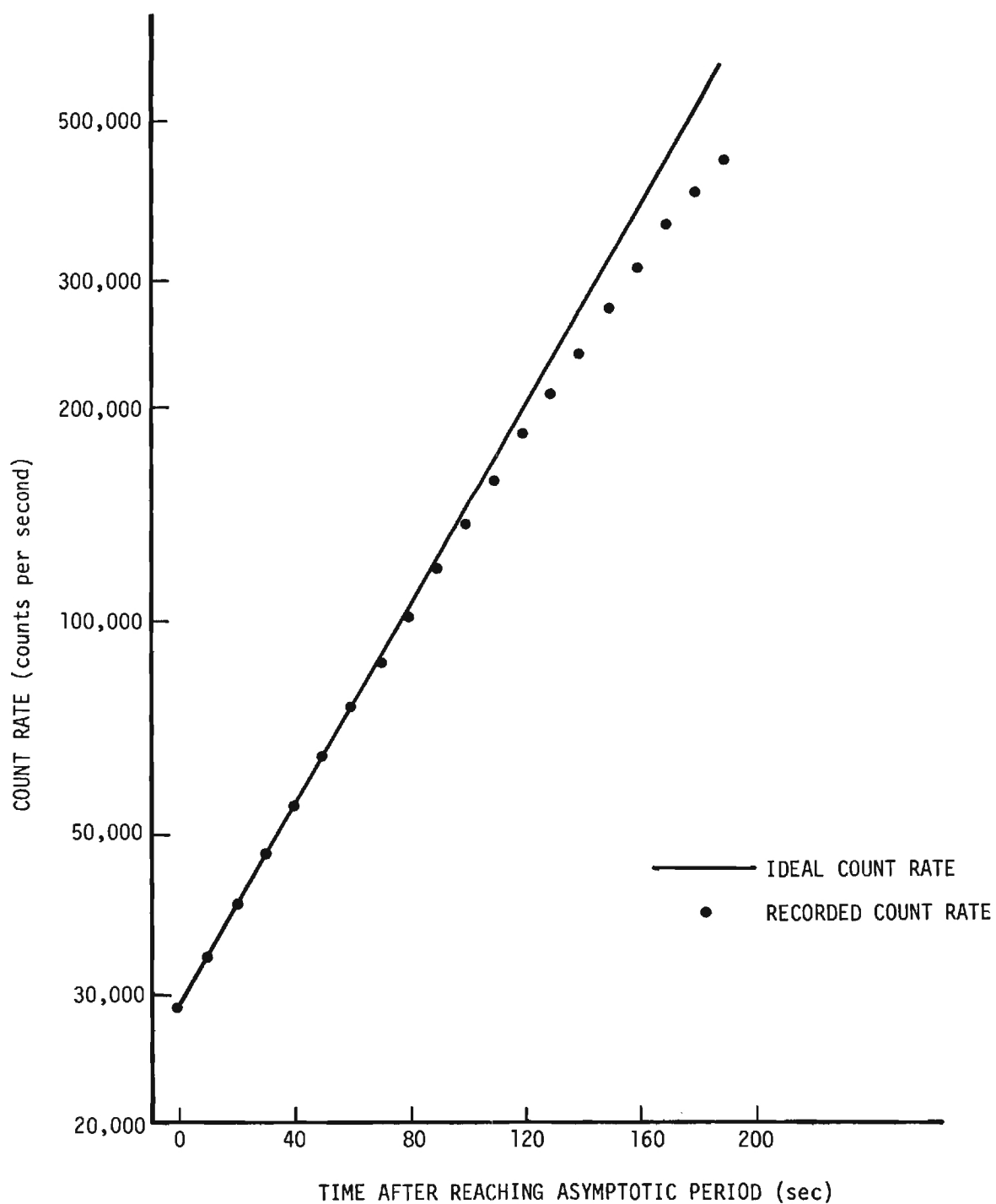


Figure 15. Detector-Analyzer System Response with Reactor on a Positive Asymptotic Period

count rates yielded a value of system resolving time. These tests indicated a total detection system pulse resolution capability of 530 nanoseconds for each of the two systems. This value corresponds with that obtained in a separate system test using a Rutherford pulse generator providing a pulse whose shape was made to resemble that of the discriminator output pulse in rise time, amplitude, and width. In this test, it was found that the maximum count rate, as observed on the oscilloscope, was also obtained for pulses separated by 530 nanoseconds.

#### Delayed Neutron Precursor Concentration Buildup

By referring to Figure 16, a logical flow chart of information in process, one may observe the central importance of the delayed neutron precursor concentrations. The buildup of precursors may affect the results of control rod calibrations, experiment zero time adjustment, and the correction of parameters for sub-critical multiplication. A simple assessment of the fraction of equilibrium concentration of a precursor which exists at the time a control rod is dropped to start a flux decay experiment may be made by use of the familiar formula:

$$Q_i = 1 - e^{-\lambda_i(t_p - t_d)}$$

where  $Q_i$  represents the equilibrium fraction of the  $i^{\text{th}}$  precursor,  $\lambda_i$  is that precursor's decay constant, and  $(t_p - t_d)$  is the time interval before rod drop over which the reactor has been operating at a level power.

When the longer-lived photoneutron precursors are involved, such a procedure may lead to gross inaccuracies since the level power operation



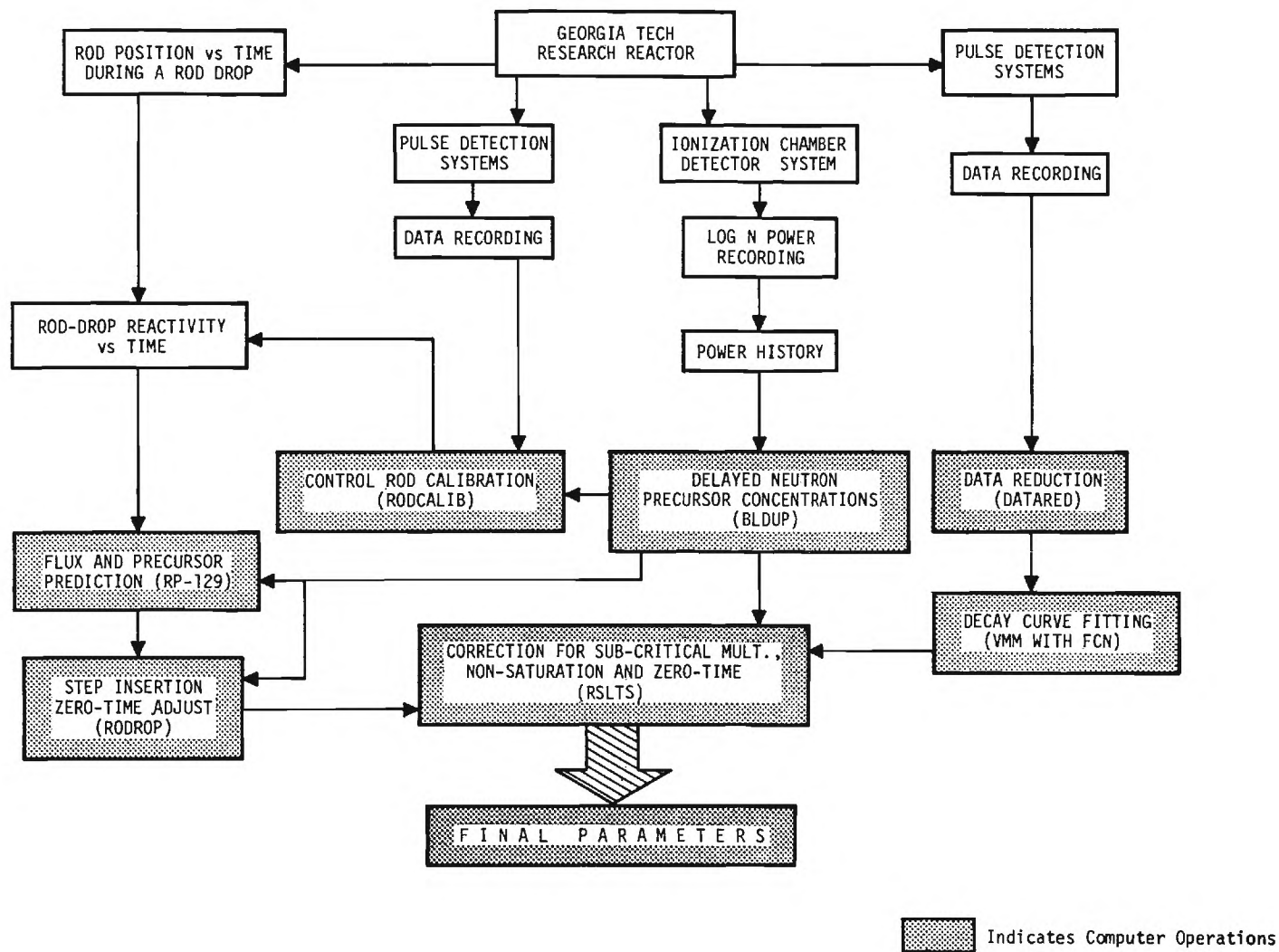


Figure 16. Logical Flow Chart of Information in Process

time may be short compared with precursor half-life. Therefore, it was decided to improve the estimate of equilibrium fraction by processing the reactor's power history using a computer program, BLDUP, developed for the Burroughs B-5500 computer at Georgia Tech. This program and the equations which it solves are included in Appendix B.

The incorporation of reactor power history into computer-readable form, i.e. punched cards, is expected to produce desirable long-term research benefits. It will permit realistic future interpretation of the residual "sources" within the reactor and will also afford the basic information necessary for an accurate burn-up assessment. It is believed that this is the first time that this refinement in calculating precursor concentrations has been included in either parameter determinations or kinetics calculations.

#### Rod Drop Zero Time Determination

In this research, reactor kinetics parameters have been determined by fitting the expression,  $\frac{n(t)}{n(0)} = \sum_{i=1}^M a_i e^{-\lambda_i' t}$ , to the flux decay data. This method employs the commonly used assumption that, at time zero, an instantaneous step insertion of negative reactivity was provided. The time required to drop a rod in the Georgia Tech Research Reactor has been measured by electronic and high speed photographic methods and, as one might expect, it differs considerably between rods, depending on the initial rod position before the drop and the operating characteristics of the dashpot. In any event, while more than 90 percent of the reactivity is invariably inserted in less than one-half second, this is not a truly instantaneous insertion.

It should be evident that a discrepancy of the order of one-half second is of little importance at times in the order of hours, but it may have some bearing on the results obtained for precursors having half-lives of the order of some hundred milliseconds. One might choose the start of rod drop motion as zero time, the completion of rod drop as zero time, or select some time between these two. The latter technique has been followed. In determining the constructive step insertion time, it is desired to choose a time such that a flux versus time calculation using the actual functional description of reactivity insertion versus time will produce results which match those obtained using the step description of reactivity insertion at some time after the drop.

A typical control rod has been calibrated from the banked-critical position ( $19.5^\circ$  withdrawn to full-in) using the RODCALIB method.<sup>30</sup> The results are shown in Figure 17. Thus, the relation between reactivity and rod position may be estimated. Electronic measurement using a Baldwin shaft-position encoder has provided the information on rod position as a function of time in a drop. These results appear in Figure 18. Using these results, a mean value for reactivity insertion as a function of time has been plotted (Figure 19). The representation of this reactivity change as a ramp insertion completed in one-fourth second permits one to apply the ALGOL version of the computer program RP-129.<sup>31</sup> This formulation, originally coded at the Argonne National Laboratory in FORTRAN, solves the one-group, space-independent reactor kinetics equations which were discussed in Chapter I. The output of RP-129 consists of neutron flux and delayed neutron precursor concentrations at uniformly spaced time intervals. These results form the basic input for the ALGOL version of another ANL-originated

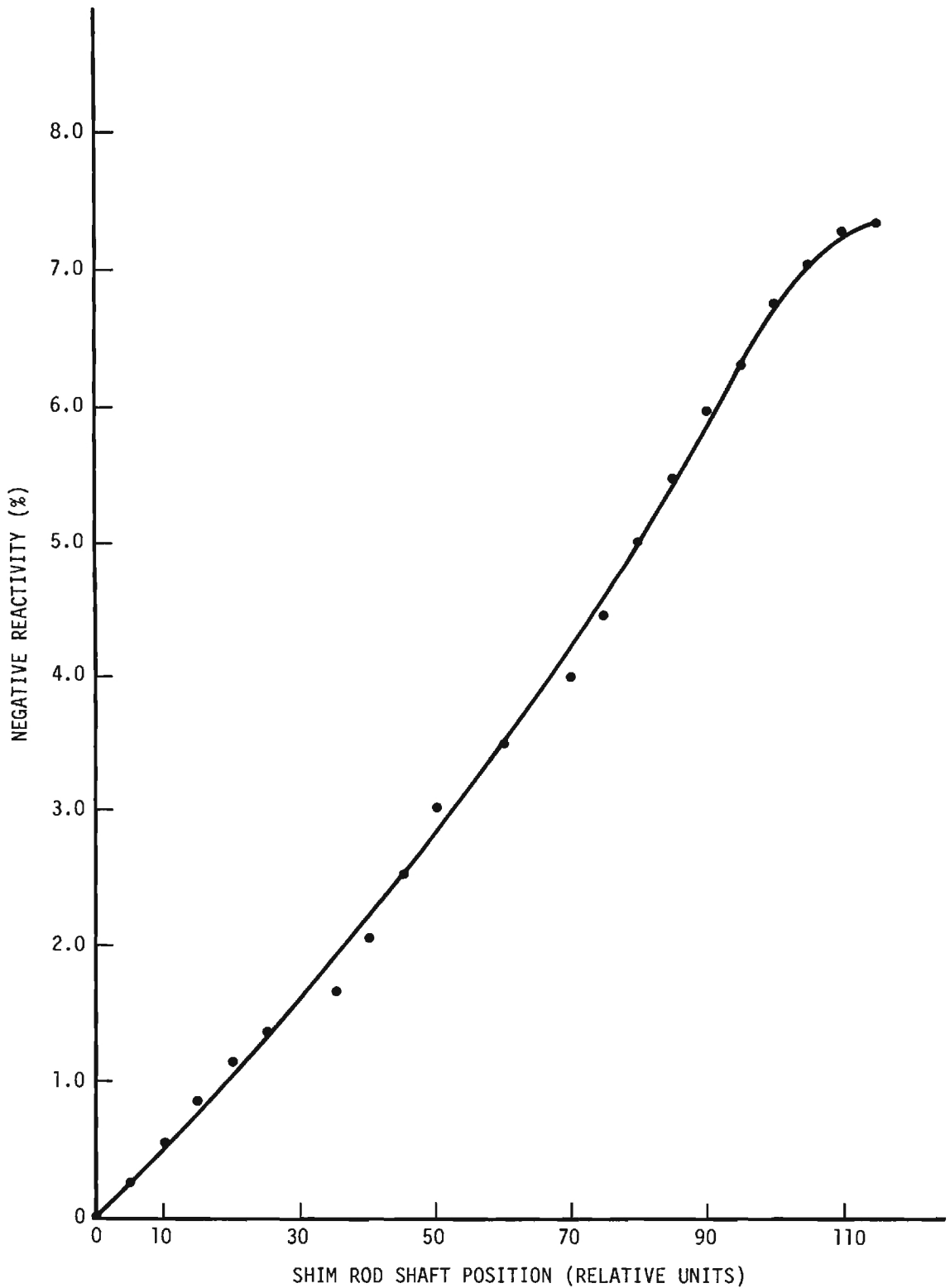


Figure 17. Shim Safety Control Rod Calibration from the Banked-Critical Position to Full-in

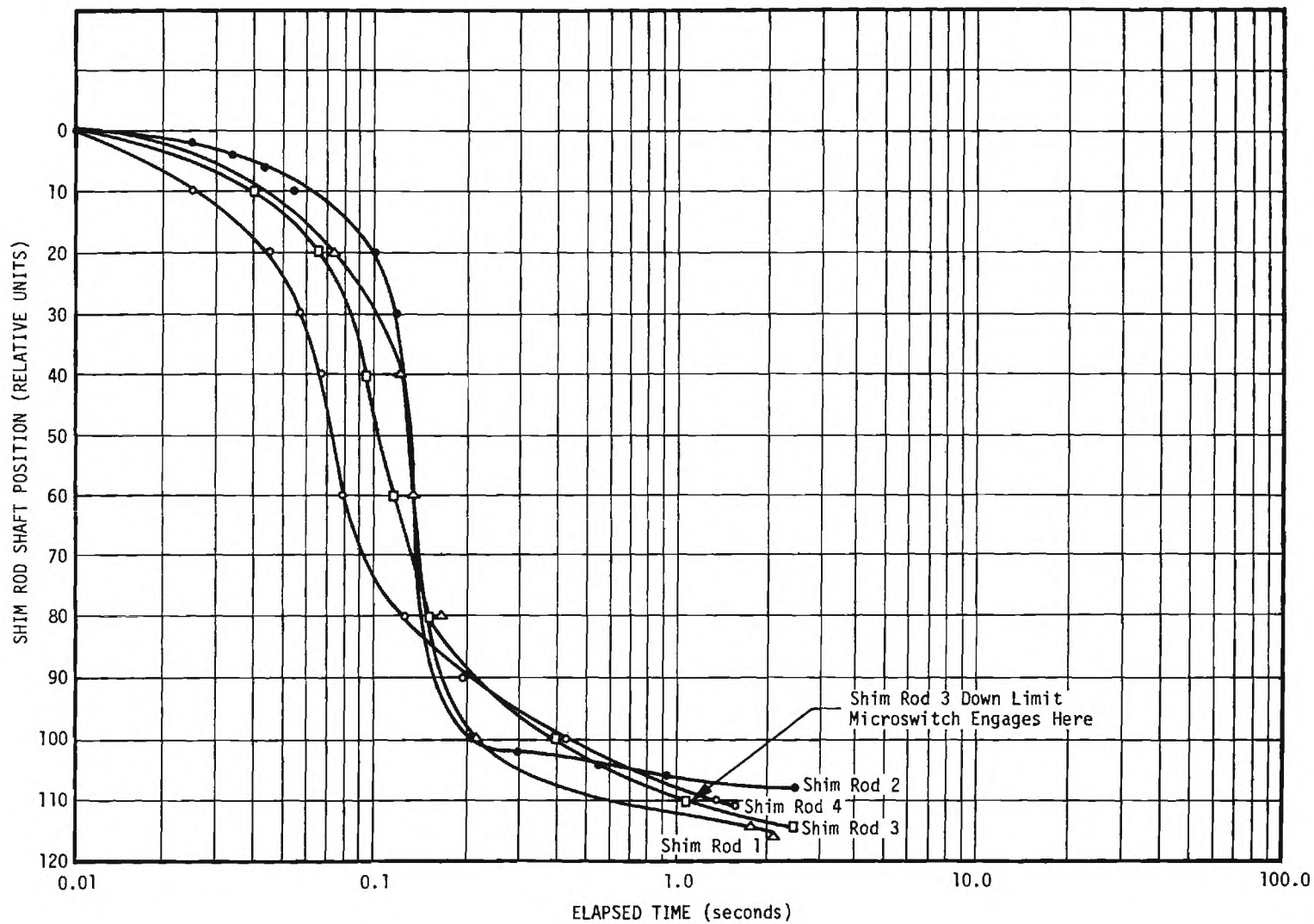


Figure 18. Shim Safety Control Rod Position as a Function of Time Following a Drop from the Banked-Critical Position

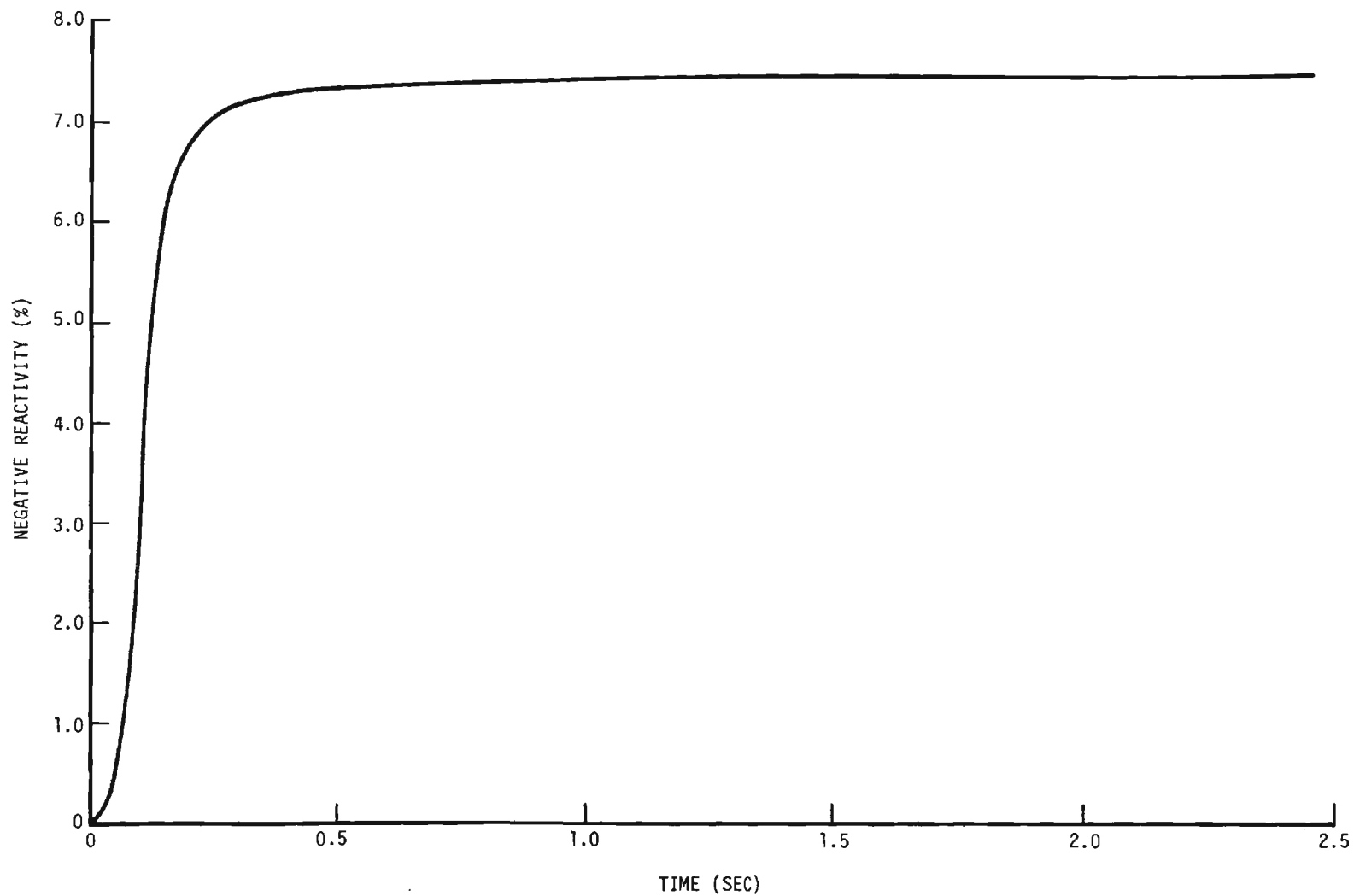


Figure 19. Shim Safety Control Rod -- Negative Reactivity Insertion as a Function of Time Following a Drop from the Banked-Critical Position

FORTTRAN program entitled RODROP.<sup>32</sup> Both of these computer programs are included in Appendix C. The purpose of RODROP is to determine the time at which an instantaneous insertion of negative reactivity would have produced, several minutes later, a flux value which approximates closely that flux predicted by the RP-129 calculation. The RP-129 calculation was based on a more realistic ramp insertion of reactivity. Both calculations assume the same total negative reactivity insertion. They were both made using the best available estimates of kinetics parameters.<sup>11</sup> While one might question the desirability of using estimated kinetics parameters to obtain corrections to other kinetics parameters, this is in fact a valid procedure since this calculation is not sensitive to the details of the assumed parameters. This is particularly true because of the shape of the reactivity-versus-time curve of the rod drop in which most of the reactivity insertion occurs in a short time.

#### Data Collection

The data recording equipment has been described in Chapter II. The procedure followed for data collection using this equipment will now be detailed.

The fission chamber detector and scintillation detector were positioned in the through-tubes. It was considered desirable to obtain data with two different detectors in order to determine any inconsistency or detector-analyzer system malfunction. The comparative results will be discussed in Chapter IV. The reactor was started up and operated at steady power for various lengths of time. The antimony-beryllium start-up source was removed. All four shim rods were dropped and data collection initiated

on a start signal from the down-limit microswitch of one of the control rods. All three multiscalers were sequenced by pulses from the same clock. Analyzer 1 received fission chamber system counts, analyzer 2 scintillation detector system counts, and analyzer 3 received a 1 kc time pulse as a check on clock accuracy. The initial dwell time per channel setting was 0.1 sec. At preselected times, the dwell time setting was advanced. In this fashion, a single 400 channel multiscaler was capable of collecting data for several days without relief or recycle of analyzers. During the course of a counting experiment, the reactor top reflector remained at its operating level. No modifications of reactor configuration were permitted, i.e. no insertions or removals.

The punched paper tapes produced in the readout operation were converted to the punched cards required by the B-5500 computer using an I.B.M. Tape-to-Card Printing Punch with a wired program that checks for punch errors and reproduces the digitized description of the experiment on each card.

#### Data Reduction and Fitting

The flux decay data on punched cards contained the raw information necessary for the curve fitting Variable Metric Minimization (VMM) program,<sup>33</sup> but preliminary reduction and processing were required. These were accomplished by the computer procedure DATARED which is reproduced and discussed in Appendix D. The purpose of DATARED was to test the data for proper sequencing, convert multiscaler dwell time and channel number to elapsed experiment real time, correct data for detector dead time, combine original data points, if required, to provide a reasonable number of final data points



for curve fitting, and to calculate the statistical deviation of each final data point.

Weighted least squares fitting of the flux decay data to the expression  $\frac{n(t)}{n(0)} = \sum_i a_i e^{-\lambda_i' t}$  was accomplished using VMM with an integral function procedure. VMM is a relatively new method for numerically determining the local minimum of a differentiable function of several variables. Instead of using matrix inversion as is frequently done in such problems, VMM starts with an estimate of the inverted matrix and attempts to improve the estimate with each iteration. This technique was devised by its originator, W. C. Davidon, in order to avoid the difficulties of ill-conditioned matrices of the sort encountered in some radioactive decay problems. A discussion of the method has been given by Davidon<sup>33</sup> and by Fletcher and Powell.<sup>34</sup> Since VMM is a general purpose method, the value of the specific function to be minimized, along with its derivatives with respect to each variable, must be calculated in a separate procedure supplied by the user. The function incorporates the goodness-of-fit criterion desired, which in this case is weighted least squares. The details of this function and its derivatives, along with the computer program itself may be found in Appendix E.

After the data have been analyzed to find the parameters producing a best fit, they must be corrected in order to make them applicable under other power history and shut-down conditions. These corrections, which are accomplished in Procedure RSLTS, account for any variation of delayed neutron precursor concentration from an equilibrium value (using BLDUP), the effect of sub-critical neutron multiplication on decay constant parameters, and the change in relative group abundance between the rod drop calculated

zero time and the time at which data collection was started (with zero time having been computed using RP-129 and RODROP). The theory by which these corrections are calculated is detailed in Appendix F.

## CHAPTER IV

### RESULTS

Flux decay data for up to 75 hours after shutdown were obtained on ten separate occasions during the low-power operation of the Georgia Tech Research Reactor. Several preliminary data sets were deemed unacceptable due to interval timer malfunctions or control error. On two occasions, power failures interrupted the experiment for extended periods. In one instance, at the last crucial moment the flexing of a power cable broke a solder joint, incapacitating one of the two detectors from which parallel data were desired. Undoubtedly the most elusive difficulty was that of noise interference. Until the most extreme and sometimes redundant measures for eliminating line and radiated interference were employed, random noise counts from some known and other still unknown sources were apparent. Considerable attention was given to component grounding and shielding and cable shielding. The laboratory regulated power supply was filtered by a Sorensen A.C. regulator. Special D.C. filament supplies were built for the detector preamplifiers.

Two satisfactory experiments, henceforth designated A and B, were carried out in late April and early May, 1965. In each of these, both detectors operated in an acceptable manner. In the discussion which follows, the Test A data obtained with the scintillation detector system will be referred to as A(s); that obtained with the fission chamber system will be designated A(f). Similar designations will apply to Test B results, i.e.

$B(s)$  for scintillation detector data and  $B(f)$  for fission chamber data.

Preliminary fitting attempts very early indicated the necessity for accurate first estimates of the parameters and the uncertainty in these estimates. The square of this uncertainty estimate is a starting value for the error matrix which is refined by the Variable Metric Minimization method. This error matrix controls the magnitude of the parameter-correction step and, after fitting, provides an estimate of the precision with which each parameter has been determined. Initial estimates were based on the decay constants and relative abundances found in the literature, specifically Keepin's compilation.<sup>11</sup> It was found to be helpful to improve these estimates initially by treating the data collected over various time intervals as count rates associated with the mid-point of the time interval. The data collection time interval varied from 0.1 second per data point at the rod drop to 1100 seconds per data point in the final phase of counting. It is believed that this approach provides faster initial convergence because of the greater simplicity of the count rate fitting function and its derivatives.

In the first count rate function fits of the data sets  $A(s)$ ,  $A(f)$ ,  $B(s)$ , and  $B(f)$ , it was evident that  $A(s)$  would be amenable to the closest fit. With 349 data points, an eight-group fit resulted in an  $F$  value of 344.8 (see Equation 6 on page 123) and a weighted variance of fit,  $V$ , of 1.035. The other three tests had eight-group weighted variances of 1.21, 1.25, and 1.24. Since each fit to a different number of groups required at least one-half hour of B-5500 computer time, it was decided to select the number of groups required for the fit by investigating the  $A(s)$  data set in detail, using the exact integral fit method, and then analyzing the other

data sets with selected numbers of groups based on the A(s) outcome. Figure 20 illustrates the result of integral function fits as A(s) data were fitted to the expression,

$$n(t_j \rightarrow t_j + \Delta t_j) = \sum_{i=1}^M \int_{t_j}^{t_j + \Delta t_j} a_i' e^{-\lambda_i' t} dt$$

with a successively larger number of delayed neutron groups, M. A minimum in F value as well as figure-of-merit, V, occurred at 13 groups. One of these 13 was identified as a background term since its decay constant was  $2.73 \times 10^{-10} \text{ sec}^{-1}$ , corresponding to a steady term. Therefore, it was concluded that these data indicate a best fit with twelve delayed neutron groups plus a background group. It should be mentioned at this point that a figure-of-merit value of about 1.0 is the region of acceptable fitting results. In this region of acceptability, roughly two-thirds of the data points will fall within one standard deviation of their calculated values and the remaining points will be sufficiently well-behaved that the average residual (difference between observed and calculated values divided by the standard deviation of the observed data) will have a value slightly less than 1. On this basis, it may be seen that almost all of the fits indicated in Figure 20 were acceptable, although the 13-group fit was best. Plots of data, calculated fit, and residuals for Tests A(s) and B(f) appear in Appendix A. The relative abundances and decay constants for the A(s) fit are presented in Table 1, along with some interesting correction factors which are worthy of comment.

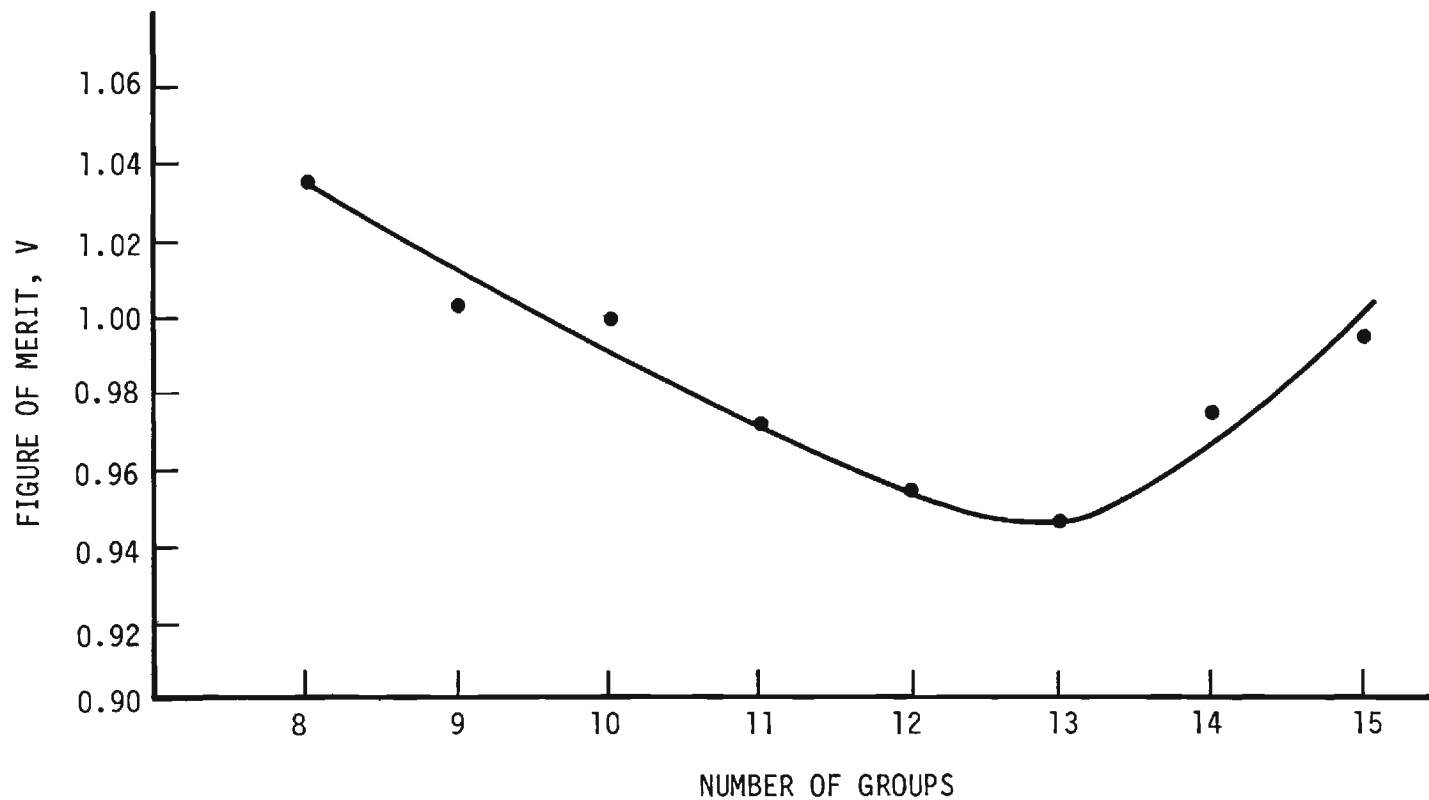


Figure 20. Figure-of-Merit for Test A(s) Parameters as a Function of Number of Delayed Neutron Groups Used in the Fitting

Table 1. Test A(s) 13-Group Parameters with Correction Terms

Group	Resolved $\lambda(\text{sec}^{-1})$	Corrected $\lambda(\text{sec}^{-1})$	Equilibrium Fraction	Zero-Time Enhancement	Relative Abundance
1	1.92	$1.96(\pm 0.25)$	1.00	8.30	$0.245(\pm 0.043)$
2	$4.39 \times 10^{-1}$	$4.41(\pm 0.38) \times 10^{-1}$	1.00	1.62	$0.0812(\pm 0.0105)$
3	$2.83 \times 10^{-1}$	$2.88(\pm 0.09) \times 10^{-1}$	1.00	1.36	$0.273(\pm 0.020)$
4	$1.16 \times 10^{-1}$	$1.17(\pm 0.04) \times 10^{-1}$	1.00	1.14	$0.160(\pm 0.015)$
5	$3.01 \times 10^{-2}$	$3.05(\pm 0.05) \times 10^{-2}$	1.00	1.03	$0.198(\pm 0.004)$
6	$9.22 \times 10^{-3}$	$9.25(\pm 0.28) \times 10^{-3}$	0.988	1.01	$0.0337(\pm 0.0022)$
7	$2.27 \times 10^{-3}$	$2.27(\pm 0.32) \times 10^{-3}$	1.37	1.00	$0.00309(\pm 0.00026)$
8	$7.73 \times 10^{-4}$	$7.73(\pm 0.14) \times 10^{-4}$	5.94	1.00	$0.00200(\pm 0.00008)$
9	$3.15 \times 10^{-4}$	$3.15(\pm 0.06) \times 10^{-4}$	7.55	1.00	$0.00142(\pm 0.00004)$
10	$1.18 \times 10^{-4}$	$1.18(\pm 0.004) \times 10^{-4}$	4.82	1.00	$0.00225(\pm 0.00003)$
11	$5.85 \times 10^{-5}$	$5.85(\pm 0.06) \times 10^{-5}$	2.80	1.00	$0.000503(\pm 0.000014)$
12	$1.37 \times 10^{-5}$	$1.37(\pm 0.07) \times 10^{-5}$	0.993	1.00	$0.0000272(\pm 0.0000014)$
13 (Background)	$2.73 \times 10^{-10}$	$2.73(\pm 0.08) \times 10^{-10}$	-----	----	0.58 counts/sec



Figure 21 is a reproduction of the log n power record for the GTRR at-power periods immediately preceding the initiation of Test A by rod drop. It reveals an approximate half-hour interval at 20 watts power followed by a shutdown (to insert detectors) and a return to 1 watt power for about 10 minutes before rod drop. Since it was planned to account for precursor equilibrium fraction by an analysis of the power history, as discussed in Appendix B, and since the reactor had not operated at appreciable power since startup, this mode of operation was chosen in order to enhance the contribution to the decaying flux of intermediate and longer-lived precursors relative to the short-lived components whose presence would be readily apparent in any event. The result of this enhancement is evident in the equilibrium fraction column of Table 1, in which it may be seen that some groups even exceeded their saturation value, based on power level at the drop. This was possible since precursor atoms generated at the 20 watt level had not had sufficient time to decay away and reach equilibrium at the 1 watt level. The group possessing the largest equilibrium fraction, 7.55, has a half-life of 36.6 minutes and was thus short-lived enough to be at nearly 50 percent equilibrium based on the 20 watt level and sufficiently long-lived not to decay away markedly before shutdown. This equilibrium fraction provided a correction term that was applied before the calculation of the relative abundances in order that all abundances might be based on the saturation value of precursors.

The second correction factor in Table 1, labeled zero-time enhancement, is due to the 1.1 second lag between the time of the constructive step insertion of reactivity and the time that the down-limit microswitch on shim rod #3 was engaged, starting data collection. The constructive zero-

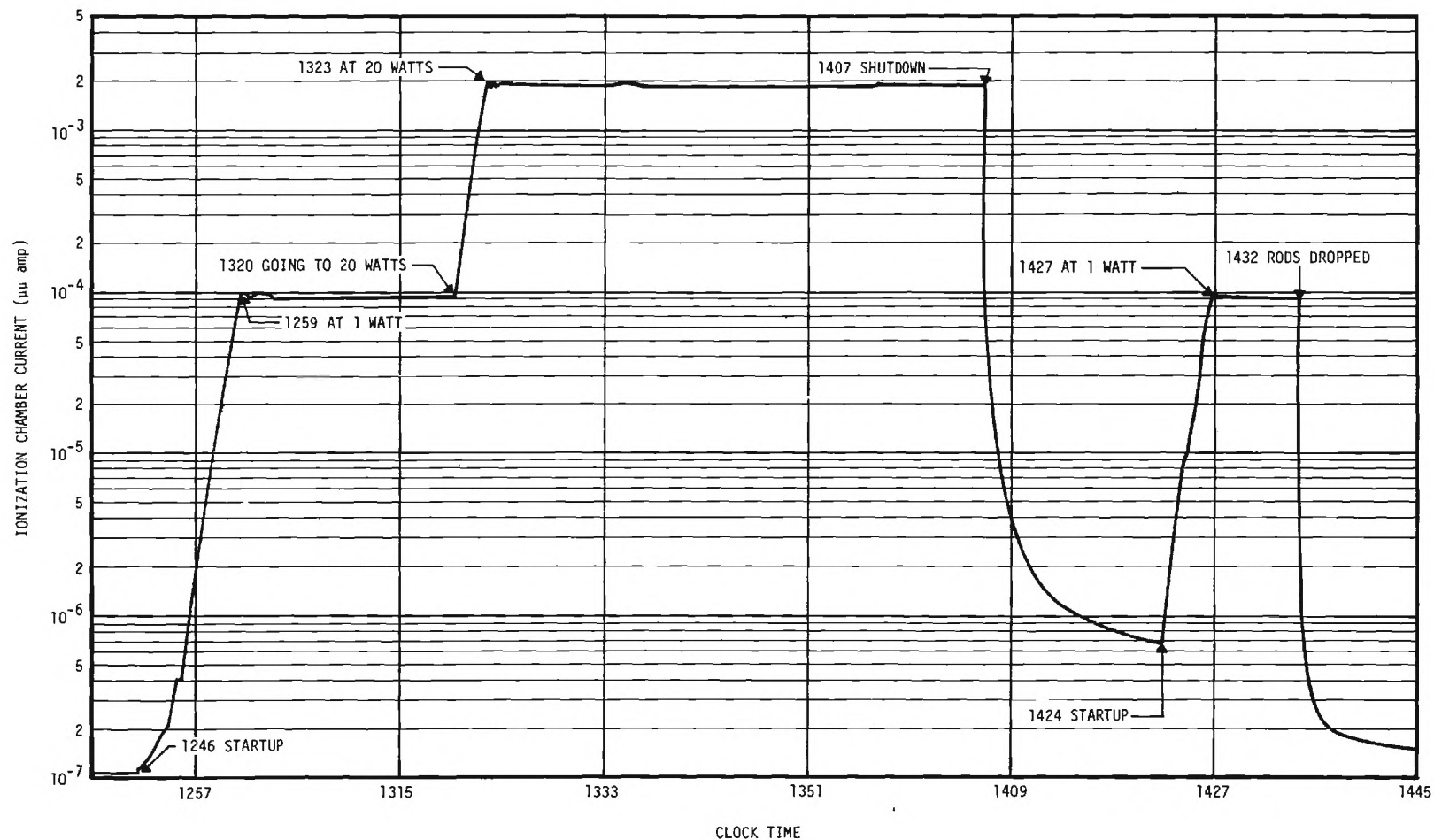


Figure 21. Log n Power Recording for the Georgia Tech Research Reactor At-Power Periods Immediately Preceding the Start of Test A

time for these experiments was calculated by the methods described in Appendix C to be 0.038 second, and the total drop time from the banked-critical position to the engaging of the microswitch was measured and found to be 1.13 to 1.14 seconds. This enhancement was most apparent in the shortest-lived group with a decay constant of  $1.96 \pm 0.25 \text{ sec}^{-1}$ . This corresponds to a half-life of 0.353 second; thus over a 1.1 second interval this group would be expected to decay away to less than one-eighth of its zero-time abundance.

Table 2 presents the parameters obtained by fitting the data of Test A(s) with several different numbers of delayed neutron groups. In order to ascertain how good a fit Keepin's suggested decay constants would provide for these data, we have included a fit to 14 groups, in which the abundances were free to be varied by the VMM program while the decay constants were constrained to remain at the values suggested by Keepin,<sup>11</sup> with one exception. The shortest-lived group, with a half-life of 0.179 second, was omitted since the conditions of this experiment did not favor its resolution, if it does in fact exist. The resolution of this group was sought in a special rod drop experiment with the GTRR in which data were collected at 0.1 second per channel from before a drop until 22 seconds after the drop and analyzed beginning at 0.5 second after the start of rod motion. The best fit to the data of this special experiment resulted when the shortest-lived group had a half-life of 0.452 second, indicating that a 0.179 second group could not be resolved.

Table 3 compares the 13-group fits of Tests A(s), A(f), B(s), and B(f). Test B(s) did not fit well and the 13-group fit to its data resulted in a weighted variance of 1.38. Since this figure-of-merit indicates a

Table 2. Test A(s) Parameters

Groups	8 Group Fit		10 Group Fit		12 Group Fit		13 Group Fit		14 Group Fit with Literature <sup>11</sup> Values of $\lambda_i$ $V = 1.215$	
	$V = 1.035$		$V = 1.005$		$V = 0.9568$		$V = 0.9470$			
	$\beta_{eff}/\beta_{eff}$	$\lambda_i(\text{sec}^{-1})$	$\beta_{eff}/\beta_{eff}$	$\lambda_i(\text{sec}^{-1})$	$\beta_{eff}/\beta_{eff}$	$\lambda_i(\text{sec}^{-1})$	$\beta_{eff}/\beta_{eff}$	$\lambda_i(\text{sec}^{-1})$	$\beta_{eff}/\beta_{eff}$	$\lambda_i(\text{sec}^{-1})$
1					0.174	1.63	0.245	1.96	0.0645	1.40
2					0.311	$3.27 \times 10^{-1}$	0.0812	$4.41 \times 10^{-1}$	0.332	$3.11 \times 10^{-1}$
3	0.628	$2.37 \times 10^{-1}$	0.606	$2.57 \times 10^{-1}$	0.0893	$2.62 \times 10^{-1}$	0.273	$2.88 \times 10^{-1}$	0.0992	$2.77 \times 10^{-1}$
4					0.176	$1.04 \times 10^{-1}$	0.160	$1.17 \times 10^{-1}$	0.206	$1.15 \times 10^{-1}$
5	0.312	$3.33 \times 10^{-2}$	0.231	$4.32 \times 10^{-2}$	0.212	$2.82 \times 10^{-2}$	0.198	$3.05 \times 10^{-2}$	0.214	$3.17 \times 10^{-2}$
6			0.0972	$2.46 \times 10^{-2}$					0.0264	$1.69 \times 10^{-2}$
7	0.0489	$8.33 \times 10^{-3}$	0.0538	$9.77 \times 10^{-3}$	0.00660	$8.97 \times 10^{-3}$	0.0337	$9.25 \times 10^{-3}$	0.0375	$1.27 \times 10^{-2}$
8					0.0232	$6.83 \times 10^{-3}$	0.00309	$2.27 \times 10^{-3}$	0.00982	$4.81 \times 10^{-3}$
9	0.00348	$8.89 \times 10^{-4}$	0.00376	$1.06 \times 10^{-3}$	0.00268	$8.84 \times 10^{-4}$	0.00200	$7.73 \times 10^{-4}$	0.00370	$1.50 \times 10^{-3}$
10	0.00222	$3.03 \times 10^{-4}$	0.00232	$3.54 \times 10^{-4}$	0.00174	$3.15 \times 10^{-4}$	0.00142	$3.15 \times 10^{-4}$	0.00278	$4.28 \times 10^{-4}$
11	0.00320	$1.09 \times 10^{-4}$	0.00319	$1.18 \times 10^{-4}$	0.00258	$1.13 \times 10^{-4}$	0.00225	$1.18 \times 10^{-4}$	0.00324	$1.17 \times 10^{-4}$
12	0.000398	$4.54 \times 10^{-5}$	0.000613	$5.39 \times 10^{-5}$	0.000401	$4.97 \times 10^{-5}$	0.000503	$5.85 \times 10^{-5}$	0.000467	$4.37 \times 10^{-5}$
13			0.0000204	$3.65 \times 10^{-6}$			0.0000272	$1.37 \times 10^{-5}$	0.0000212	$3.63 \times 10^{-6}$
14	0.00151	$5.94 \times 10^{-7}$	0.00134	$5.94 \times 10^{-7}$	0.000134	$7.77 \times 10^{-7}$			0.000305	$6.24 \times 10^{-7}$
Back-ground							0.58 counts per second	$2.7 \times 10^{-10}$		

Table 3. Comparison of 13-Group Parameters - Tests A and B

Group	Test A(s) V = 0.947		Test A(f) V = 1.14		Test B(f) V = 1.07		Test B(s) V = 1.38	
	$\beta_{i,eff}/\beta_{eff}$	$\lambda_i(\text{sec}^{-1})$	$\beta_{i,eff}/\beta_{eff}$	$\lambda_i(\text{sec}^{-1})$	$\beta_{i,eff}/\beta_{eff}$	$\lambda_i(\text{sec}^{-1})$	$\beta_{i,eff}/\beta_{eff}$	$\lambda_i(\text{sec}^{-1})$
1	0.245( $\pm 0.043$ )	1.96 ( $\pm 0.25$ )	0.286( $\pm 0.028$ )	1.99 ( $\pm 0.22$ )	0.175( $\pm 0.018$ )	1.61 ( $\pm 0.16$ )	0.518( $\pm 0.52$ )	2.07( $\pm 0.20$ )
2	0.0812( $\pm 0.0105$ )	4.41 ( $\pm 0.38$ ) $\times 10^{-1}$	0.260( $\pm 0.017$ )	3.56 ( $\pm 0.20$ ) $\times 10^{-1}$	0.297( $\pm 0.018$ )	3.76 ( $\pm 0.23$ ) $\times 10^{-1}$	0.0207( $\pm 0.0021$ )	7.43( $\pm 0.74$ ) $\times 10^{-1}$
3	0.273( $\pm 0.020$ )	2.88 ( $\pm 0.09$ ) $\times 10^{-1}$	0.0764( $\pm 0.0054$ )	2.35 ( $\pm 0.12$ ) $\times 10^{-1}$	0.0807( $\pm 0.0084$ )	2.38 ( $\pm 0.21$ ) $\times 10^{-1}$	0.230( $\pm 0.023$ )	2.19( $\pm 0.21$ ) $\times 10^{-1}$
4	0.160( $\pm 0.015$ )	1.17 ( $\pm 0.04$ ) $\times 10^{-1}$	0.154( $\pm 0.011$ )	1.16 ( $\pm 0.04$ ) $\times 10^{-1}$	0.205( $\pm 0.012$ )	1.12 ( $\pm 0.05$ ) $\times 10^{-1}$	0.0497( $\pm 0.0050$ )	1.79( $\pm 0.18$ ) $\times 10^{-1}$
5	0.198( $\pm 0.004$ )	3.05 ( $\pm 0.05$ ) $\times 10^{-2}$	0.185( $\pm 0.002$ )	3.04 ( $\pm 0.04$ ) $\times 10^{-2}$	0.209( $\pm 0.003$ )	2.76 ( $\pm 0.03$ ) $\times 10^{-2}$	0.155( $\pm 0.015$ )	3.26( $\pm 0.27$ ) $\times 10^{-2}$
6	0.0337( $\pm 0.0022$ )	9.25 ( $\pm 0.28$ ) $\times 10^{-3}$	0.0115( $\pm 0.0009$ )	1.26 ( $\pm 0.06$ ) $\times 10^{-2}$	0.0209( $\pm 0.0012$ )	8.73 ( $\pm 0.34$ ) $\times 10^{-3}$	0.00664( $\pm 0.00066$ )	8.19( $\pm 0.81$ ) $\times 10^{-3}$
7	0.00309( $\pm 0.00026$ )	2.27 ( $\pm 0.32$ ) $\times 10^{-3}$	0.00206( $\pm 0.0013$ )	7.32 ( $\pm 0.27$ ) $\times 10^{-3}$	0.00685( $\pm 0.00055$ )	4.02 ( $\pm 0.14$ ) $\times 10^{-3}$	0.0160( $\pm 0.0016$ )	7.41( $\pm 0.68$ ) $\times 10^{-3}$
8	0.00200( $\pm 0.00008$ )	7.73 ( $\pm 0.14$ ) $\times 10^{-4}$	0.00217( $\pm 0.00004$ )	8.56 ( $\pm 0.09$ ) $\times 10^{-4}$	0.00204( $\pm 0.00006$ )	9.21 ( $\pm 0.14$ ) $\times 10^{-4}$	0.00167( $\pm 0.00017$ )	6.54( $\pm 0.65$ ) $\times 10^{-4}$
9	0.00142( $\pm 0.00004$ )	3.15 ( $\pm 0.06$ ) $\times 10^{-4}$	0.00122( $\pm 0.00002$ )	3.17 ( $\pm 0.05$ ) $\times 10^{-4}$	0.00133( $\pm 0.00002$ )	3.45 ( $\pm 0.06$ ) $\times 10^{-4}$	0.000119( $\pm 0.000012$ )	2.30( $\pm 0.23$ ) $\times 10^{-4}$
10	0.00225( $\pm 0.00003$ )	1.18 ( $\pm 0.004$ ) $\times 10^{-4}$	0.00204( $\pm 0.00001$ )	1.195( $\pm 0.006$ ) $\times 10^{-4}$	0.00175( $\pm 0.00002$ )	1.239( $\pm 0.009$ ) $\times 10^{-4}$	0.00102( $\pm 0.00009$ )	1.66( $\pm 0.11$ ) $\times 10^{-4}$
11	0.000503( $\pm 0.000014$ )	5.85 ( $\pm 0.06$ ) $\times 10^{-5}$	0.000464( $\pm 0.000011$ )	5.78 ( $\pm 0.03$ ) $\times 10^{-5}$	0.000412( $\pm 0.000012$ )	6.12 ( $\pm 0.04$ ) $\times 10^{-5}$	0.000662( $\pm 0.000059$ )	8.11( $\pm 0.57$ ) $\times 10^{-5}$
12	0.0000272( $\pm 0.0000014$ )	1.37 ( $\pm 0.07$ ) $\times 10^{-5}$	0.0000207( $\pm 0.0000012$ )	1.10 ( $\pm 0.08$ ) $\times 10^{-5}$	0.0000128( $\pm 0.0000007$ )	1.07 ( $\pm 0.04$ ) $\times 10^{-5}$	0.0000227( $\pm 0.0000023$ )	2.27( $\pm 0.23$ ) $\times 10^{-5}$
Back-ground	0.58 counts/sec	2.73 ( $\pm 0.08$ ) $\times 10^{-10}$	0.52 counts/sec	8.57 ( $\pm 0.67$ ) $\times 10^{-11}$	0.70 counts/sec	1.39 ( $\pm 0.11$ ) $\times 10^{-10}$	0.52 counts/sec	2.48( $\pm 0.25$ ) $\times 10^{-10}$

poorer fit than that obtained in Tests A(s), A(f), and B(f), these parameters are included only to demonstrate that, even in this worst case, the results are still comparable to those obtained in relatively more successful fits. No conclusion has been reached as to why these data were less successfully fitted, especially since the same detector was used in Test B(s) as was used when the best results were obtained in Test A(s). A comparison of the remaining parameters in Table 3 reveals only a fair consistency and adequate agreement only in the case of some decay constants. In Test A it appears that there may be some degree of ambiguity between groups 2 and 3, which have decay constants of a similar magnitude, but which are not resolved to within their respective error estimates in the two different data sets. In Test A(s), group 3 abundance was roughly 3 times that of group 2, while in Test A(f) group 2 had an abundance something over 3 times that of group 3. This occurrence may be indicative of the reason for some lack of agreement as to parameter values among the different tests. The nature of this fitting process is such that a certain set of data is best fitted with a number of delayed neutron group parameters that is almost certainly smaller than the actual number of delayed neutron precursors present. The extent to which real groups merge together into the resolved groups and the details of such a merger may be responsible for the occurrence of two somewhat different sets of parameters, both of which permit an acceptable fit to the data of a given experiment as gathered by two different detectors. Thus, in Test A, it appears possible that the true physical situation affecting that portion of the experiment attributable to groups 2 and 3 may be satisfactorily represented in a non-unique manner. There is also a possibility that the VMM program did not accurately assess the error

matrix for all parameters for all tests. The refinement of that error matrix is accomplished in the program by making numerous steps in a random direction away from the minimum, and then finding the minimum again. In the process of searching for the minimum, additional information is gained which is used to improve the accuracy of the error matrix. More than 15 random steps were taken for Test A(s) and approximately 10 each for Tests A(f) and B(f). Each random step required about 10 - 15 minutes of B-5500 computer time. In any such experiment one would also be obliged to mention the possibility of detector gain-shift. This potential error-producing mechanism would be most appropriately suspected with respect to the scintillation detector. It has been previously mentioned in discussing this equipment that its design was directed toward minimizing gain shift from high to low counting rates, and careful consideration was given to the stability of the high voltage supply selected for this detector.

In Table 4 we have compared our best fit parameters of Test A(s) with those recommended by Keepin<sup>11</sup> (these incorporate the results of Keepin et al.,<sup>12</sup> Bernstein et al.,<sup>10</sup> and Ergen<sup>17</sup>), and those found in ZEEP.<sup>19</sup> The Keepin-Bernstein-Ergen data (henceforth to be referred to as KBE) have been combined into a single set and normalized to a total relative abundance of 1. The 1947 ZEEP experiment was conducted in order to study photoneutron parameters and the abundances were normalized to that of a prominent standard delayed group resolved from the ZEEP data which coincided in decay constant with a group reported by Hughes et al.,<sup>9</sup> using the Hughes abundance as the standard. Therefore, no complete listing of relative abundances can be derived from that data. The decay constants from ZEEP<sup>19</sup> are included for historical reasons and to indicate the



Table 4. Comparison of 13-Group Parameters of the Present Work with Literature Values

Group	Test A(s)		Avg. of Tests A(s), A(f), and B(f)		Keepin-Bernstein-Ergen <sup>11</sup>			Johns and Sargent <sup>19</sup>
	$\beta_{i\text{eff}}/\beta_{\text{eff}}$	$\lambda_i(\text{sec}^{-1})$	$\beta_{i\text{eff}}/\beta_{\text{eff}}$	$\lambda_i(\text{sec}^{-1})$	$\beta_i/\beta$	Type	$\lambda_i(\text{sec}^{-1})$	$\lambda_i(\text{sec}^{-1})$
1					0.0225	Fission	3.87	
2	0.245	1.96	0.235	1.85	0.111	Fission	1.40	
3	0.0812	$4.41 \times 10^{-1}$	0.213	$3.91 \times 10^{-1}$	0.352	Fission	$3.11 \times 10^{-1}$	
4	0.273	$2.88 \times 10^{-1}$	0.143	$2.54 \times 10^{-1}$	0.0867	Photo	$2.77 \times 10^{-1}$	
5	0.160	$1.17 \times 10^{-1}$	0.173	$1.15 \times 10^{-1}$	0.163	Fission	$1.15 \times 10^{-1}$	$1.72 \times 10^{-1}$
6	0.198	$3.05 \times 10^{-2}$	0.197	$2.95 \times 10^{-2}$	0.184	Fission	$3.17 \times 10^{-2}$	$3.33 \times 10^{-2}$
7	0.0337	$9.25 \times 10^{-3}$	0.0220	$1.02 \times 10^{-2}$	0.0272	Photo	$1.69 \times 10^{-2}$	
8					0.0329	Fission	$1.27 \times 10^{-2}$	$1.22 \times 10^{-2}$
9	0.00309	$2.27 \times 10^{-3}$	0.00400	$4.54 \times 10^{-3}$	0.00932	Photo	$4.81 \times 10^{-3}$	$3.05 \times 10^{-3}$
10	0.00200	$7.73 \times 10^{-4}$	0.00207	$8.50 \times 10^{-4}$	0.00448	Photo	$1.50 \times 10^{-3}$	$7.30 \times 10^{-4}$
11	0.00142	$3.15 \times 10^{-4}$	0.00132	$3.26 \times 10^{-4}$	0.00276	Photo	$4.28 \times 10^{-4}$	$2.30 \times 10^{-4}$
12	0.00225	$1.18 \times 10^{-4}$	0.00201	$1.21 \times 10^{-4}$	0.00312	Photo	$1.17 \times 10^{-4}$	$1.12 \times 10^{-4}$
13	0.000503	$5.85 \times 10^{-5}$	0.000460	$5.92 \times 10^{-5}$	0.000430	Photo	$4.37 \times 10^{-5}$	$4.52 \times 10^{-5}$
14	0.0000272	$1.37 \times 10^{-5}$	0.0000202	$1.18 \times 10^{-5}$	0.0000137	Photo	$3.63 \times 10^{-6}$	
15					0.0000666	Photo	$6.24 \times 10^{-7}$	
Back-ground	0.58 cps	$2.73 \times 10^{-10}$	0.60 cps	$1.66 \times 10^{-10}$				

number of groups which Johns and Sargent were able to resolve in their experiment which was similar to our own.

We have given for comparison in Table 4 a combination set of parameters obtained by averaging the corresponding groups of Tests A(s), A(f), and B(f). While this is surely a plausible set for kinetics calculations in highly enriched heavy-water reactors, and we have weighed the advisability of adopting them, we choose to use the Test A(s) parameters in the remainder of this work. We feel that they are supported by partial agreement with the A(f) and B(f) results, but are a better choice than an average with these other sets would be since a more precise fit was obtained in Test A(s).

A comparison between Test A(s) and KBE parameters is instructive, even though it is not precise. The first group of Test A(s) appears to have a decay constant,  $1.96 \text{ sec}^{-1}$ , which is close to an abundance-weighted average of the first two groups of the KBE values, i.e.

$$\frac{0.02251 \times 3.87 + 0.1108 \times 1.4}{0.1333} = 1.81$$

KBE groups 3 and 4 are difficult to compare with corresponding groups from Test A(s) due to the abundance ambiguity discussed earlier. There is, however, agreement with the decay constants of KBE groups 5 and 6. Group 6 is the important 22-second half-life by which the Bernstein photoneutron data have been incorporated into the recommended group constants of Keepin.<sup>11</sup> (Originally Bernstein et al. reported their results with respect to the 22-second group of Hughes et al.<sup>9</sup>) Since both of these groups are attributed to "standard" delayed neutrons, one may make the assumption (in agreement

with calculations made by J. Lewins for the Massachusetts Institute of Technology Reactor<sup>26</sup>) that  $\sum_i \beta_i \text{eff}$  for the GTRR is about the same as  $\sum_i \beta_i$  for the KBE parameters. Then the relative abundances of these two groups may be examined for some clue as to relative effectiveness of this category of delayed neutrons in the GTRR. The ratio of Test A(s) abundances to KBE abundances for these two groups is 1.03, suggesting a 3 percent enhancement of delayed neutron importance in the GTRR due to lower average energy. The only photoneutron group with notable agreement in decay constant value is group 12. The Test A(s) value is  $1.18 \times 10^{-4} \text{ sec}^{-1}$  and the KBE value is  $1.17 \times 10^{-4} \text{ sec}^{-1}$ . With such close agreement on decay constant, one might anticipate that the ratios of relative abundances for this group could provide an estimate of the photoneutron effectiveness in the GTRR. This ratio, 0.72, is in fact quite close to the value of 0.691 calculated for the MITR.<sup>26</sup>

An interesting feature appeared in the analysis of Test A(f) results. Fits had been obtained with moderate success using eight and nine groups. The ten-group fit was surprising in that one of the abundance terms was negative, a possibility permitted by the VMM program. When the decay constant,  $1.96 \times 10^{-5} \text{ sec}^{-1}$  was converted to a half-life value, 9.82 hours, it was recognized as being near the 9.13 hour half-life of Xe-135. Xe-135 effects had been anticipated after higher power operation, but had not been expected during low-power operation. If, indeed, this were Xe-135 it could explain the negative abundance value since the decay of a neutron sink (Xe-135) has the opposite effect of the decay of a neutron source (delayed neutron emitter). But the significance of the supposed xenon contribution was small, - 1.5 counts per second in the initial count rate of about 12,000 counts per second. A decay constant of  $1.86 \times 10^{-5} \text{ sec}^{-1}$  was found in con-

junction with a negative abundance term in the ten-group analysis of the results of Test B(s). Other than these two rather uncertain indications, such a term did not again appear until a 16-group fit to the Test A(s) data revealed a - 0.7 count per second contribution with a decay constant,  $2.09 \times 10^{-5} \text{ sec}^{-1}$ , convertible to a half-life value of 9.21 hours. This 16-group fit also included another low-abundance term with positive sign whose decay constant was close to that of I-135. The concentration of xenon as a function of time following shutdown can, of course, be derived from a solution of the differential equations describing the change in concentration of iodine and xenon. This has been done by Meghreblian and Holmes<sup>35</sup> and the result is

$$\text{Xe}(t) = \left( \text{Xe}_0 + \frac{\lambda_I I_0}{\lambda_I - \lambda_{\text{Xe}}} \right) e^{-\lambda_{\text{Xe}} t} - \left( \frac{\lambda_I I_0}{\lambda_I - \lambda_{\text{Xe}}} \right) e^{-\lambda_I t}$$

where  $\text{Xe}_0$  is the initial concentration at time zero of Xe-135,  $I_0$  is the time zero concentration of I-135, and the  $\lambda$ 's are the iodine and xenon decay constants.

If xenon were present to any appreciable extent, its change in concentration would have to be interpreted as a change in reactivity and, hence, a change in the sub-critical multiplication of the reactor. The magnitude of this effect at the time these data were collected could not exceed the value appropriate for 200 watt operation. According to Glasstone and Edlund,<sup>36</sup> for fluxes less than  $10^{11} \text{ neutrons/cm}^2\text{sec}$ , the Xe-135 poisoning effect at shutdown,  $P_0$ , may be estimated by

$$P_o \cong 8 \times 10^{-15} \phi_o$$

where  $\phi_o$  is the pre-shutdown at-power neutron flux, and the poisoning,  $P_o$ , is defined as the pre-shutdown ratio of the number of thermal neutrons absorbed by the poison to those absorbed in the fuel. At such flux levels, there is no appreciable poisoning increase after shutdown. If we assume  $\phi_o$  at 1000 kW to be  $2 \times 10^{13}$  n/cm<sup>2</sup>sec<sup>27</sup> and scale down linearly to 200 watts,  $\phi_o = 4 \times 10^9$  n/cm<sup>2</sup>sec. Thus,  $P_o \cong 3.2 \times 10^{-5}$ . This effect is so small that one would reasonably consider it to be negligible. The possibility that these data do actually indicate the presence of Xe-135 is therefore difficult to evaluate. It is concluded that these indications result either from a true fitting to Xe-135 decay near the threshold of significance or a chance coincidence of the fitting results.

## CHAPTER V

### CONCLUSIONS

Experiments have been performed with the Georgia Tech Research Reactor to determine the number of identifiable delayed neutron groups along with the parameter values for these groups. This information is required in reactor kinetics calculations.

The parameters obtained in Test A(s) of this work represent the most appropriate values of decay constants and relative abundances presently available for a highly enriched heavy-water reactor. Twelve delayed neutron and photoneutron groups are required. Since these parameters were obtained through experiments using an actual reactor of this type, they incorporate the factors affecting such values in a direct fashion. It is for this reason that the use of these parameters in kinetics calculations should represent an improvement over calculations using parameters determined by the small-sample method. The parameters reported have been given general utility by careful attention to the corrections required to account for reactor power history, finite time of rod drop, and sub-critical multiplication. It is believed that this is the first time that these methods for power history and rod drop assessment have been applied to the kinetics parameter determination problem.

In order to illustrate the value of this work and the extent to which the particular parameters one uses may affect kinetics calculations, two different sets of calculations have been made. These were first, the

determination of the reactivity calibration curve for the GTRR regulating rod, and second, the assessment of GTRR reactivity as a function of the reciprocal of positive asymptotic period. In the regulating rod problem, with the reactor initially critical, the neutron flux was recorded while the rod was driven at constant speed from full-out to full-in. These data were analyzed using the RODCALIB method,<sup>30</sup> first with KBE parameters and then with the parameters determined in the present work. The RODCALIB method is a fast calibration technique that uses a digital computer program to apply the reactor kinetics equations. Since the data that are required to perform a complete control rod calibration may be obtained in less than one minute, it is an attractive method, and one that will probably be employed frequently to provide up-to-date calibrations for this control element, which is itself a commonly used secondary standard by which other reactivities are determined.

The results of the two calculations are represented in Figure 22. It may be seen in this figure that the KBE parameters produce a calibration curve that is generally about 10 percent higher than that obtained with our parameters. Thus, negative reactivity calibrations made using the KBE parameter curve for the regulating rod as a standard will be overestimated in worth by 10 percent. The excess positive reactivity which can be compensated with this rod would also be overestimated to the same extent. In both of these rod calibration calculations, the same value of total  $\beta$  was used, i.e.  $\sum_i \beta_i = \sum_i \beta_{i\text{eff}}$ . It should be emphasized at this point that no value for total  $\beta_{\text{eff}}$  has been obtained in this work; only decay constants and relative abundances for the delayed neutron groups have been measured.



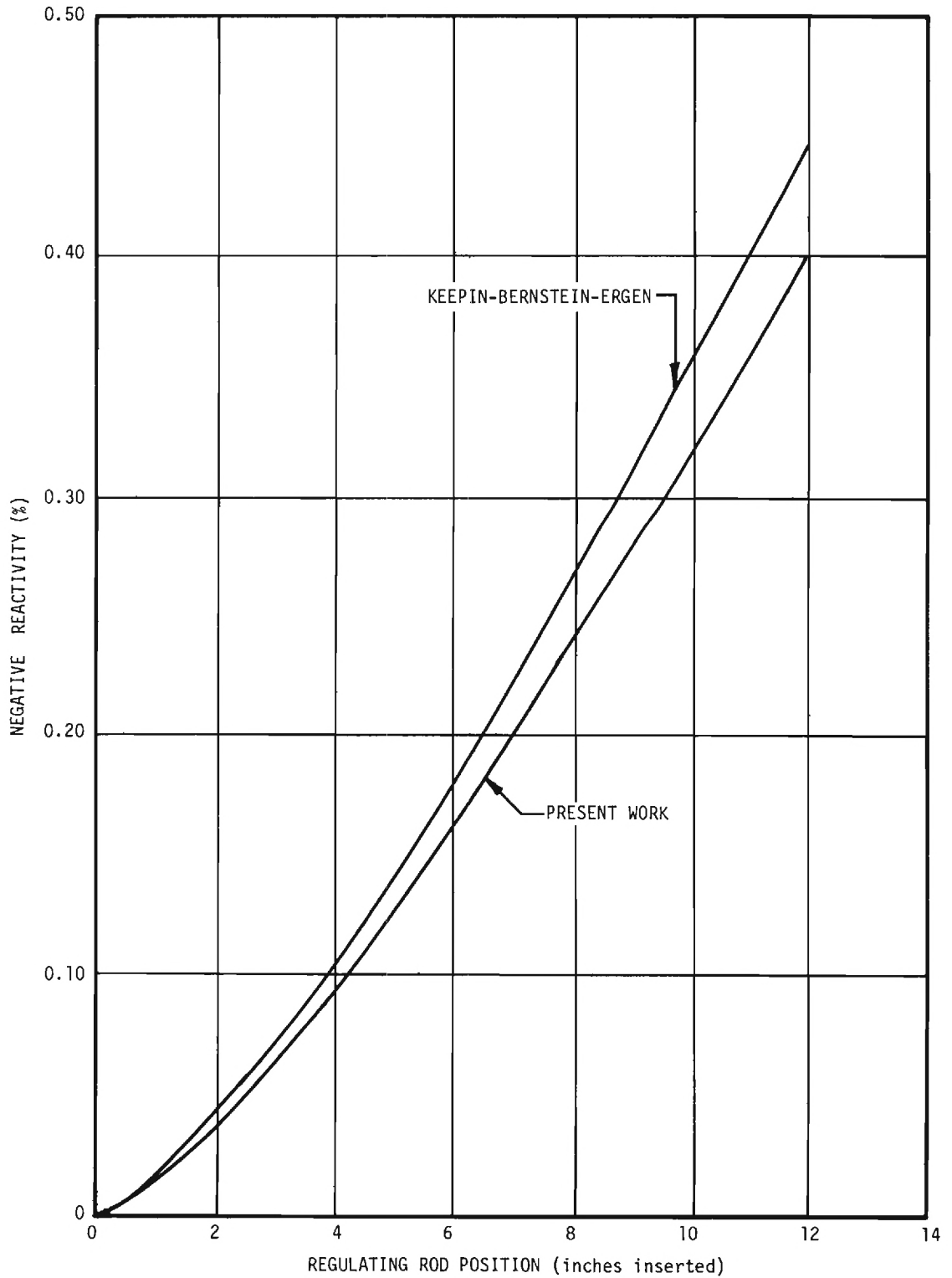


Figure 22. Georgia Tech Research Reactor -- Regulating Rod Calibration as Determined from Experimental Data by Using Both Previously Available Parameters and Those Determined in the Present Work

However, it has been mentioned in the previous chapter that calculations by Lewins<sup>26</sup> at MITR have indicated that  $\beta_{\text{eff}}$  for the MITR, which is a highly enriched heavy-water research reactor similar to the GTRR, may be very close to the  $\beta$  value suggested by Keepin.<sup>11</sup>

In the asymptotic period problem, these same two sets of parameters were applied in turn to calculate the steady rising reactor period which would be associated with a wide range of positive reactivity step insertions. Computer program NE-1 was used for these calculations.<sup>37</sup> The results are represented in Figure 23. In this figure we have chosen to plot positive reactivity as a function of the reciprocal of asymptotic period since this is an effective way to emphasize the difference which the choice of parameters makes over a wide range of asymptotic periods. Once again, a reactivity calibration which is obtained using the asymptotic period method and KBE parameters would indicate approximately 10 percent greater worth than would a calibration using the same period data and our parameters. The basic reason for these differences in kinetics calculation results is that, for GTRR applications, the KBE parameters overestimate the photoneutron contribution and simultaneously do not properly account for the enhanced importance of the standard delayed neutrons. Since, on the whole, the photoneutrons with which we are concerned here have longer half-lives than do the other delayed neutrons, KBE parameter calculations may be expected to accentuate the "sluggish" effect which photoneutrons have on reactor transients. With a given set of GTRR data, such as the RODCALIB data previously discussed, the KBE parameter calculation compensates for overestimated sluggishness by overestimating the reactivity.

The detection and data recording equipment employed in this work

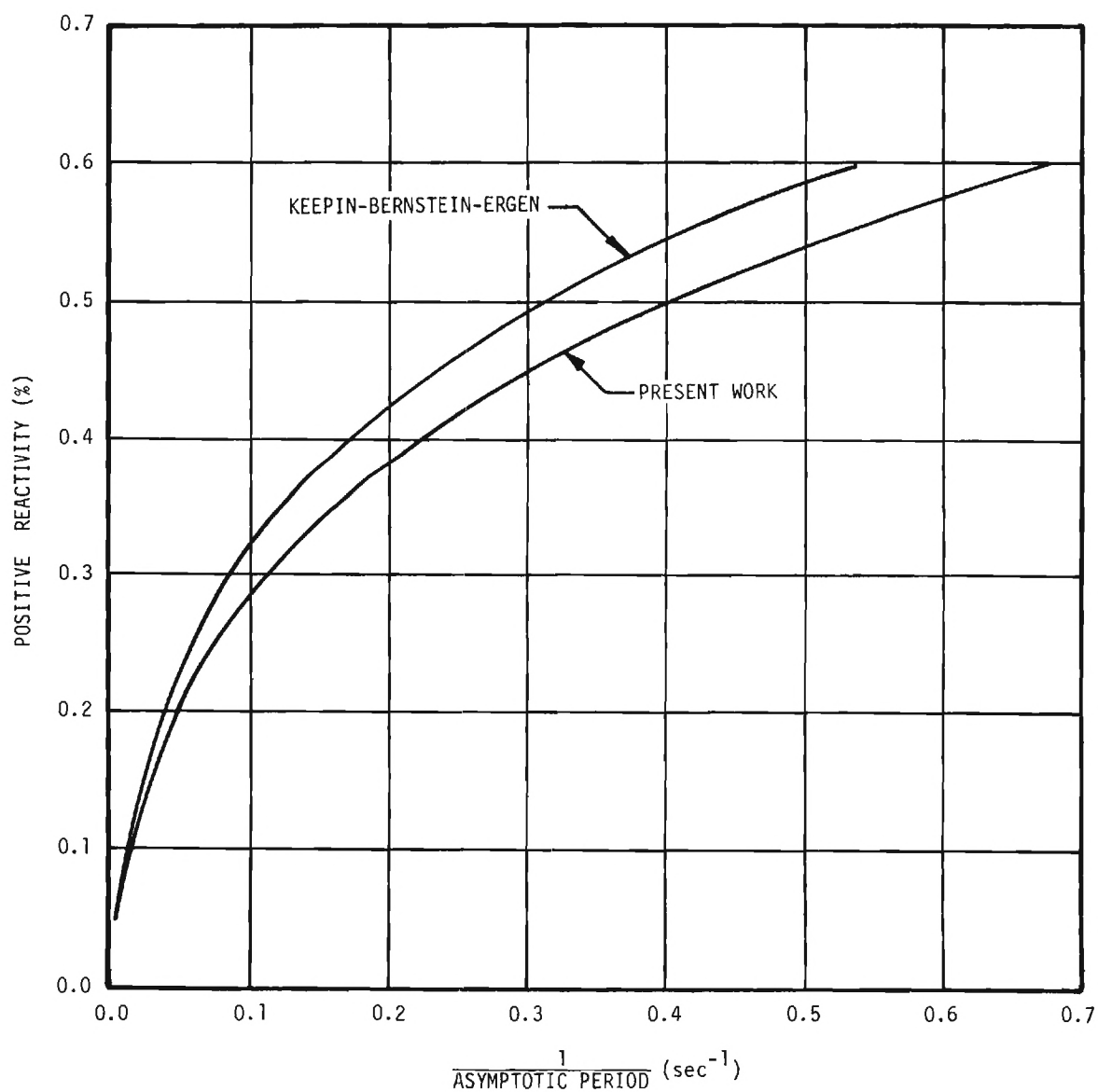


Figure 23. Positive Reactivity as a Function of the Reciprocal of Asymptotic Period Calculated by Using Previously Available and Present Work Parameters

were of the most modern design. Two different neutron detector types, a scintillation detector and a fission chamber, were used. Both detection systems possessed 530 nanosecond pulse resolution times. The experience of this work indicates no consistent advantage of one system over another as far as accuracy and reliability, although precise agreement of results between detectors would have more convincingly validated their equivalence. It is anticipated that, because of their different construction arrangements, the scintillation detector-preamplifier will be more readily affected by radiation damage, and thus have a shorter useful lifetime than the fission chamber assembly.

The purposes of this thesis as set down in Chapter I have been realized. The required number of delayed neutron groups was determined to be 12; relative abundances and decay constants have been provided. A comparison has been made between previously available and presently determined parameters. Furthermore, some of the methods which have been devised in this work offer prospects for useful application to other similar problems in the general area of reactor kinetics.

## CHAPTER VI

## RECOMMENDATIONS

An immediate extension of this work can be realized by repeating this experiment following higher power operation. The advantage in doing so is that improved statistical precision of data will result. The data collection system described in Chapter II has a resolving time of 530 nanoseconds. The limiting component is the multiscaler. It is anticipated that rather minor improvements of the fission chamber detector will provide for it a resolution of less than 100 nanoseconds. It is, therefore, recommended that this system be improved for higher count rates by the addition of appropriate fast prescalers between the discriminators and the multiscalers. As a matter of operational reliability and reproducibility, it is also recommended that automatic programming of the multiscaler channel dwell time selection be added to the existing equipment.

The values obtained for relative abundances of delayed neutron groups must be related to an appropriate total  $\beta_{\text{eff}}$ ,  $\sum_i \beta_{i,\text{eff}}$ , in order to be applied to kinetics calculations. A value has been determined in the small-sample experiments previously described which may or may not be appropriate. It is recommended that both calculation and experimental technique be applied to the determination of an absolute value of  $\beta_{\text{eff}}$  which is appropriate to a highly enriched heavy-water reactor. The calculational method might also yield values of relative abundance which could be compared with those obtained in the present work. In addition, if an independent experi-

mental value of the prompt neutron lifetime,  $\ell^*$ , were obtained, a direct comparison could be made with the parameter  $\beta_{\text{eff}}/\ell^*$  as obtained by both noise analysis and pile oscillator methods. The calculation of gamma-ray attenuation by the fuel element in the energy region above the 2.23 MeV threshold energy for photoneutron production in heavy water would provide additional understanding of the details of this process and permit more accurate prediction of the adjustment of abundance parameters necessary for different types of fuel elements.

This work has demonstrated the usefulness of the Variable Metric Minimization method for curve fitting. Methods for its efficient operation should be tested further and optimized techniques for speeding its convergence should be developed.

## APPENDICES



## APPENDIX A

## EXPERIMENTAL RESULTS

The following pages in this appendix include figures which illustrate the success of the curve-fitting operation for Tests A(s) and B(f). Flux decay data were actually accumulated over different time intervals,  $\Delta t_j$ , varying from 0.1 to 1100 seconds. These data values have been divided by the appropriate time,  $\Delta t_j$ , to obtain the count rates represented in Figures 24 and 25. The improved statistical precision associated with a higher total count is evident in these figures; as the collection time per channel increases in Figures 24 and 25, the actual count rates are more consistently described by the computed fit.

In Figures 26 and 27, the value of the weighted residual for each data point is plotted. This residual is the difference between the observed and computed-fit count, divided by the square root of the observed value. From these figures it may be seen that, in both of the tests illustrated, roughly two-thirds of the data points are within one standard deviation of the computed value, and the differences between actual and computed values are randomly positive and negative. If one were to square each of the values indicated in Figure 26, sum up these squares, and then divide by the number of data points (349) minus the number of parameters (26), the result would be the figure-of-merit,  $V$ , for this test.

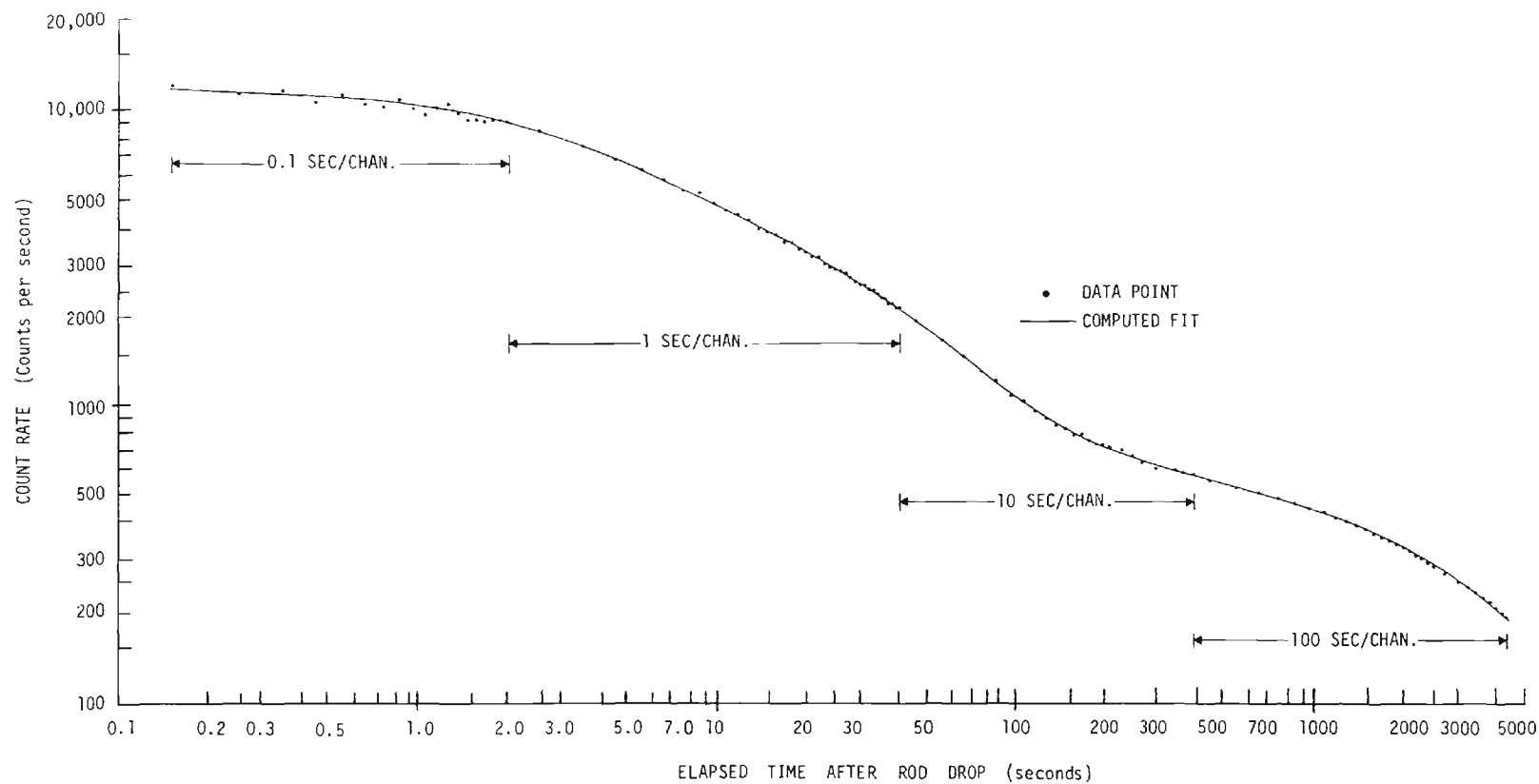


Figure 24a. Representation of Test A(s) Data and Calculated 13-Group Fit from 0.1 - 4000 Seconds (some data points omitted for clarity)

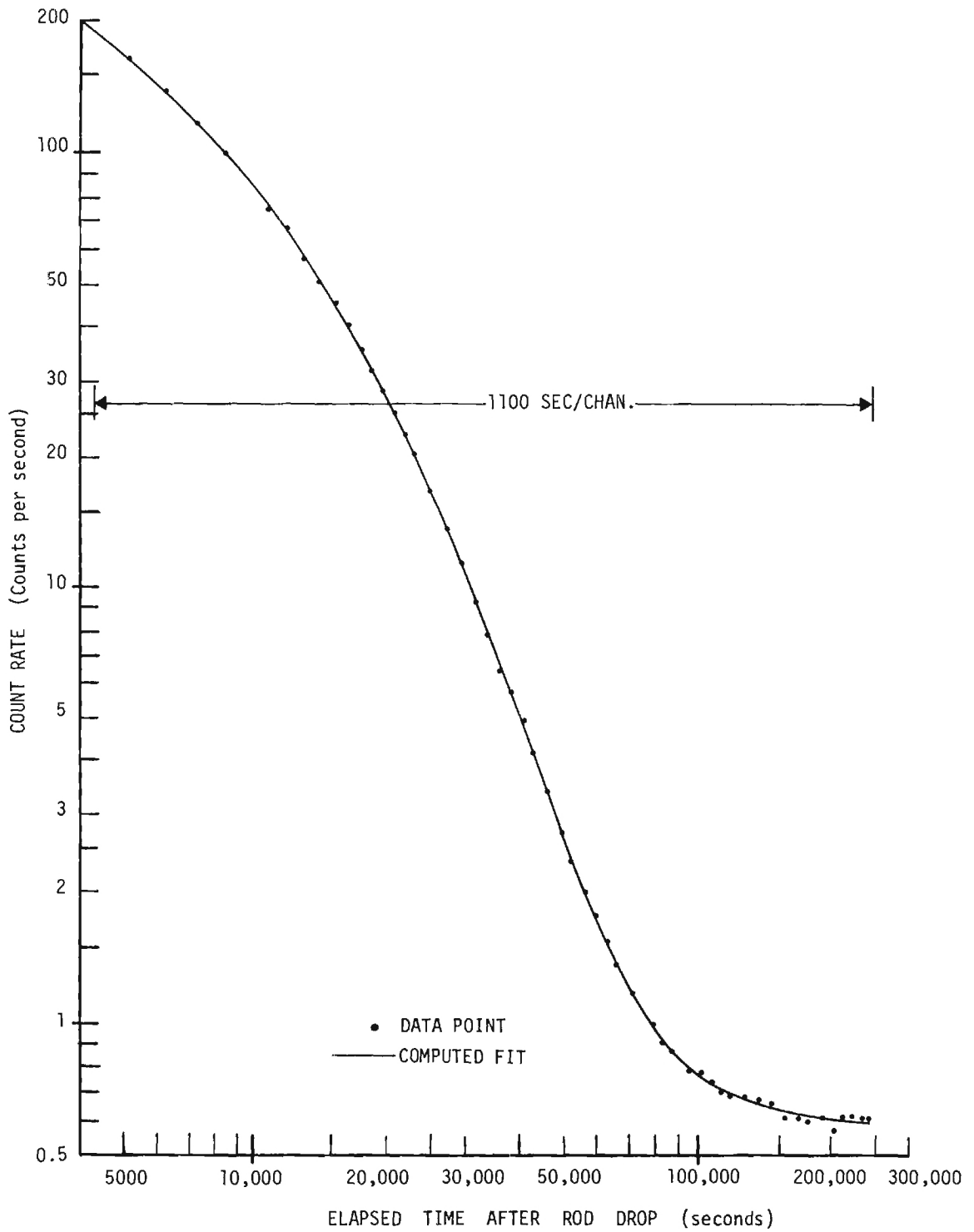


Figure 24b. Representation of Test A(s) Data and Calculated 13-Group Fit from 4000 - 250,000 Seconds (some data points omitted for clarity)

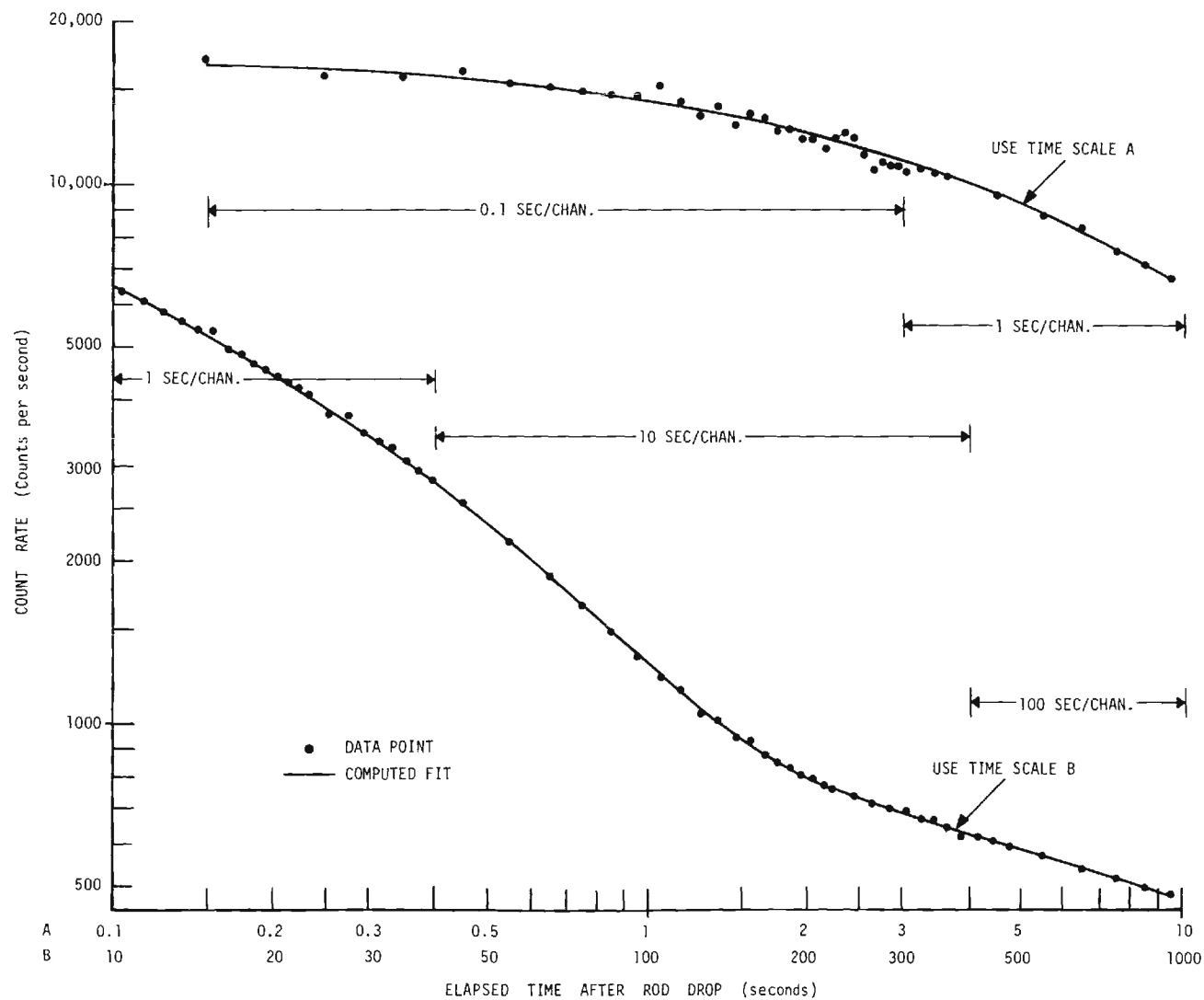


Figure 25a. Representation of Test B(f) Data and Calculated 13-Group Fit from 0.1 - 1000 Seconds (some data points omitted for clarity)

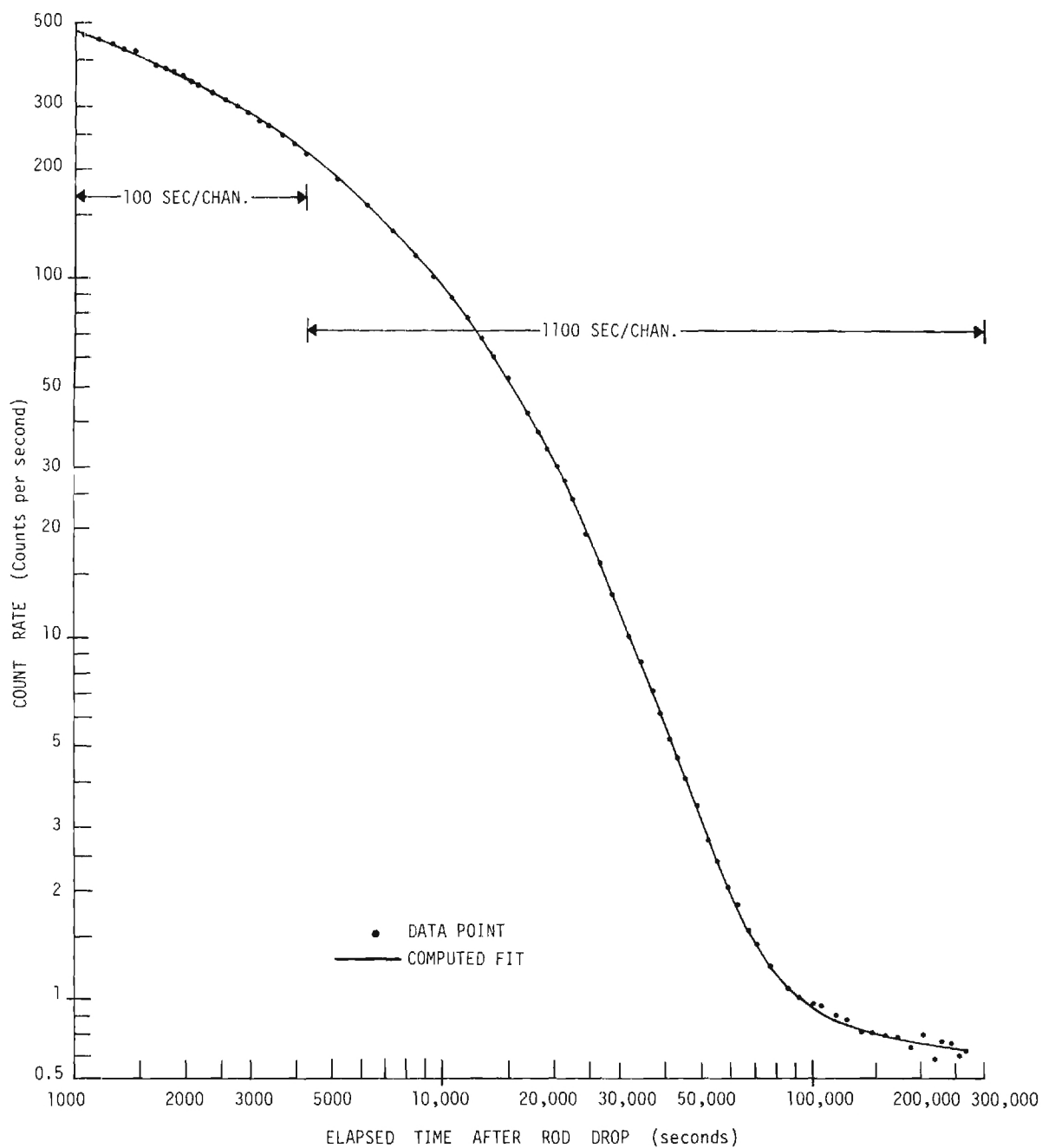


Figure 25b. Representation of Test B(f) Data and Calculated 13-Group Fit from 1000 - 275,000 Seconds (some data points omitted for clarity)

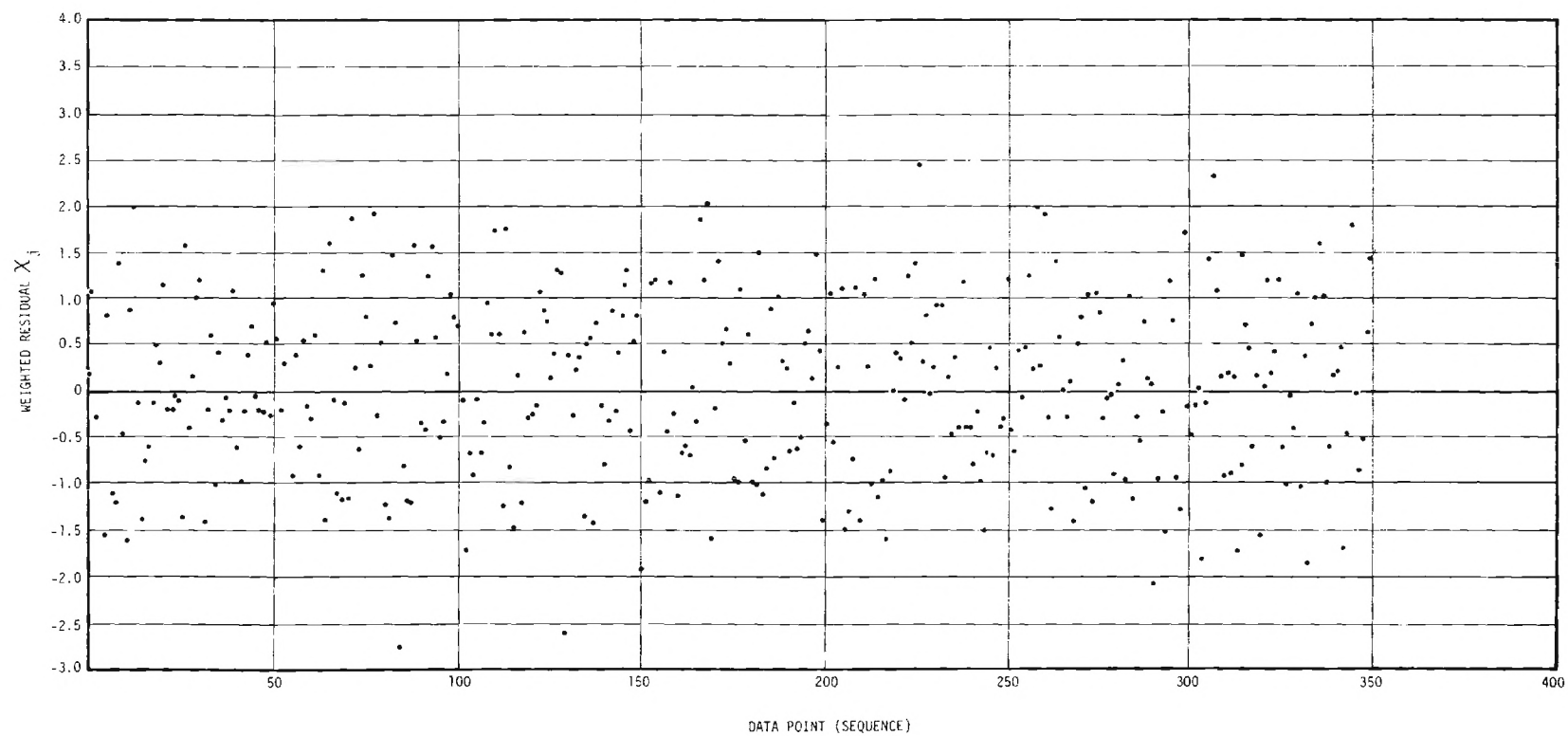


Figure 26. Test A(s) Residuals for Each Data Point in the 13-Group Fit

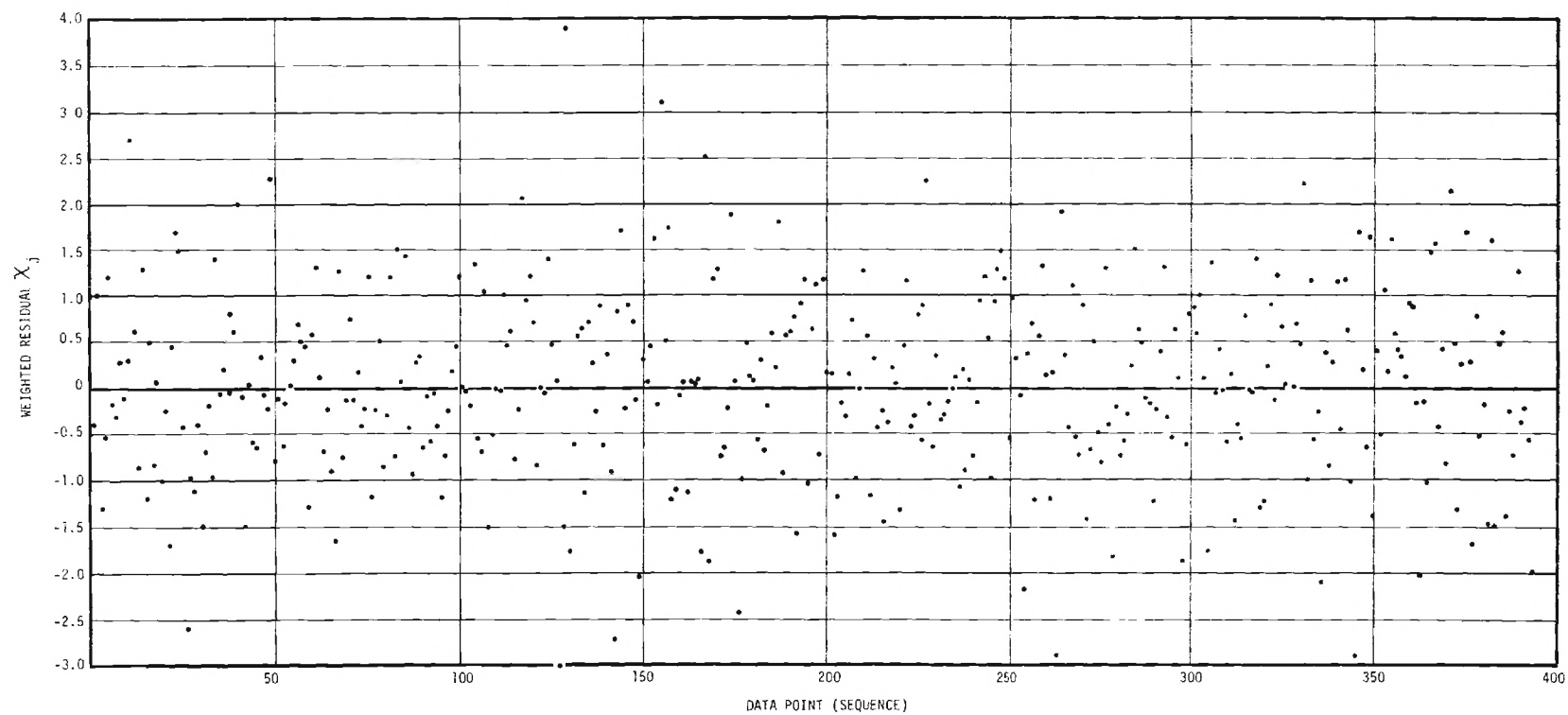


Figure 27. Test B(f) Residuals for Each Data Point in the 13-Group Fit



## APPENDIX B

## PROCEDURE BLDUP

BLDUP is a B-5500 computer program written in the ALGOL language. It analyzes the power history of the reactor from initial startup to any later time in order to assess the equilibrium fraction of delayed neutron precursors. This equilibrium fraction is expressed as a percent of the saturation value which is associated with the power level existing at the time of interest. In the work reported in this thesis, the time of interest is a specific rod drop time, or alternatively the time at which a control rod calibration by the digital method, RODCALIB,<sup>30</sup> was commenced.

The input data for this program include information taken from the log n recording of reactor power. The recorder receives its signal from a micromicroammeter which operates in conjunction with a compensated ionization chamber located in one of the reactor instrument positions. The ionization chamber is a General Electric Model No. GE-5467870-GR11; the micromicroammeter is General Electric Catalog No. 534E745G3.

Appropriate intervals of reactor operation as recorded on the log n chart are categorized by either exponential or linear approximations and the time and current values are recorded on coding sheets for punched card entries. The only other input quantities required are the decay constants of the delayed neutron precursors, which are determined by the Variable Metric Minimization curve fitting program.

To determine the sequential history of the reactor neutron population, we begin with the standard kinetics equation which describes the

change in delayed neutron precursor concentration with time at a fixed position in the reactor:

$$\frac{dC_i(t)}{dt} = -\lambda_i C_i(t) + \frac{k}{p} \beta_i \Sigma_a \phi(t)$$

By use of an integrating factor,  $e^{\lambda_i t}$ , this differential equation may be rewritten as

$$\frac{d[C_i(t) e^{\lambda_i t}]}{dt} = \frac{k}{p} \beta_i \Sigma_a \phi(t) e^{\lambda_i t}$$

and integrated to obtain

$$\int d[C_i(t') e^{\lambda_i t'}] = \int \frac{k}{p} \beta_i \Sigma_a \phi(t') e^{\lambda_i t'} dt'$$

Now we define  $C_i(t=0) = C_{i_0}$ , and  $t_d$  as the rod drop time of interest, and perform the integration,

$$C_i(t_d) = C_{i_0} e^{-\lambda_i t_d} + \frac{k}{p} \beta_i \Sigma_a e^{-\lambda_i t_d} \int_{t=0}^{t'=t_d} \phi(t') e^{\lambda_i t'} dt' \quad (3)$$

Now, the reference interval is that interval at level power immediately preceding the initiation of an experiment (e.g. rod drop). For the reference case  $\phi(t) = \phi^R$ , a constant. The equilibrium fraction desired for

each precursor is the number of precursor atoms present under actual conditions divided by the number that would have been present had the reactor been operating at the reference level for an infinite length of time.

Therefore we obtain the reference concentration,

$$C_i^R(t_d) = \frac{k}{p} \frac{\beta_i}{\lambda_i} \sum_a \phi^R \quad (4)$$

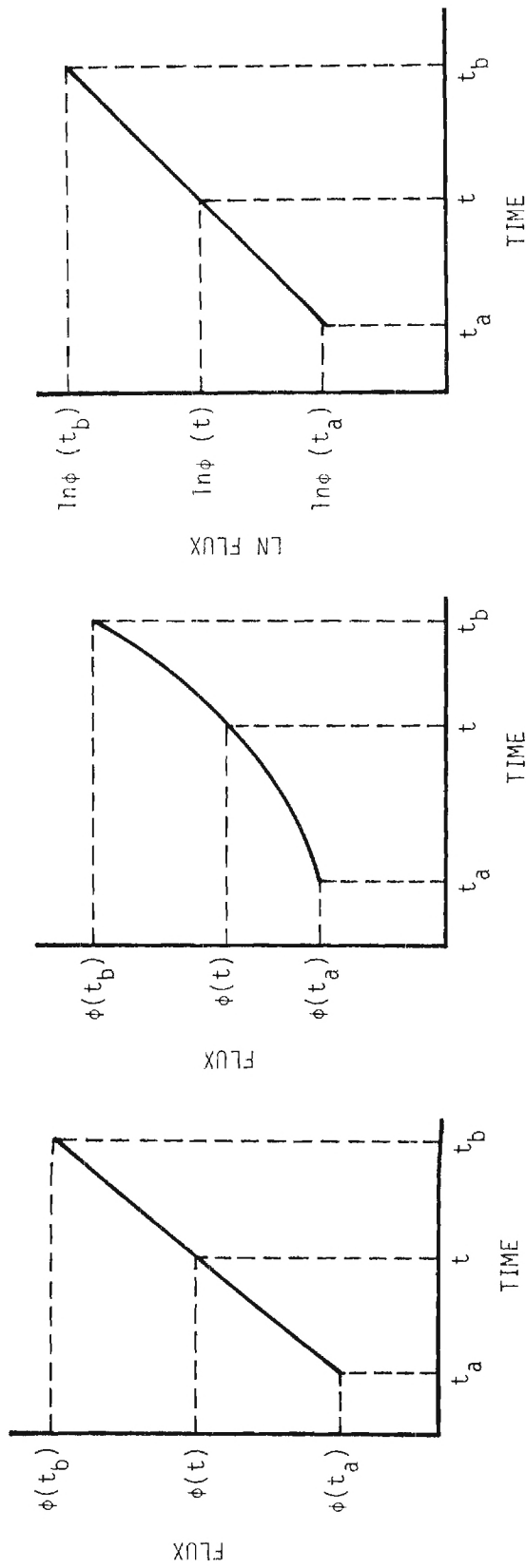
The actual concentration is expressed in Equation 3 above. The equilibrium fraction is:

$$Q_i(t_d) = \frac{C_i(t_d)}{C_i^R(t_d)} \quad (5)$$

The problem then reduces to one of finding the value of the integral in Equation 3 for the exponential or linear portions which make up the integral. In the linear case, referring to Figure 28a, we make the following formulation:

$$\frac{\phi(t) - \phi(t_a)}{t - t_a} = \frac{\phi(t_b) - \phi(t_a)}{t_b - t_a}$$

$$\phi(t) = \phi(t_a) + \frac{t - t_a}{t_b - t_a} [\phi(t_b) - \phi(t_a)]$$



a. Linear Flux Change Representation      b. Exponential Flux Change Representation      c. Logarithmic Representation of Exponential Flux Change

Figure 28. Standardized Approximations for Reactor Power-History Record

$$\phi(t) = \frac{t_b \phi(t_a) - t_a \phi(t_b)}{t_b - t_a} + \frac{[\phi(t_b) - \phi(t_a)] t}{t_b - t_a}$$

Evaluate  $\int_{t=t_a}^{t'=t_b} \phi(t') e^{\lambda_1 t'} dt'$ , with the substitution of  $\phi(t)$  developed

above for  $\phi(t')$  in the integral. Define the value of this integral to be  $L$ .

$$L = \frac{[t_b \phi(t_a) - t_a \phi(t_b)]}{t_b - t_a} \int_{t=t_a}^{t'=t_b} e^{\lambda_1 t'} dt' +$$

$$+ \frac{[\phi(t_b) - \phi(t_a)]}{t_b - t_a} \int_{t=t_a}^{t'=t_b} t' e^{\lambda_1 t'} dt'$$

$$L = \frac{[t_b \phi(t_a) - t_a \phi(t_b)]}{t_b - t_a} \frac{1}{\lambda_1} (e^{\lambda_1 t_b} - e^{\lambda_1 t_a}) +$$

$$+ \left\{ \frac{[\phi(t_b) - \phi(t_a)]}{(t_b - t_a)} \right\} \left\{ \frac{(t_b e^{\lambda_1 t_b} - t_a e^{\lambda_1 t_a})}{\lambda_1} + \frac{(e^{\lambda_1 t_a} - e^{\lambda_1 t_b})}{\lambda_1^2} \right\}$$

Similarly, in the exponential case illustrated in Figures 28b and 28c, we obtain the following representation:

$$\phi(t) = \phi(t_a) e^{\alpha(t - t_a)}$$

where  $\alpha$  is some appropriate coefficient to describe the exponential change.

Then

$$\ln \frac{\phi(t)}{\phi(t_a)} = \frac{t - t_a}{t_b - t_a} \ln \frac{\phi(t_b)}{\phi(t_a)}$$

$$\phi(t) = \phi(t_a) \left[ \frac{\phi(t_b)}{\phi(t_a)} \right]^{\frac{t - t_a}{t_b - t_a}}$$

Defining the value of the integral,

$$\int_{t=t_a}^{t'=t_b} \phi(t') e^{\lambda_i t'} dt'$$

as  $E$  in this exponential case, we obtain

$$E = \phi(t_a) \int_{t=t_a}^{t'=t_b} \left[ \frac{\phi(t_b)}{\phi(t_a)} \right]^{\frac{t' - t_a}{t_b - t_a}} e^{\lambda_i t'} dt'$$

We solve this by substitution as follows:

$$\text{Let } y = \frac{t'}{t_b - t_a} . \quad \text{Then } t' = y(t_b - t_a) \text{ and } dt' = (t_b - t_a)dy$$

$$E = \phi(t_a) \left[ \frac{\phi(t_b)}{\phi(t_a)} \right]^{\frac{-t_a}{t_b - t_a}} (t_b - t_a) \int_{y = \frac{t_a}{t_b - t_a}}^{y = \frac{t_b}{t_b - t_a}} \left[ \frac{\phi(t_b)}{\phi(t_a)} \right]^y e^{\lambda_i(t_b - t_a)y} dy$$

The integral is of the form,  $\int a^y e^{by} dy$ , or  $\int e^{y \ln a} e^{by} dy$ , which reduces to  $\int e^{(\ln a + b)y} dy$  and is integrated to produce

$$\left| \frac{e^{(\ln a + b)y}}{(\ln a + b)} \right|_{\frac{t_a}{t_b - t_a}}^{\frac{t_b}{t_b - t_a}}$$

Transforming back to the variables of interest and collecting terms, we obtain:

$$E = (t_b - t_a) \phi(t_a) \left[ \frac{1}{\ln \frac{\phi(t_b)}{\phi(t_a)} + \lambda_i(t_b - t_a)} \right] \left[ \frac{\phi(t_b)}{\phi(t_a)} e^{\lambda_i t_b} - e^{\lambda_i t_a} \right]$$

We have thus demonstrated the method for evaluating the integral in Equation 3 if the power history record is broken up into intervals approximating either linear or exponential changes in flux.

In evaluating Equations 3 and 4 it is not necessary to assess the value of the terms  $k$ ,  $p$ ,  $\beta_i$ , and  $\Sigma_a$  since they are always present in



both numerator and denominator. For the calculation from startup, the  $C_{i_0}$  values are all zero. For subsequent analyses, starting at the rod drop time of the previous analysis and calculating forward in time, the values of  $C_{i_0}$  are simply the values of  $C_i(t_d)$  which were calculated for the last rod drop time if the decay constants remain unchanged. It is evident that successive analyses must be contiguous in time.

The computer procedure, BLDUP, delivers in printed and punched form the values of equilibrium fractions according to Equation 5 and also punches the values of  $C_i(t_d)$  for use in the next succeeding analysis.

The listing of this procedure is reproduced, beginning on the following page.

```

COMMENT  B L O U P J
BEGIN FILE IN CARD 0 (2, 15) J %

FILE OUT PUNCH 0 (2, 10) J %
FILE OUT PRINT 1 (2, 15) J %
INTEGER NP, I, CONIND, TPREV, TCON, NOINT, K, TO, Z, M, TSTART,
INTEGER ARRAY TYPE (0 : 1022), T (0 : 1022),
REAL PHIO, SUMINT, FAC1, FAC2, FAC3, FAC5, FAC6, FAC7, L, E,
REAL ARRAY LAM (0 : 20), CZERO (0 : 20), PHI (0 : 1022), CR (0 :
20), THA (0 : 20), TIMIN (0 : 20), CT (0 : 20), EQFRAC (0 : 20),
LABEL L1, L8, L2, L3, L4, LA, L5, L6, L7,
ALPHA C1, C2, C3, C4, C5, C6, C7, C8, C9, C10, C11, C12, C13, C14,
FORMAT FL1 (

START OF SEGMENT ***** 0002
200 0005
300 0010
400 0015
500 0015
600 0019
700 0019
800 0025
900 0035
1000 0035
1100 0035

START OF SEGMENT ***** 0003
"      BLDUP, A H=5500 ALGOL PROCEDURE FOR CALCULATING THE
CONCENTRATION OF DELAYED NEUTRON PRECURSORS
", FL2 (14 A5), FL3 (/ / / "DATE OF THIS CALCULATION IS ", 14 A5
), FL4 (I10 / (6 E12, 5)), FL5 (" I          LAMBDA          "),
FL6 (/ X2, I2, X12, R10, 5), FL7 (3 I10), FL8 (/ /
" THE PREVIOUS BUILLOUP ANALYSIS ENDED AT ", I6, /
" THIS ANALYSIS BEGINS AT ", I6), FL9 (6 E12, 5), FL10 (I10), FL11
(I12, I12, R12, 4), FL12 (I10, R12, 4), FL13 (I10, X10, R12, 4),

0003 IS 0118 LONG, NEXT SEG 0002
1900 0035
2000 0052
2100 0058
2200 0069
2300 0077
2400 0086
2500 0094
2600 0104
2700 0110
2800 0116
2900 0123
3000 0131
3100 0143
3200 0153
3300 0156
3400 0159
3500 0163
3600 0167
3700 0171
3800 0175
3900 0184
4000 0188

LIST LIST1 (C1, C2, C3, C4, C5, C6, C7, C8, C9, C10, C11, C12, C13
, C14) J %
LIST LIST2 (NP, FOR I + 1 STEP 1 UNTIL NP DO LAM (I))
LIST LIST3 (I, LAM (I)) J %
LIST LIST4 (CONIND, TPREV, TCON) J %
LIST LIS5 (TPREV, TCON) J %
LIST LIST6 (FOR I + 1 STEP 1 UNTIL NP DO CZERO (I))
LIST LIST10 (NOINT) J %
LIST LIST11 (FOR K + 1 STEP 1 UNTIL NOINT DO (TYPE (K), T (K), PHI
(K))) J %
LIST LIST12 (TO, PHIO) J %
LIST LIST13 (FOR I + 1 STEP 1 UNTIL NP DO (I, EQFRAC (I)))
LIST LIST14 (FOR I + 1 STEP 1 UNTIL NP DO CT (I))
WRITE (PRINT (PAGE)) J %
WRITE (PRINT, FL1) J %
READ (CARD, FL2, LIST1) J %
WRITE (PRINT, FL3, LIST1) J %
READ (CARD, FL4, LIST2) J %
WRITE (PRINT, FL5) J %
FOR I + 1 STEP 1 UNTIL NP DO WRITE (PRINT, FL6, LIST3)
READ (CARD, FL7, LIST4) J %
WRITE (PRINT, FL8, LIST5) J %

```

READ (CARD, FL9, LIST6) ; %	4100	0191
READ (CARD, FL10, LIST10) ; %	4200	0195
READ (CARD, FL11, LIST11) ; %	4300	0199
READ (CARD, FL12, LIST12) ; %	4400	0203
FOR K + 1 STEP 1 UNTIL NUINT DO T [K] = T [K] * 60;	4500	0207
TD = TD * 60 ; %	4600	0218
I = 0 ; %	4700	0219
L1: I = I + 1 ; %	4800	0220
IF (I > NP) THEN GO TO L8 ; %	4900	0222
T [NUINT + 1] = TD ; %	5000	0223
PHI [NUINT + 1] = PHID ; %	5100	0225
CR [I] = (PHID / LAM [I]) ; %	5200	0227
THA [I] = 0.693 / LAM [I] ; %	5300	0229
TTMIN [I] = TD = 8 * THA [I] ; %	5400	0231
SUMINT = 0 ; %	5500	0233
Z = NUINT ; %	5600	0234
IF (TTMIN [I] ≤ TCON) THEN GO TO L4;	5700	0235
L2: IF (TTMIN [I] ≥ T [Z]) THEN GO TO L3;	5800	0236
Z = Z + 1 ; %	5900	0238
GO TO L2 ; %	6000	0240
L3: TSTART = T [Z] ; %	6100	0242
GO TO L4 ; %	6200	0243
L4: TSTART = TCON ; %	6300	0243
Z = 1 ; %	6400	0244
L4: FOR M + Z STEP 1 UNTIL NUINT DO	6500	0245
BEGIN IF (TYPE [M] ≠ 0) THEN GO TO L6;	6600	0247
L5: FAC1 = T [M + 1] - T [M] ; %	6700	0248
FAC2 = EXP (LAM [I] * (T [M + 1] - TD));	6800	0251
FAC3 = EXP (LAM [I] * (T [M] - TD));	6900	0254
FAC5 = (T [M + 1] * PHI [M] - T [M] * PHI [M + 1]) / FAC1;	7000	0257
FAC6 = FAC2 - FAC3 ; %	7100	0262
FAC7 = (PHI [M + 1] - PHI [M]) / FAC1;	7200	0263
L = FAC5 * FAC6 / LAM [I] + FAC7 * ((T [M + 1] * FAC2 - T [M] * FAC3) / LAM [I] - FAC6 / LAM [I] * LAM [I]);	7300	0266
SUMINT = SUMINT + L ; %	7400	0269
GO TO L7 ; %	7500	0274
L6: FAC1 = T [M + 1] - T [M] ; %	7600	0275
FAC2 = EXP (LAM [I] * (T [M + 1] - TD));	7700	0276
FAC3 = EXP (LAM [I] * (T [M] - TD));	7800	0278
FAC6 = LN (PHI [M + 1] / PHI [M]);	7900	0281
E = FAC1 * PHI [M] * (1 / (FAC6 + LAM [I] * FAC1)) * ((PHI [M + 1] / PHI [M]) * FAC2 - FAC3) ; %	8000	0284
SUMINT = SUMINT + E ; %	8100	0287
	8200	0290
	8300	0293

```

      L7:
END J %
CT [I] = CZERO [I] * EXP (- LAM [I] * (TSTART - TPREV)) + SUMINTJ
EQFRAC [I] = CT [I] / CR [I] J &
GD TO L1 J %
LR: WRITE (PRINT, FL13, LIST13) J %
WRITE (PUNCH, FL9, LIST14) J %
END.

```

```

8400 0295
8500 0295
8600 0297
8700 0301
8800 0304
8900 0304
9000 0308
9100 0312

```

## APPENDIX C

## RP-129 AND RODROP

RP-129 is a FORTRAN program which solves the one-group, space-independent reactor kinetics equations for neutron density if the reactor kinetics parameters and the excess reactivity as a function of time are given. A complete description of the method of solution is given by Kaganove.<sup>31</sup> This program has been translated into ALGOL for the B-5500. It permits several optional functional representations of reactivity as a function of time plus an interrupt feature which enables a redefining of reactivity function in the middle of the transient solution for neutron flux.

RP-129 has been modified somewhat in order to provide punched output which can be efficiently used in a second program, RODROP,<sup>32</sup> which has also been translated into ALGOL. RP-129 provides, at selected times, the relative neutron density and current value of delayed neutron precursor concentration. These quantities, along with the kinetics parameters, represent the input to RODROP. It is the purpose of RODROP to ascertain at what time during a non-instantaneous insertion of reactivity the instantaneous insertion of the same amount of reactivity would be most nearly equivalent, in terms of resulting neutron density.

Following the insertion of a fixed amount of reactivity,  $\Delta k$  remains constant, a static reactor configuration exists, and the reactor flux may

be expressed as

$$\phi(t) = \sum_{i=1}^N a_i e^{s_i(t-T)}$$

where  $T$  = reactivity insertion time

$t$  = elapsed time.

The  $s_i$  are inhour equation roots and are found in the same fashion as in References 8 and 37. The  $a_i$  may be calculated from the values of flux and precursor concentration provided by RP-129.

If the time for reactivity insertion is not instantaneous, the value of  $T$  to be used for calculational purposes is questionable, since neither the start of drop nor the stop of the drop are necessarily the "best time."

The conclusion that, for some long time after a reactivity insertion, instantaneous or otherwise, the detailed history of the insertion should have little effect on the flux leads to the proposal that a time  $T'$  be chosen such that

$$a_1 e^{s_1(t-T)} = a_1' e^{s_1(t-T')}$$

Here,  $s_1$  is the smallest in magnitude of the  $s_i$  (and is associated with the longest half-life of interest) and the  $a_1'$  is the coefficient which is found in the analysis of an instantaneous drop. The output of this program is the constructive time of insertion of a  $\Delta k$  in a stepwise manner which is most nearly equivalent at a later time to the true insertion. In investi-

gating results from these two programs, it has been found by Cohn<sup>32</sup> that, for a linear reactivity insertion, the ratio of  $T/T'$  is always less than 0.5 and approaches that maximum as the absolute value of the  $\Delta k$  decreases. The equivalent instantaneous drop flux predicted by the RODROP program is always less than that of the actual non-instantaneous insertion.

These programs in the ALGOL language are included for reference in the following pages.



COMMENT R P = 1 2 9 J		0000
BEGIN FILE OUT PUNCH 0 (2, 10) J %	100	0000
	START OF SEGMENT ***** 00n2	
FILE TAPE6 1 (2, 15) J %	200	0005
FILE TAPE7 0 (2, 15) J %	300	0010
BOOLEAN ARRAY SENSL (0 : 4) J %	400	0015
REAL Q, XPR J %	500	0017
INTEGER K J %	600	0017
REAL PROCEDURE INT (ARG1) J %	700	0017
VALUE ARG1 J %	800	0017
REAL ARG1 J %	900	0017
BEGIN INT = (SIGN (ARG1) * ENTIER (ABS (ARG1)))	1000	0017
END J %	1100	0020
REAL PROCEDURE MAX (ARG1, ARG2) J %	1200	0025
VALUE ARG1, ARG2 J %	1300	0025
REAL ARG1, ARG2 J %	1400	0025
BEGIN MAX = (IF ARG1 ≥ ARG2 THEN ARG1 ELSE ARG2)	1500	0025
END J %	1600	0027
REAL PROCEDURE MIN (ARG1, ARG2) J %	1700	0030
VALUE ARG1, ARG2 J %	1800	0030
REAL ARG1, ARG2 J %	1900	0030
BEGIN MIN = (IF ARG1 ≤ ARG2 THEN ARG1 ELSE ARG2)	2000	0030
END J %	2100	0032
PROCEDURE SRASYMPR (JREX, JALPHA, JMAXI, SVBETA, SVFLAM, JBETASU,	2200	0035
JVITA, JSOURCE) J %	2300	0035
INTEGER JMAXI J %	2400	0035
REAL JREX, JALPHA, JBETASU, JVITA, JSOURCEJ	2500	0035
REAL ARRAY SVBETA (0), SVFLAM (0)	2600	0035
BEGIN INTEGER JI J %	2700	0035
	START OF SEGMENT ***** 00n3	
REAL JN, JSUM, JALPHAG, JSUM2, JX, JYJ	2800	0000
LABEL DUMMY, L1, L10, L20 J %	2900	0000
IF JREX > 0 THEN GO TO L1 J %	3000	0000
JALPHA = 0 J %	3100	0001
GO TO DUMMY J %	3200	0002
COMMENT CALCULATE INITIAL GUESS BY EMPIRICAL FORMULAJ	3300	0002
L1: JR = 1 + JREX J %	3400	0002
JSUM = 0 J %	3500	0004
JJ = 1 J %	3600	0005
DO	3700	0005
BEGIN JSUM = JSUM + SVBETA (JJ) / SVFLAM (JJ)	3800	0005
END UNTIL (JJ + (JJ + 1)) > JMAXIJ	3900	0006
JALPHAG = JREX / (JVITA + JR * JSUM / (1 + (.2 * JREX / JBETASU)	4000	0010
* 2 / SQRT (JVITA))) J %	4100	0012

```

COMMENT ITERATE USING NEWTONS METHOD UNTIL 6 SIGNIFICANT FIGURES;
L10: JSUM = 0 ; *
JSUM2 = 0 ; *
JI = 1 ; *
DO
  BEGIN JX = 1 / (JALPHAG + SVFLAM [JI]);
    JY = SVBETA [JI] * SVFLAM [JI] * JX;
    JSUM = JSUM + JY ; *
    JSUM2 = JSUM2 + JY * JX
  END UNTIL (JI + (JI + 1)) > JMAX;
  JALPHA = JALPHAG = (JVITA * JALPHAG - JREX - JH * (JSUM -
    JBETASU)) / (JVITA + JH * JSUM2);
  IF (ABS ((JALPHA - JALPHAG) / JALPHA) < 1E-6) THEN GO TO DUMMY;
  JALPHAG = JALPHA ; *
  GO TO L10 ; *
L20: GO TO DUMMY ; *
DUMMY:
END ; *

0003 IS 0044 LONG, NEXT SEG 0002

PROCEDURE MAINPRU ; *
BEGIN REAL ARRAY ARRAY1 [0 : 10] ; *

START OF SEGMENT ***** 0004

DEFINE SVTESTO = ARRAY1 [0] ; *
DEFINE JT = ARRAY1 [1] ; *
DEFINE JALPHA = ARRAY1 [5] ; *
DEFINE JTHERM = ARRAY1 [4] ; *
DEFINE JPHI = ARRAY1 [3] ; *
DEFINE JREX = ARRAY1 [2] ; *
REAL ARRAY SVBETA [0 : 20], SVFLAM [0 : 20], SVCIDOT [0 : 20],
SVADENT [0 : 10], SVP [0 : 100], SVTLIM [0 : 20], SVTLIP [0 : 20],
SVRLTI [0 : 20], SVBLTI [0 : 20], SVC [0 : 20], SVPDT [0 :
100] ; *
INTEGER DX1 ; *
OWN INTEGER ASVKHTN ; *
INTEGER JIFBLAM, JNUMOPT, JICHECK, JINTRUP, JIFLAG, JIMAX, JI,
JNUMEXC, JJC, JINTM, JPRINT, JNUMREX, JNREAD, JK, JJ, JL;
REAL JMUERY, JBETASU, JTLAST, JVITA, JS, JEPSILO, JSUM, JRHO,
JSOURCE, JPERIOD, JENDOT, JENDUT2, JELTATC, JSTEPK, JPHIZ, JH,
JBLT, JSUMDOT, JSL, JTTEST, JT2, JRT2, JRISQR, JDELNM1, JDELNM2,
JT2L, JRLT2, JBLTVIT, JDELAT, JCBLT, JCBLT2, JCBLT3, JDELPHI,
JT1, JA, JB, JTRY, JDELK, JDELK3N, JX, JDELK1, JOK1, JOK2, JOK3;
COMMENT THE FOLLOWING SUBROUTINES ARE REQUIRED:
  SRASYMPN ; *
  FUMMAT FL1001 (2 I4, 10 A6, X9, 13), FL1 (/

```

START OF SEGMENT ***** 0005		
"JICHECK TEST FAILED"), FL1005 (112 / (6 R12, 1)), FL1015 (6	8400	0024
R12, 1), FL1060 (6 R12, 1), FL1080 (	8500	0024
" NP129 ONE GROUP, SPACE INDEPENDENT REACTOR KINETICS"), FL1085 (	8600	0024
/ " ", 10 A6), FL3003 (" " / 10 A6), FL1090 (/	8700	0024
" NUMBER OF PRECURSORS=", I2 / X15, "I", X11, "BETA", X10,	8800	0024
"LAMBDA", X7, "L*(C DOT)" / (I16, 3 R16, 5)), FL1095 (/ " ", X5,	8900	0024
"KEX(0-)", X7, "PERIOD(0-)", X6, "NDOT/N (0-)" / 3 R16, 5),	9000	0024
FL1100 (" ", X5, "WHERE NDOT/N (0-) WAS INPUT INFORMATION"),	9100	0024
FL1105 (" ", X5, "WHERE KEX(0-) WAS INPUT INFORMATION"), FL1110 (	9200	0024
" ", X5, "WHERE KEX(0-) AND THE CIONTS WERE INPUT INFORMATION"),	9300	0024
FL1115 (/ " ", X3, "INITIAL TIME", X4, "FINAL TIME", X8,	9400	0024
"SOURCE", X9, "LIFETIME" / 4 R16, 6), FL1200 (3 I12, 3 R12, 1),	9500	0024
FL1350 (/ " REACTIVITY OPTION", X7, I2 / " REACTIVITY STEP", X5,	9600	0024
R16, 6 / " INTERRUPT OPTION", X9, I2 / " INTERRUPT VALUE", R20,	9700	0024
6 / / " ", (6 R20, 6)), FL1355 (/ " DELTA T=", R12, 4,	9800	0024
"RESULTS PRINTED EVERY", I6, " STEPS."), FL1360 (/ " ", X8,	9900	0024
"TIME", X12, "FLUX", X10, "PERIOD", X9, "INTEGRAL N", X6,	10000	0024
"K EXCESS"), FL1480 (5 R16, 6), FL3001 (6 R20, 10), FL3002 (4	10100	0024
R20, 10) ; *	10200	0024
0005 IS 0233 LONG, NEXT SEG 0004		
LIST LIST1 (JIFBLAM, JNUMUPT, FOR DX1 + 1 STEP 1 UNTIL 10 DO	10300	0024
SVADENT (DX1), JICHECK) ; *	10400	0029
LIST LIST2 (JIMAX, FOR DX1 + 1 STEP 1 UNTIL JIMAX DO SVBETA (DX1	10500	0038
), FOR DX1 + 1 STEP 1 UNTIL JIMAX DO SVFLAM (DX1)) ;	10600	0042
LIST LIST3 (JT, JLAST, JVITA, JALPHA, JS, JPHI, JREX, JEPSILO);	10700	0054
LIST LIST4 (FOR DX1 + 1 STEP 1 UNTIL JIMAX DO SVCIDOT (DX1));	10800	0070
LIST LIST5 (FOR DX1 + 1 STEP 1 UNTIL 8 DO SVADENT (DX1));	10900	0080
LIST LIST6 (JIMAX, FOR DX1 + 1 STEP 1 UNTIL JIMAX DO (DX1,	11000	0090
SVBETA (DX1), SVFLAM (DX1), SVCIDOT (DX1));	11100	0095
LIST LIST7 (JREX, JPERIOD, JALPHA);	11200	0106
LIST LIST8 (JT, JLAST, JS, JVITA);	11300	0115
LIST LIST9 (JNUMEXC, JINTRUP, JJC, JELTATC, JQUERY, JSTEPK);	11400	0125
LIST LIST10 (FOR DX1 + 1 STEP 1 UNTIL JNREAD DO SVP (DX1));	11500	0138
LIST LIST11 (JNUMREX, JSTEPK, JINTRUP, JQUERY, FOR DX1 + 1 STEP	11600	0148
1 UNTIL JNHEAD DO SVP (DX1)) ; *	11700	0154
LIST LIST12 (JDELTAT, JPRINT) ; *	11800	0163
LIST LIST13 (JT) ; *	11900	0171
LIST LIST14 (JT, JPHI, JPERIOD, JTHERM, JREX);	12000	0178
LIST LIST15 (FOR DX1 + 1 STEP 1 UNTIL JIMAX DO SVC (DX1));	12100	0190
LIST LIST16 (JT, JMEX, JPHI, FOR DX1 + 1 STEP 1 UNTIL JIMAX DO	12200	0200
SVC (DX1)) ; *	12300	0207
LABEL L1, L2, L10, L15, L20, L30, L50, L60, L70, L100, L105,	12400	0214
L110, L115, L200, L210, L220, L235, L245, L5000, L5001, L5002,	12500	0214

L5003, L5050, L250, L300, L301, L302, L303, L304, L350, L400,	12600	0214
L406, L407, L420, L440, L446, L459, L460, L465, L480, L490,	12700	0214
L2100, L2101, L2102, L2103, L2200, L2210, L2215, L2104, L2105,	12800	0214
L2000, L2001, LEND, L71 ; %	12900	0214
SWITCH ASSIGN + L406, L407 ; %	13000	0214
SWITCH SWGD1 + L20, L30, L60 ; %	13100	0219
SWITCH SWGD2 + L100, L105, L110 ;	13200	0224
SWITCH SWGD3 + L5000, L5001, L5002, L5003 ;	13300	0229
SWITCH SWGD4 + L301, L302, L303, L304 ;	13400	0235
SWITCH SWGD5 + L2100, L2102, L2200, L2104 ;	13500	0241
SWITCH SWGD6 + L2101, L2103, L2200, L2105 ;	13600	0247
L1: READ (TAPE7, FL1001, LIST1) [LEND] ;	13700	0253
IF (JICHECK = 129) THEN GO TO L2 ;	13800	0259
GO TO L2001 ; %	13900	0260
L2: JINTRUP + 0 ; %	14000	0262
JIFLAG + 0 ; %	14100	0262
JQUERY + 0 ; %	14200	0263
IF (XPR + (JIFBLAM)) > 0 THEN GO TO L15 ;	14300	0264
IF XPR < 0 THEN GO TO L10 ; %	14400	0266
READ (TAPE7, FL1005, LIST2) ; %	14500	0267
JBETASU + SVBETA [1] ; %	14600	0271
JI + 2 ; %	14700	0272
DO	14800	0273
BEGIN JBETASU + JBETASU + SVBETA [JI]	14900	0273
END UNTIL (JI + (JI + 1)) > JIMAX ;	15000	0273
GO TO L15 ; %	15100	0276
L10: SVBETA [1] + .00025 ; %	15200	0279
SVBETA [2] + .00166 ; %	15300	0280
SVBETA [3] + .00213 ; %	15400	0281
SVBETA [4] + .00241 ; %	15500	0282
SVBETA [5] + .00085 ; %	15600	0284
SVBETA [6] + .00025 ; %	15700	0285
JBETASU + .00755 ; %	15800	0286
SVFLAM [1] + .01246 ; %	15900	0287
SVFLAM [2] + .0315 ; %	16000	0288
SVFLAM [3] + .1535 ; %	16100	0289
SVFLAM [4] + .456 ; %	16200	0291
SVFLAM [5] + 1.612 ; %	16300	0292
SVFLAM [6] + 14.3 ; %	16400	0293
JIMAX + 6 ; %	16500	0294
L15: READ (TAPE7, FL1015, LIST3) ;	16600	0295
JSUM + 0 ; %	16700	0300
GO TO SWGD1 [JNUMOPT] ; %	16800	0300
L20: JI + 1 ; %	16900	0302

DD	17000	0303
BEGIN JSUM = JSUM + SVBETA (JI) / (SVFLAM (JI) + JALPHA)	17100	0303
END UNTIL (JI + (JI + 1)) > JIMAX	17200	0305
JRHU = JALPHA * (JVITA + JSUM) / (JALPHA * JVITA + 1)	17300	0309
JREX = JRHU / (1 - JRHU) %	17400	0312
GO TO L50 %	17500	0315
L301 SHASMPR (JREX, JALPHA, JIMAX, SVBETA, SVFLAM, JBETASU,	17600	0329
JVITA, JSOURCE) %	17700	0332
L501 JI + 1 %	17800	0333
DD	17900	0333
BEGIN SVCIDOT (JI) = SVBETA (JI) * JPHI * JALPHA * (1 + JREX) / (	18000	0333
SVFLAM (JI) + JALPHA)	18100	0337
END UNTIL (JI + (JI + 1)) > JIMAX	18200	0338
GO TO L70 %	18300	0341
L601 READ (TAPE7, FL1060, LIST4)	18400	0342
JSUM = SVCIDOT (1) %	18500	0347
JI + 2 %	18600	0348
DD	18700	0348
BEGIN JSUM = JSUM + SVCIDOT (JI)	18800	0348
END UNTIL (JI + (JI + 1)) > JIMAX	18900	0349
JALPHA = (JREX - JSUM / JPHI) / JVITA	19000	0352
L701 IF JALPHA = 0.0 THEN GO TO L71	19100	0355
JPERIOD = 1 / JALPHA %	19200	0357
L711 JENDOT = JPHI * JALPHA %	19300	0359
JENDOT2 = JALPHA * JENDOT %	19400	0360
WRITE (TAPE6, FL1080) %	19500	0362
WRITE (TAPE6, FL1085, LIST5) %	19600	0365
WRITE (PUNCH, FL3003, LIST5) %	19700	0369
WRITE (TAPE6, FL1090, LIST6) %	19800	0373
WRITE (TAPE6, FL1095, LIST7) %	19900	0377
GO TO SWGD2 (JNUMOPT) %	20000	0380
L1001 WRITE (TAPE6, FL1100) %	20100	0382
GO TO L115 %	20200	0386
L1051 WRITE (TAPE6, FL1105) %	20300	0388
GO TO L115 %	20400	0391
L1101 WRITE (TAPE6, FL1110) %	20500	0392
L1151 WRITE (TAPE6, FL1115, LIST8)	20600	0395
L2001 READ (TAPE7, FL1200, LIST9)	20700	0399
JPHI2 = JPHI %	20800	0404
JINTM = - JINTHUP %	20900	0405
IF (JNUMEXC + JINTRUP + JJC) # 0 THEN GO TO L210	21000	0406
IF (JELTATC + JQUERY + JSTEPK) = 0 THEN GO TO L1	21100	0408
L2101 IF (XPR + (JJC)) = 0 THEN GO TO L220	21200	0410
IF XPR < 0 THEN GO TO L1 %	21300	0412

JJPRINT + JJC / %	21400	0414
L220: IF JSTEPK = 0 THEN GO TO L235;	21500	0414
JREX + JREX + JSTEPK / %	21600	0414
JW + JPHI * JSTEPK / %	21700	0418
JI + 1 / %	21800	0419
DO	21900	0420
BEGIN SVCIDOT [JI] + SVCIDOT [JI] + SVBETA [JI] * JW	22000	0420
END UNTIL (JI + (JI + 1)) > JIMAX;	22100	0422
JALPHA + JALPHA + (1 - JBETASU) * JSTEPK / JVITA;	22200	0425
IF JALPHA = 0.0 THEN GO TO L235;	22300	0429
JPERIOD + 1 / JALPHA / %	22400	0430
L235: IF JNUMEXC # 0 THEN GO TO L245;	22500	0432
IF (XPM + (JELTATC)) > 0 THEN GO TO L250;	22600	0433
IF XPR = 0 THEN GO TO L350 ELSE GO TO L1;	22700	0435
L245: JNUMREX + JNUMEXC / %	22800	0436
GO TO SWG03 [JNUMREX] / %	22900	0437
L5000: JNREAD + 2 / %	23000	0439
GO TO L5050 / %	23100	0440
L5001: JNREAD + 8 / %	23200	0443
GO TO L5050 / %	23300	0443
L5002: JNREAD + 3 / %	23400	0444
GO TO L5050 / %	23500	0445
L5003: JNREAD + 3 / %	23600	0446
L5050: READ (TAPE/, FL1060, LIST10);	23700	0447
IF (XPM + (JELTATC)) * 0 THEN GO TO L300;	23800	0452
IF XPR < 0 THEN GO TO L1 / %	23900	0453
L250: JBLT + 0 / %	24000	0455
JSUMDOT + 0 / %	24100	0455
JSL + JS * JVITA / %	24200	0456
JTTEST + JTLAST - .0005 * JELTATC;	24300	0457
JT2 + 0.5 * JELTATC / %	24400	0459
JR12 + 0.5 / JELTATC / %	24500	0460
JR15GR + 1 / JELTATC * 2 / %	24600	0462
JDELNM1 + JELTATC * (JENDOT - 0.5 * JELTATC * JENDOT2);	24700	0463
JDELNM2 + JELTATC * (JENDOT - 1.5 * JELTATC * JENDOT2);	24800	0466
JI + 1 / %	24900	0469
DO	25000	0470
BEGIN JT2L + JT2 * SVFLAM [JI] / %	25100	0470
SVTLIM [JI] + 1 = JT2L / %	25200	0471
SVTLIP [JI] + 1 + JT2L / %	25300	0473
SVRLTI [JI] + 1 / SVTLIP [JI];	25400	0475
JSUMDOT + JSUMDOT + SVCIDOT [JI] * SVRLTI [JI];	25500	0477
SVBLTI [JI] + SVBETA [JI] * SVRLTI [JI];	25600	0479

JBLT = JBLT + SVBLT1 / J11 / %	25700	0481
END UNTIL (JJ + (J1 + 1)) > JIMAX	25800	0483
JBLT2 = 0.5 * JBLT / %	25900	0485
JBLTVIT = JBLT2 + JVITA / JELTATC	26000	0486
JCBLT = 1 - JBLT / %	26100	0488
JCBLT2 = 0.5 * JCBLT / %	26200	0489
JCBLT3 = 0.333333333333 * JCBLT	26300	0490
JDELPHI = JELTATC * (JENDUT + JENDUT2 * JT2)	26400	0492
JDELTAT = JELTATC / %	26500	0494
L300: GO TO SWG04 [JNUMREX] / %	26600	0495
L301: SVPDT [1] = SVP [1] * JDELTAT	26700	0497
SVPDT [2] = SVP [2] * JDELTAT / %	26800	0499
SVPDT [3] = SVPDT [2] * 0.5 / %	26900	0501
GO TO L350 / %	27000	0503
L302: SVPDT [1] = ((SVP [4] * JDELTAT + SVP [3]) * JDELTAT +	27100	0509
SVP [2]) * JDELTAT + SVP [1]) * JDELTAT	27200	0511
SVPDT [2] = ((SVP [4] * 4 * JDELTAT + 3 * SVP [3]) * JDELTAT + 2	27300	0514
* SVP [2]) * JDELTAT / %	27400	0518
SVPDT [3] = (SVP [4] * 6 * JDELTAT + 3 * SVP [3]) * JDELTAT	27500	0520
SVPDT [4] = SVP [4] * 4 * JDELTAT	27600	0525
SVPDT [5] = SVP [5] * JDELTAT / %	27700	0527
SVPDT [6] = SVP [6] * 2 * JDELTAT	27800	0529
SVPDT [7] = SVP [7] * 3 * JDELTAT	27900	0532
SVPDT [8] = SVP [8] * 4 * JDELTAT	28000	0534
SVPDT [9] = SVP [6] * JDELTAT * JDELTAT	28100	0537
SVPDT [10] = SVPDT [7] * JDELTAT	28200	0539
SVPDT [11] = SVPDT [8] * 1.5 * JDELTAT	28300	0541
SVPDT [12] = SVPDT [10] * .3333333333 * JDELTAT	28400	0544
SVPDT [13] = SVPDT [11] * .66666666667 * JDELTAT	28500	0546
SVPDT [14] = SVPDT [13] * .25 * JDELTAT	28600	0549
JT1 = 0 / %	28700	0551
GO TO L350 / %	28800	0552
L303: SVPDT [1] = SVP [1] * JDELTAT	28900	0557
GO TO L350 / %	29000	0559
L304: SVPDT [1] = 2 * SVP [1] * SIN (SVP [3] * JDELTAT * 0.5)	29100	0559
SVPDT [2] = SVP [2] * JDELTAT / %	29200	0564
SVPDT [3] = SVPDT [2] * 0.5 / %	29300	0566
SVPDT [4] = SVP [3] * JDELTAT * 0.5	29400	0568
L350: WRITE (TAPE6, FL1350, LIST1)	29500	0570
WRITE (TAPE6, FL1355, LIST2) / %	29600	0574
WRITE (TAPE6, FL1360) / %	29700	0578
L400: JK = 1 / %	29800	0582



DD	29900	0582
BEGIN JJ + 1 ; %	30000	0582
DD	30100	0583
BEGIN JA + JPHI * JREX = JSUMDOT + JSL	30200	0583
JB + JPHI * JCBLT2 ; %	30300	0586
SVC [1] + JBLTVIT = JREX * JCBLT2 ;	30400	0587
ASVKHTN + 1 ; %	30500	0590
GO TO SWG05 [JNUMREX] ; %	30600	0591
L406: ASVKRTN + 2 ; %	30700	0593
JL + 1 ; %	30800	0593
DD	30900	0594
BEGIN JTRY + JOELK ; %	31000	0594
JOELPHI + (JA + JB * JTRY) / (SVC [1] - JCBLT3 * JTRY) ;	31100	0595
GO TO SWG06 [JNUMREX] ; %	31200	0598
L407: IF (ABS (JTRY - JOELK) ≤ JEPSILO) THEN GO TO L420 ;	31300	0600
END UNTIL (JL + (JL + 1)) > 100 ;	31400	0603
WRITE (TAPE6, FL1015, LIST13) ;	31500	0605
JIFLAG + 1 ; %	31600	0609
GO TO L465 ; %	31700	0610
L420: JOELPHI + (JA + JB * JOELK) / (SVC [1] - JCBLT3 * JOELK) ; %	31800	0612
JOELK3N + 0.333333333333 * JOELK * JOELPHI ;	31900	0614
JTHERM + JTHERM + (JPHI + JOELPHI * 0.5) * JOELTAT ;	32000	0615
JSUMDOT + 0 ; %	32100	0617
JX + JOELK * JPHI + (1 + JREX + 0.666666666666 * JOELK) * JOELPHI ; %	32200	0621
JX + JOELK * JPHI + (1 + JREX + 0.666666666666 * JOELK) * JOELPHI ; %	32300	0621
JX + JOELK * JPHI + (1 + JREX + 0.666666666666 * JOELK) * JOELPHI ; %	32400	0624
JX + JOELK * JPHI + (1 + JREX + 0.666666666666 * JOELK) * JOELPHI ; %	32500	0626
DD	32600	0626
BEGIN SVCIDOT [JI] + (SVBETA [JI] * (JX + SVTLIP [JI] * JOELK3N) + SVCIDOT [JI] * SVTLIM [JI]) * SVRLTI [JI] ;	32700	0626
JSUMDOT + JSUMDOT + SVCIDOT [JI] * SVRLTI [JI] ;	32800	0628
END UNTIL (JI + (JI + 1)) > JIMAX ;	32900	0632
JREX + JREX + JOELK ; %	33000	0634
JPHI + JPHI + JOELPHI ; %	33100	0636
JPHI + JPHI + JOELPHI ; %	33200	0638
JOELNM2 + JOELNM1 ; %	33300	0640
JOELNM1 + JOELPHI ; %	33400	0641
JENDOT + (3 * JOELNM1 - JOELNM2) * JRT2 ;	33500	0642
JENDOT2 + (JOELNM1 - JOELNM2) * JRTSQR ;	33600	0644
JALPHA + JENDOT / JPHI ; %	33700	0646
JOELPHI + 2 * JOELNM1 - JOELNM2 ;	33800	0648
JT + JT + JOELTAT ; %	33900	0650
JT1 + JT1 + JOELTAT ; %	34000	0652
IF (JT < JTTEST) THEN GO TO L440 ;	34100	0653

JIFLAG ← 1 ; %	34200	0654
GO TO L465 ; %	34300	0655
L440: IF (XPR + (JINTRUP)) = 0 THEN GO TO L460;	34400	0660
IF XPR < 0 THEN GO TO L446 ; %	34500	0661
IF (SVTESTO (JINTRUP) ≥ JQUERY) THEN GO TO L459 ELSE GO TO	34600	0663
L460 ; %	34700	0664
L446: IF (SVTESTO (JINTM) > JQUERY) THEN GO TO L460;	34800	0665
L459: JIFLAG ← 1 ; %	34900	0666
GO TO L465 ; %	35000	0667
L460:	35100	0668
END UNTIL (JJ + (JJ + 1)) > JJPRINT;	35200	0669
L465: JPERIOD ← 1 / JALPHA ; %	35300	0671
WRITE (TAPE6, FL1480, LIST14);	35400	0673
J1 ← 1 ; %	35500	0677
DO	35600	0678
BEGIN SVC (J1) + ((1 + JREX) × SVBETA (J1) × JPHI = SVCIDDT [	35700	0678
J1]) / (JVITA × SVFLAM (J1))	35800	0681
END UNTIL (J1 + (J1 + 1)) > JIMAX;	35900	0682
WRITE (TAPE6, FL3001, LIST15);	36000	0685
WRITE (PUNCH, FL3002, LIST16);	36100	0689
IF JIFLAG ≠ 0 THEN GO TO L480;	36200	0693
END UNTIL (JK + (JK + 1)) > 1000;	36300	0694
L480: IF (XPR + (JIFLAG)) > 0 THEN GO TO L490;	36400	0696
IF XPR = 0 THEN GO TO L400 ; %	36500	0698
JIFLAG ← 0 ; %	36600	0700
GO TO L1 ; %	36700	0700
L490: JIFLAG ← 0 ; %	36800	0701
GO TO L200 ; %	36900	0702
L2100: JDELK1 ← SVPDT [1] + SVPDT [2] × JPHI;	37000	0703
L2101: JDELK ← JDELK1 + SVPDT [3] × JDELPHI;	37100	0706
GO TO L2000 ; %	37200	0709
L2102: JDELK1 ← ((SVPDT [4] × JT1 + SVPDT [3]) × JT1 + SVPDT [2]	37300	0709
) × JT1 + SVPDT [1] ; %	37400	0712
JDK1 ← ((SVPDT [8] × JTHERM + SVPDT [7]) × JTHERM + SVPDT [6]) ×	37500	0714
JTHERM + SVPDT [5] ; %	37600	0718
JDK2 ← (SVPDT [11] × JTHERM + SVPDT [10]) × JTHERM + SVPDT [9];	37700	0720
JDK3 ← SVPDT [13] × JTHERM + SVPDT [12];	37800	0724
L2103: JX ← JPHI + 0.5 × JDELPHI;	37900	0726
JDELK ← JDELK1 + JX × ((JX × SVPDT [14] + JDK3) × JX + JDK2) ×	38000	0729
JX + JDK1 ; %	38100	0732

GO TO L2000 ; *	38200	0734
L2200: JX = JOELPHI / JPHI ; *	38300	0736
IF (ABS (JX) < .01) THEN GO TO L2210;	38400	0737
JX = SVP [2] * LN (1 + JX) ; *	38500	0739
GO TO L2215 ; *	38600	0741
L2210: JX = JX * (1 + JX * (= .5 + JX * (.3333333333333333 - .25 * JX))) * SVP [2] ; *	38700	0743
L2215: JOELK = (ABS (SVPDT [1]) * SIGN (SVP [3] - JT)) + JX;	38800	0745
L2104: JOELK1 = SVPDT [1] * COS (SVP [3] * JT + SVPDT [4]) + SVPDT [2] * (JPHI - JPHIZ) ; *	38900	0748
L2105: JOELK = JOELK1 + SVPDT [3] * JOELPHI;	39000	0754
L2000: GO TO ASSIGN (ASVKRTN) ; *	39100	0757
L2001: WRITE (TAPE6, FL1) ; *	39200	0759
LEND:	39300	0762
END ; *	39400	0764
	39500	0767
	39600	0768

0004 IS 0798 LONG, NEXT SEG 0002

COMMENT INITIALIZING BLOCK ; *	39700	0035
XPR = Q + K + 0 ; *	39800	0035
SENSL [1] = FALSE ; *	39900	0036
SENSL [2] = FALSE ; *	40000	0038
SENSL [3] = FALSE ; *	40100	0039
SENSL [4] = FALSE ; *	40200	0040
MAIVPRO END.	40300	0041

COMMENT	R O D R O P J	
BEGIN FILE TAPE6 1 (2, 15) J %	100	0000
		START OF SEGMENT ***** 0002
FILE TAPE7 0 (2, 15) J %	200	0005
FILE XXXXXX 2 (2, 15) J %	300	0010
SWITCH FILE FILES# + XXXXXX, XXXXXX, XXXXXX, XXXXXX, XXXXXX,	400	0015
XXXXXX, TAPE6, TAPE7 J %	500	0023
BOOLEAN ARRAY SENSL [0 : 4], SENSW [0 : 6];	600	0027
REAL ARRAY SVDC [0 : 20], SVBETA [0 : 20], SVS [0 : 21], SVBSD [0	700	0031
: 21, 0 : 20], SVBDD [0 : 21, 0 : 20];	800	0037
INTEGER JN J %	900	0041
INTEGER K J %	1000	0041
REAL JPNL J %	1100	0041
REAL Q, XPR J %	1200	0041
LABEL FINIS J %	1300	0041
FORMAT F ( / / / / / "STOP / PAUSE NO. ", I5)	1400	0041
		START OF SEGMENT ***** 0003
		0003 IS 0013 LONG, NEXT SEG 0002
REAL PROCEDURE INT (ARG1) J %	1500	0041
VALUE ARG1 J %	1600	0041
REAL ARG1 J %	1700	0041
INT + SIGN (ARG1) * ENTIER (ABS (ARG1));	1800	0041
REAL PROCEDURE TANH (ARG1) J %	1900	0049
VALUE ARG1 J %	2000	0049
REAL ARG1 J %	2100	0049
TANH + ((1 + EXP (ARG1 * 2)) - 1) / (1 + 1);	2200	0049
REAL PROCEDURE MAX (ARG1, ARG2) J %	2300	0055
VALUE ARG1, ARG2 J %	2400	0055
REAL ARG1, ARG2 J %	2500	0055
MAX + IF ARG1 ≥ ARG2 THEN ARG1 ELSE ARG2;	2600	0055
REAL PROCEDURE MIN (ARG1, ARG2) J %	2700	0060
VALUE ARG1, ARG2 J %	2800	0060
REAL ARG1, ARG2 J %	2900	0060
MIN + IF ARG1 ≤ ARG2 THEN ARG1 ELSE ARG2;	3000	0060
REAL PROCEDURE DIM (ARG1, ARG2) J %	3100	0065
VALUE ARG1, ARG2 J %	3200	0065
REAL ARG1, ARG2 J %	3300	0065
DIM + MAX (ARG1 - ARG2, 0) J %	3400	0065
PROCEDURE ERROR (ARG1) J %	3500	0069
VALUE ARG1 J %	3600	0069
REAL ARG1 J %	3700	0069
BEGIN WRITE (TAPE6, F, ARG1) J %	3800	0069
GO TO FINIS	3900	0077
END J %	4000	0078

PROCEDURE SRROUTIN (JK) ; %	4100	0080
VALUE JR ; %	4200	0080
REAL JR ; %	4300	0080
BEGIN INTEGER JNA, JK, JJ, JI, JI;	4400	0080
	START OF SEGMENT *****	0004
REAL JRHO, JRHOFS, JSD, JOEV, JPREDEV, JU, JV, JRHOQT, JDELTA;	4500	0000
LABEL L7, L139, L17, L19, L23, L20, L26, L250, L134;	4600	0000
JNA + JN + 1 ; %	4700	0000
JRHO + JR ; %	4800	0001
SVS [1] + 0 ; %	4900	0002
JK + 2 ; %	5000	0003
DO	5100	0004
BEGIN SVS [JK] + = (SVDC [JK] + SVDC [JK - 1]) / 2	5200	0004
END UNTIL (JK + (JK + 1)) > JN ; %	5300	0006
SVS [JNA] + = (1 / JPNL + SVDC [JN]) / 2;	5400	0009
JJ + 1 ; %	5500	0013
DO	5600	0013
BEGIN JI + 1 ; %	5700	0013
L7: JRHOFS + 0 ; %	5800	0014
JI + 1 ; %	5900	0015
DO	6000	0016
BEGIN JSD + SVS [JJ] + SVDC [JI];	6100	0016
SVBSD [JJ, JI] + SVBETA [JI] / JSD;	6200	0018
SVBOD [JJ, JI] + SVBSD [JJ, JI] / JSD;	6300	0021
JRHOFS + JRHOFS + SVBSD [JJ, JI];	6400	0024
END UNTIL (JI + (JI + 1)) > JN;	6500	0026
JRHOFS + SVS [JJ] * (JPNL + JRHOFS) / (1 + JPNL * SVS [JJ]);	6600	0029
JOEV + JRHOFS - JRHO ; %	6700	0032
IF NOT (JIT > 1) THEN GO TO L139;	6800	0034
IF (XPR + (JOEV * JPREDEV)) = 0 THEN GO TO L134;	6900	0035
IF XPR < 0 THEN GO TO L139 ; %	7000	0037
IF NOT (ABS (JOEV) < ABS (JPREDEV)) THEN GO TO L134;	7100	0038
L139: IF NOT (JIT < 100) THEN GO TO L134;	7200	0040
JPREDEV + JOEV ; %	7300	0042
JIT + JIT + 1 ; %	7400	0043
JU + 0 ; %	7500	0044
JV + 0 ; %	7600	0045
JI + 1 ; %	7700	0045
DO	7800	0046
BEGIN JU + JU + SVBSD [JJ, JI];	7900	0046
JV + JV + SVBOD [JJ, JI]	8000	0048
END UNTIL (JI + (JI + 1)) > JN;	8100	0050
JRHOQT + ((JPNL + JU) / (1 + JPNL * SVS [JJ]) - SVS [JJ] * JV	8200	0053

)/ (1 + JPNL * SVS [JJ]) / %	8300	0056
JDELTA = JDEV / JRMDDOT / %	8400	0059
IF (JJ ≤ 1) THEN GO TO L17 / %	8500	0060
IF (JJ = JN ≥ 1) THEN GO TO L20 ELSE GO TO L19	8600	0062
L17: IF (SVS [JJ] + JDELTA + SVDC [1]) > 0 THEN GO TO L250	8700	0064
JDELTA = JDELTA / 10 / %	8800	0067
GO TO L17 / %	8900	0069
L19: IF (SVS [JJ] + JDELTA + SVDC [JJ]) > 0 THEN GO TO L23	9000	0069
JDELTA = JDELTA / 10 / %	9100	0072
GO TO L19 / %	9200	0074
L23: IF (= SVDC [JJ = 1] = SVS [JJ] > JDELTA) THEN GO TO L250	9300	0074
JDELTA = JDELTA / 10 / %	9400	0076
GO TO L23 / %	9500	0079
L20: IF (SVS [JJ] + JDELTA + 1 / JPNL) > 0 THEN GO TO L26	9600	0079
JDELTA = JDELTA / 10 / %	9700	0083
GO TO L20 / %	9800	0084
L26: IF (= SVDC [JN] = SVS [JJ] > JDELTA) THEN GO TO L250	9900	0084
JDELTA = JDELTA / 10 / %	10000	0087
GO TO L26 / %	10100	0088
L250: SVS [JJ] + SVS [JJ] + JDELTA	10200	0089
GO TO L7 / %	10300	0092
L134:	10400	0092
END UNTIL (JJ + (JJ + 1)) > JNA	10500	0093
END / %	10600	0095
	0004 IS 0101 LONG, NEXT SEG 0002	
PROCEDURE MAINPRD / %	10700	0080
BEGIN INTEGER ARRAY SVIDENT (0 : 9)	10800	0080
	START OF SEGMENT ***** 0005	
REAL ARRAY SVC (0 : 20), SVA (0 : 21), SVAA (0 : 21), SVAB (0 : 21) / %	10900	0002
INTEGER DX1 / %	11000	0008
INTEGER JNA, JJJ, JII, JJ, JL / %	11100	0010
REAL JTDROP, JEXX, JPSTART, JEFK, JRHO, JSUMA, JSUMAA, JSUMD,	11200	0010
JDELTAT, JDELT, JFRACT, JX, JT, JPH, JPI, JFACTOR, JERRDR	11300	0010
COMMENT THE FOLLOWING SUBROUTINES ARE REQUIRED:	11400	0010
	11500	0010
SRRDOTIN / %	11600	0010
FORMAT FL2 (I12, R12, 5 / (6 R12, 5)), FL1 (9 A6), FL3 (4 R20,	11700	0010
	START OF SEGMENT ***** 0006	
10), FL4 (" ", 9 A6 / / " PNL =", R20, 10, " EXCESS K =", R20,	11800	0010
10, " REACTIVITY =", R20, 10 / / " DROP TIME =", R20, 10,	11900	0010
" SECONDS, STARTING FLUX =", R20, 10 / /	12000	0010
"	12100	0010
LAMDA                    DELTA STARTING TIME, CUR, " /	12200	0010
/ (3 R20, 10)), FL8 (/ " TIME DISPLACEMENT", R20, 10, " SECONDS"	12300	0010
/ /		

"	ROOT	A(IDEAL)	"	12400	0010
,	"	A(REAL)	A(IDEAL)CORRECTED" / (4 E25. 10)), FL21	12500	0010
(/	"	EQUIVALENT DROP", R20. 9, "	SECONDS OR", R15. 9,	12600	0010
"	DROP TIMES AFTER TIME ZERO"	, FL9 (/		12700	0010
"	TIME AFTER DROP	REAL FLUX	IDEAL FLU"	12800	0010
,	"X(DISPLACED)	RELATIVE ERROR"	, FL12 (R25. 2, 3 R25.	12900	0010
10) ; *				13000	0010
				0006 IS 0142 LONG, NEXT SEG 0005	
LIST LIST1 (JN, JPNL, FOR DX1 + 1 STEP 1 UNTIL JN DO SVBETA (DX1				13100	0010
), FOR DX1 + 1 STEP 1 UNTIL JN DO SVDC (DX1))				13200	0015
LIST LIST2 (FOR DX1 + 1 STEP 1 UNTIL 9 DO SVIDENT (DX1))				13300	0027
LIST LIST3 (JTOROP, JEXK, JPSTART, SVC (1))				13400	0037
LIST LIST4 (FOR DX1 + 2 STEP 1 UNTIL JN DO SVC (DX1))				13500	0047
LIST LIST5 (FOR DX1 + 1 STEP 1 UNTIL 9 DO SVIDENT (DX1), JPNL,				13600	0057
JEXK, JRHO, JTOROP, JPSTART, FOR DX1 + 1 STEP 1 UNTIL JN DO (				13700	0065
SVDC (DX1), SVBETA (DX1), SVC (DX1))				13800	0071
LIST LIST6 (JDELTA, FOR DX1 + 1 STEP 1 UNTIL JNA DO (SVS (DX1),				13900	0081
SVA (DX1), SVAA (DX1), SVAB (DX1))				14000	0086
LIST LIST7 (JDELTA, JFRACT) ; *				14100	0097
LIST LIST8 (JT, JPN, JP1, JERROR)				14200	0105
LABEL L20, L14, L15, LEND ; *				14300	0115
READ (TAPE7, FL2, LIST1) ; *				14400	0115
L20: READ (TAPE7, FL1, LIST2) (LEND)				14500	0119
L14: READ (TAPE7, FL3, LIST3) ; *				14600	0124
IF JTOROP ≤ 0 THEN GO TO L20 ; *				14700	0128
READ (TAPE7, FL3, LIST4) ; *				14800	0129
JEFK + JEXK + 1 ; *				14900	0133
JRHO + JEXK / JEFK ; *				15000	0134
WRITE (TAPE6 (PAGE)) ; *				15100	0135
WRITE (TAPE6, FL4, LIST5) ; *				15200	0139
SRHOOTIN (JRHO) ; *				15300	0142
JNA + JN + 1 ; *				15400	0143
JJJ + 1 ; *				15500	0144
DO				15600	0145
BEGIN JSUMA + 0 ; *				15700	0145
JSUMAA + 0 ; *				15800	0146
JSUMD + 0 ; *				15900	0147
JII + 1 ; *				16000	0147
DO				16100	0148
BEGIN JSUMA + JSUMA + SVBSD (JJJ, JII)				16200	0148
JSUMAA + JSUMAA + SVC (JII) * SVDC (JII) / (SVS (JJJ) + SVDC				16300	0150
(JII)) ; *				16400	0152
JSUMD + JSUMD + SVDC (JII) * SVBDD (JJJ, JII)				16500	0154

END UNTIL (JII + (JII + 1)) > JNJ	16600	0156
JSUMD + JSUMD * JEFK / JPNL + 1	16700	0159
SVA [JJJ] + (1 + JSUMA / JPNL) / JSUMD	16800	0162
SVAA [JJJ] + (JPSTART + JSUMAA) / JSUMD	16900	0164
END UNTIL (JJJ + (JJJ + 1)) > JNA	17000	0166
JDELTAT + LN (SVAA [1] / SVA [1]) / SVS [1]	17100	0169
JJ + 1	17200	0172
DO	17300	0173
BEGIN SVAB [JJ] + SVA [JJ] * EXP (SVS [JJ] * JDELTAT)	17400	0173
END UNTIL (JJ + (JJ + 1)) > JNA	17500	0174
WRITE (TAPE4, FL6, LIST6)	17600	0178
JDELT + JTORUP = JDELTAT	17700	0182
JFNACT + JDELT / JTOROP	17800	0183
WRITE (TAPE6, FL21, LIST7)	17900	0184
WRITE (TAPE6, FL9)	18000	0188
JX + .01	18100	0192
L15: JL + 1	18200	0192
DO	18300	0193
BEGIN JT + JX * JL	18400	0193
JPR + 0	18500	0195
JPI + 0	18600	0195
JJ + 1	18700	0196
DO	18800	0197
BEGIN JFACTOR + EXP (SVS [JJ] * JT)	18900	0197
JPR + JPR + SVAA [JJ] * JFACTOR	19000	0199
JPI + JPI + SVAB [JJ] * JFACTOR	19100	0201
END UNTIL (JJ + (JJ + 1)) > JNA	19200	0202
JERRUR + (JPR - JPI) / JPR	19300	0205
WRITE (TAPE6, FL12, LIST8)	19400	0207
END UNTIL (JL + (JL + 1)) > 9	19500	0211
IF (JX ≥ 100) THEN GO TO L14	19600	0213
JX + JX * 10	19700	0214
GO TO L15	19800	0215
LEND:	19900	0222
END	20000	0222

0005 IS 0234 LONG, NEXT SEG 0002

COMMENT INITIALIZING BLOCK	20100	0080
XPR + Q + K + 0	20200	0080
SENSW [1] + FALSE	20300	0081
SENSW [2] + FALSE	20400	0083
SENSW [3] + FALSE	20500	0084
SENSW [4] + FALSE	20600	0085
SENSW [5] + FALSE	20700	0086
SENSW [6] + FALSE	20800	0088



SENSL [1] + FALSE ; *	20900	0089
SENSL [2] + FALSE ; *	21000	0090
SENSL [3] + FALSE ; *	21100	0091
SENSL [4] + FALSE ; *	21200	0093
MAINPRD ; *	21300	0094
FINIS: END.	21400	0094

## APPENDIX D

## PROCEDURE DATARED

The purpose of this data reduction procedure for the B-5500 computer is to process the data and coded information which is collected at the reactor before commencing the least squares curve fitting. The coded information consists of a test number, multiscaler sequence, and multiscaler dwell-time code. This information is manually punched into the leader of the paper tape prior to data readout onto the tape from a multiscaler. The data which follow the coded information are simply the contents of each memory location of the multiscaler, punched serially. An IBM tape-card printing punch has been provided with a wired-board program to convert this information into punched cards since the B-5500 is not provided with a paper tape input reader. These punched cards form a portion of the input to DATARED. The other input required is the test number, total number of tapes for which information is being processed, a code indicating whether the number of channels from the multiscaler was other than 400, the switching time between multiscalers, the detection and recording system dead time, the dwell time to be associated with a special non-standard dwell-time code, and the time after experiment start to be associated with the first piece of data. In addition, if the code indicates other than 400 channels of data, the number of channels must be provided. The final input is a reduction factor for each time code. This factor tells the procedure how many channels of data to combine

into a single data point for economy in analysis. This factor gives the fine control on total number of data points which must be processed.

In the program, data are corrected for dead time losses and combined with other data points as determined by the reduction factor described above. A value of the standard deviation,  $\sigma$ , is obtained by taking the square root of the corrected counts for the data point. Using the dwell time per channel, elapsed time prior to the start of the multiscaler being considered, and multiscaler switching time, an interval start and stop time are calculated for each combined data point. The end result consists of one punched card per final data point and includes interval start and stop time, total counts over the interval, and the standard deviation.

Procedure DATARED is listed on the following pages.

COMMENT DATA READ ;		0000
BEGIN FILE IN TAPE7 0 (2, 15) ; %	100	0000
	START OF SEGMENT *****	0002
FILE OUT PUNCH 0 (2, 10) ; %	200	0005
FILE OUT TAPE6 1 (2, 15) ; %	300	0010
COMMENT DATARED ; %	400	0015
INTEGER I, CHAND, NOTEST, TESTNO, TUTAPE, CODE, FIN, DIG, TCODE,	500	0015
PTAPE, INIT, START, NOTWIN ; %	600	0015
INTEGER JB, JMODE, K ; %	700	0015
REAL ELAP ; %	800	0015
REAL TCHAN, EXTCH, DEL, SUM, TAU ; %	900	0015
INTEGER ARRAY REDFACT (0 : 20) ; %	1000	0015
REAL ARRAY SVY (0 : 1022), SVSIGMA (0 : 1022), SVT (0 : 1022), SVU	1100	0017
(0 : 1022), TZERO (0 : 1022) ; %	1200	0023
LABEL LSTART, L30, L1, L3, L4, L5, L6, L7, L8, L9, L10, L11, L12,	1300	0027
L13, L14, L15, L16, LCHEN, L17, L18, L19, L41, L43, L45, LEND,	1400	0027
DUMMY, L181, L182, L183, L184 ; %	1500	0027
FORMAT FL3001 (3 I1), FL1 (R10, 4, X4, R10, 4, X4, R14, 6, X4,	1600	0027
	START OF SEGMENT *****	0003
R14, 6), FL2 (R12, 4), FL9 (20 I3), FL3002 (X19, 5 (X4, I6)),	1700	0027
FL3003 (4 I4, 4 R13, 3), FL3004 (I5), FL3005 (/	1800	0027
"ERROR1=DISCREPANCY BETWEEN INPUT TEST NUMBER AND TEST	1900	0027
NUMBER ON PAPER TAPE"), FL3006 (	2000	0027
"ERROR2=PAPER TAPE DOES NOT APPEAR TO BE CORRECTLY SEQUENCED"),	2100	0027
FL3007 (/ "ERROR3=PAPER TAPE TIME CODE IS INVALID ZERO"), FL3008 (	2200	0027
/ "ERROR4=PAPER TAPE TIME CODE IS INVALID"), FL5001 (/	2300	0027
" T Y SIGMA ", FL6001 (/	2400	0027
" ", 3 E14, 6) ; %	2500	0027
	0003 IS 0113 LONG, NEXT SEG	0002
LIST LIST1 (TZERO (I), SVU (I), SVY (I), SVSIGMA (I));	2600	0027
LIST LIST5 (TESTNO, DIG, TCODE) ; %	2700	0038
LIST LIST6 (FOR I + INIT STEP 1 UNTIL FIN DO SVY (I));	2800	0047
LIST LIST7 (NOTEST, TUTAPE, CODE, JMODE, DEL, EXTCH, TAU, SVU (0))	2900	0057
; %	3000	0068
LIST LIST8 (CHAND) ; %	3100	0072
COMMENT REDFACT MUST BE ABLE TO DIVIDE INTO CHAND WITHOUT REMAINDER;	3200	0078
LIST LIST9 (FOR I + 1 STEP 1 UNTIL 20 DO REDFACT (I));	3300	0078
LIST LIST41 (SVT (I), SVY (I), SVSIGMA (I));	3400	0088
LSTART: HEAD (TAPE7, FL3003, LIST7) (LEND);	3500	0098
READ (TAPE7, FL9, LIST9) ; %	3600	0103
PTAPE + 1 ; %	3700	0107
INIT + 0 ; %	3800	0107
FIN + 0 ; %	3900	0108

READ (TAPE7, FL2, ELAP) ; *	4000	0109
IF CODE = 0 THEN GO TO L30 ELSE GO TO L1;	4100	0121
L30: CHAN = 400 ; *	4200	0123
GO TO L3 ; *	4300	0123
L1: READ (TAPE7, FL3004, LIST8) ; *	4400	0124
L3: READ (TAPE7, FL3001, LIST5) ; *	4500	0129
IF NUTEST = TESTNU THEN GO TO L5 ELSE GO TO L4;	4600	0133
L4: WRITE (TAPE6, FL3005) ; *	4700	0134
GO TO LEND ; *	4800	0138
L5: IF DIG = PTAPE THEN GO TO L7 ELSE GO TO L6;	4900	0141
L6: WRITE (TAPE6, FL3006) ; *	5000	0142
GO TO LEND ; *	5100	0146
L7: IF TCODE = 0 THEN GO TO L8 ELSE GO TO L9;	5200	0147
L8: WRITE (TAPE6, FL3007) ; *	5300	0148
GO TO LEND ; *	5400	0152
L9: IF TCODE = 1 THEN GO TO L10 ELSE GO TO L11;	5500	0153
L10: TCHAN = 0.01 ; *	5600	0154
GO TO LCHEN ; *	5700	0155
L11: IF TCODE = 2 THEN GO TO L12 ELSE GO TO L13;	5800	0158
L12: TCHAN = 0.1 ; *	5900	0159
GO TO LCHEN ; *	6000	0160
L13: IF TCODE = 3 THEN GO TO L14 ELSE GO TO L15;	6100	0163
L14: TCHAN = 1.0 ; *	6200	0164
GO TO LCHEN ; *	6300	0165
L15: IF TCODE = 4 THEN GO TO L16 ELSE GO TO L17;	6400	0168
L16: TCHAN = 10.0 ; *	6500	0169
GO TO LCHEN ; *	6600	0170
L17: IF TCODE = 5 THEN GO TO L18 ELSE GO TO L181;	6700	0173
L18: TCHAN = 100.00 ; *	6800	0174
GO TO LCHEN ; *	6900	0175
L181: IF TCODE = 6 THEN GO TO L182 ELSE GO TO L183;	7000	0178
L182: TCHAN = 1100.0 ; *	7100	0179
GO TO LCHEN ; *	7200	0180
L183: IF TCODE = 7 THEN GO TO L184 ELSE GO TO L19;	7300	0183
L184: TCHAN = EXTCH ; *	7400	0184
GO TO LCHEN ; *	7500	0185
L19: WRITE (TAPE6, FL3008) ; *	7600	0186
GO TO LEND ; *	7700	0190
LCHEN: INIT = FIN + 1 ; *	7800	0191
STAR = INIT ; *	7900	0192
FIN = INIT + CHAN - 1 ; *	8000	0193
READ (TAPE7, FL3002, LIST6) ; *	8100	0194
I = INIT ; *	8200	0198

FIN = INIT + CHANO / REDFACT [TCODE] = 1)	8300	0199
DO	8400	0202
BEGIN SVU [I] = ELAP + (1 - START + 1) * REDFACT [TCODE] * TCHAN;	8500	0202
TZERO [I] + SVU [I] = REDFACT [TCODE] * TCHAN;	8600	0206
SUM = 0 ; %	8700	0208
FOR K = INIT STEP 1 UNTIL (INIT + REDFACT [TCODE] = 1) DO	8800	0209
BEGIN SUM = SUM + SVY [K] / (1 - (SVY [K] / TCHAN) * TAU)	8900	0214
END ; %	9000	0216
SVY [I] = SUM ; %	9100	0220
SVSIGMA [I] = SQRT (SVY [I]) ; %	9200	0221
INIT = INIT + REDFACT [TCODE] ; %	9300	0223
END UNTIL (1 + (I + 1)) > FIN ; %	9400	0224
FOR I = START STEP 1 UNTIL FIN DO	9500	0227
BEGIN WRITE (TAPE6, FL1, LIST1) ; %	9600	0228
WRITE (PUNCH, FL1, LIST1)	9700	0231
END ; %	9800	0235
IF PTAPE = TOTAPE THEN GO TO L45 ELSE GO TO L41;	9900	0237
L41: PTAPE = PTAPE + 1 ; %	10000	0239
ELAP = ELAP + CHANO * TCHAN + DEL;	10100	0241
L43: GO TO L1 ; %	10200	0243
L45: HEAD (TAPE7, FL3004, NOTHIN) [LEND];	10300	0244
IF NOTHIN = 0 THEN GO TO LSTART ; %	10400	0256
LEND: END.	10500	0257

## APPENDIX E

## VARIABLE METRIC MINIMIZATION WITH INTEGRAL FUNCTION PROCEDURE

Variable Metric Minimization<sup>33</sup> is a method for determining numerically the local minima of differentiable functions of several variables. In the process of determining these minima, there is generated a matrix which characterizes the behavior of the function about the minimum.

Variable Metric Minimization was originally coded in FORTRAN at the Argonne National Laboratory and subsequently translated into ALGOL at Georgia Tech for the B-5500 computer. It is a general purpose method in that any differentiable function may be minimized. A separate procedure must be provided in which the value of the particular function and its derivatives with respect to each variable are evaluated at a given trial point. In the method employed in this work, weighted least squares was the goodness-of-fit criterion used. Thus, an expression was developed which incorporated this method of curve fitting into the required function to be minimized. The Variable Metric Method is explained in detail in Reference 33; only the special integral function procedure will be described herein.

If flux decay data were taken by means of instantaneous samplings at progressively longer times after shutdown, then an appropriate weighted least squares function to be minimized would be

$$F = \sum_{j=1}^B \left( \frac{y_j - \sum_{i=1}^M a_i' e^{-\lambda_i' t_j}}{\sigma_j} \right)^2 \quad (6)$$

where  $B$  = number of data points

$M$  = number of delayed neutron groups

$y_j$  = experimentally observed neutron count at the  $j^{\text{th}}$  time,  $t_j$

$\sigma_j$  = standard deviation of  $j^{\text{th}}$  data point (the weighting factor)

$t_j$  = time associated with the  $j^{\text{th}}$  data point

$a_i'$  = group abundance term, initial count rate attributable to  $i^{\text{th}}$  group

$\lambda_i'$  = group decay constant uncorrected for sub-critical multiplication

In fact, since the data are not observed instantaneously, but over an interval,  $\Delta t_j$ , starting at  $t_j$ , the function which in practice must be minimized is

$$F = \sum_{j=1}^B \left( \frac{y_j - \sum_{i=1}^M \int_{t_j}^{t_j + \Delta t_j} a_i' e^{-\lambda_i' t} dt}{\sigma_j} \right)^2$$

When the integration is performed, the result is

$$F = \sum_{j=1}^B \left( \frac{y_j - \sum_{i=1}^M \frac{a_i'}{\lambda_i'} [e^{-\lambda_i' t_j} - e^{-\lambda_i' (t_j + \Delta t_j)}]}{\sigma_j} \right)^2$$



and the gradient vector is obtained from

$$\frac{\partial F}{\partial \vec{a}_i} = \sum_{j=1}^B -2 \left[ y_j - \sum_{i=1}^M \frac{a_i'}{\lambda_i'} \left( e^{-\lambda_i' t_j} - e^{-\lambda_i' (t_j + \Delta t_j)} \right) \right] \times$$

$$\left[ \frac{e^{-\lambda_i' t_j}}{\sigma_j^2 \lambda_i'} \left( 1 - e^{-\lambda_i' \Delta t_j} \right) \right]$$

and

$$\frac{\partial F}{\partial \lambda_i'} = \sum_{j=1}^B -2 \left[ y_j - \sum_{i=1}^M \frac{a_i'}{\lambda_i'} \left( e^{-\lambda_i' t_j} - e^{-\lambda_i' (t_j + \Delta t_j)} \right) \right] \times$$

$$\left[ \frac{a_i' e^{-\lambda_i' t_j}}{\lambda_i'^2} \left( \Delta t e^{-\lambda_i' \Delta t_j} + (e^{-\lambda_i' \Delta t_j} - 1) \left( t_j + \frac{1}{\lambda_i'} \right) \right) \right]$$

Thus, each time the main Variable Metric Minimization Program calls this Integral Function Procedure, it passes to it the one-dimensional array representing the present estimate of the parameters  $a_i'$  and  $\lambda_i'$  and receives back the value of the least squares function calculated using those estimates, plus the one-dimensional array representing the gradient vector at the point defined by the parameter estimates. This gradient vector is then used by the main program in conjunction with the error matrix, which carries the most current information on the uncertainty of the present parameter estimates, to obtain a correction value which may be added to the parameters before their next trial. This iteration procedure continues until the predicted improvement for the next cycle is less than an input-specified con-

vergence criterion.

As a final check on the accuracy of the minimization process, a selected number of steps in a random direction away from the position of the minimum may be taken. Each time a step is taken, a new minimum is searched for. In this process, refinement of the error matrix representing the uncertainty of the final parameters is also accomplished. It has also been suggested by Cohn<sup>32</sup> that the final refinement of the error matrix may be facilitated by redefining the variables in the fitting problem in such a manner that the terms in the error matrix are of the same order of magnitude. This can be accomplished by modifying the VMM program to represent the  $a_i'$  and  $\lambda_i'$  terms as the product of new variables,  $q_i$  and  $r_i$ , and the best fit parameters previously obtained. This is equivalent to fixing the best fit parameters already obtained, defining new variables,  $q_i$  and  $r_i$  which have initial values of 1.0, and making a number of random steps in which the  $a_i$  and  $\lambda_i'$  of Equation 6 are represented as  $q_i a_i'$  and  $r_i \lambda_i'$  respectively. The final error estimates are then the product of the fixed parameters,  $a_i'$  and  $\lambda_i'$ , and the error estimates for the parameters  $q_i$  and  $r_i$ .

The ALGOL version of Variable Metric Minimization incorporating the Integral Function Procedure, FCN, is listed on the following pages.

```

COMMENT VARIABLE METRIC MINIMIZATION
BEGIN FILE OUT PUNCH 0 (2, 10)

                                0000
                                100 0000
                                START OF SEGMENT ***** 0002

FILE TAPE6 1 (2, 15) / %                                200 0005
FILE TAPE7 0 (2, 15) / %                                300 0010
BOOLEAN ARRAY SENSL [0 : 4] / %                          400 0015
BOOLEAN ARRAY SENSH [0 : 6] / %                          500 0017
REAL Q, XPR / %                                           600 0019
INTEGER K / %                                             700 0019
REAL ARRAY SVH [0 : 40, 0 : 40], SVX [0 : 40], SVG [0 : 40], SVS [
0 : 40], SVXP [0 : 40], SVGP [0 : 40], SVT [0 : 1022], SVGB [0 :
40], SVU [0 : 1022], SVC [0 : 10, 0 : 40], SVCTEM [0 : 40], TZERO [
0 : 1022] / %                                           1000 0033
REAL ARRAY SVY [0 : 1022], SVSIGMA [0 : 1022], SVYCALC [0 : 1022],
SVDF [0 : 1022] / %                                     1100 0042
REAL ARRAY SVA [0 : 38, 0 : 395] / %                     1200 0043
INTEGER JL, JIT, JN, JM, JM1, JMS, JK, JMODE, JMM, JB;   1300 0049
INTEGER I, J / %                                         1400 0051
REAL JGS, JE, JF, JEL, JSL, JFP, JGSP, JFB, JDELTA, JTD, JGSB, JA,
JQ, JGSS, JP, JRAND, JFO, JGIT, JGTP, TAU, ELAP;        1500 0053
LABEL L1 / %                                             1600 0053
REAL PROCEDURE FNOEXP (JX) / %                           1700 0053
VALUE JX / %                                             1800 0053
REAL JX / %                                             1900 0053
BEGIN REAL JOEXP / %                                     2000 0053
                                START OF SEGMENT ***** 0003

LABEL DUMMY, L1, L4, L3 / %                             2100 0053
IF (ABS (JX) < 0.1) THEN GO TO L1;                       2200 0000
JOEXP = 1 / %                                           2300 0001
IF (JX + 25.0) > 0 THEN GO TO L4 ELSE GO TO DUMMY;       2400 0002
L1: JOEXP = (1 + JX * (.5 + JX * (.16666666667 + JX * (
.4166666667*-1 + JX * (.8333333333*-2 + JX * (.13888888888*-2 +
JX * .1984126984*-3)))))) * JX / %                   2500 0004
GO TO DUMMY / %                                         2600 0006
L4: JOEXP = JOEXP + EXP (JX) / %                       2700 0007
L3: GO TO DUMMY / %                                     2800 0012
DUMMY: FNOEXP = JOEXP                                  2900 0021
END / %                                                 3000 0022
                                3100 0023
                                3200 0024
                                0003 IS 0028 LONG, NEXT SEG 0002

REAL PROCEDURE INT (ARG1) / %                            3300 0028
VALUE ARG1 / %                                           3400 0028
REAL ARG1 / %                                           3500 0028
BEGIN INT = (SIGN (ARG1) * ENTIER (ABS (ARG1)))          3600 0053
                                3700 0053
                                3800 0053
                                3900 0053

```

```

END ; %
REAL PROCEDURE MAX (ARG1, ARG2) ; %
VALUE ARG1, ARG2 ; %
REAL ARG1, ARG2 ; %
BEGIN MAX ← (IF ARG1 ≥ ARG2 THEN ARG1 ELSE ARG2)
END ; %
REAL PROCEDURE MIN (ARG1, ARG2) ; %
VALUE ARG1, ARG2 ; %
REAL ARG1, ARG2 ; %
BEGIN MIN ← (IF ARG1 ≤ ARG2 THEN ARG1 ELSE ARG2)
END ; %
PROCEDURE SRMATMPY (JM, JN, SVH, SVG, SVS);
INTEGER JM, JN ; %
REAL ARRAY SVH (0, 0), SVG (0), SVS (0);
BEGIN INTEGER JI, JJ ; %

```

START OF SEGMENT \*\*\*\*\* 0004

```

LABEL DUMMY ; %
JI ← 1 ; %
DO
BEGIN SVS [JI] ← 0 ; %
JJ ← 1 ; %
DO
BEGIN SVS [JI] ← SVH [JI, JJ] × SVG [JJ] + SVS [JI]
END UNTIL (JJ + (JJ + 1)) > JN
END UNTIL (JI + (JI + 1)) > JM ; %
GO TO DUMMY ; %
DUMMY:
END ; %

```

0004 IS 0015 LONG, NEXT SEG 0002

```

PROCEDURE SRFCN (JM, SVG, JF, SVX, JM1);
INTEGER JM, JM1 ; %
REAL JF ; %
REAL ARRAY SVG (0), SVX (0) ; %
BEGIN INTEGER UX1 ; %

```

START OF SEGMENT \*\*\*\*\* 0005

```

INTEGER JI, JQ, JL, JJ ; %
REAL JT1, JT2, JCHISQ, JCHI, TTAU, TEX1, XDT, DLT;
REAL FX ; %
FORMAT FL2000 (2 I6), FL3000 (6 (F8, 1, X4)), FL4000 (/ " T=", 8

```

START OF SEGMENT \*\*\*\*\* 0006

```

E14, 6 / (/ " ", 8 E14, 6)), FL1 (R10, 4, X4, R10, 4, X4, R15,
9, X4, R10, 4), FL2 (2 I4), FL5000 (/
" T1
T2 Y SIGMA Y CALC "
```

, " CHI	SUM CHISQ"), FL7000 (/ " DECAY CONSTANT", 14,	7900	0000
" NEGATIVE, SET EQUAL TO ZERO"), FL6000 (/ " ", 7 E(4, 6))		8000	0000
	0006 IS 0088 LONG, NEXT SEG 0005		
LIST LIST1 (TZERO [I], SVU [I], SVY [I], SVSIGMA [I])		8100	0000
LIST LIST3 (FOR DX1 + 1 STEP 1 UNTIL JM DO SVX [DX1])		8200	0011
LIST LIST4 (TZERO [J], SVU [J], SVY [J], SVSIGMA [J],		8300	0021
SVYCALC [J], JCH, JCHISQ) J %		8400	0028
LIST LIST7 (JQ) J %		8500	0036
LABEL DUMMY, L8, L10, L190, L220, L250, L260, L290		8600	0042
LABEL L12 J %		8700	0042
SWITCH SWG01 + L220, L8 J %		8800	0042
SWITCH SWG02 + L260, L290 J %		8900	0047
IF TIME (2) - J > 36000 THEN		9000	0052
BEGIN J + TIME (2) J %		9100	0054
BREAK J %		9200	0056
END J %		9300	0057
IF (XPR + (JM - 2)) > 0 THEN GO TO L250		9400	0057
IF XPR = 0 THEN GO TO L10 ELSE GO TO L190		9500	0059
L8: JMM + JM DIV 2 J %		9600	0061
L10: JL + 0 J %		9700	0063
DO		9800	0064
BEGIN TTAU + SVU [JL + 1] J %		9900	0064
DLT + TTAU - TZERO [JL + 1] J %		10000	0066
SVYCALC [JL + 1] + 0 J %		10100	0068
JQ + 1 J %		10200	0070
DO		10300	0070
BEGIN IF (SVX (2 * JQ) ≤ 1.0E-15) THEN		10400	0070
BEGIN IF JL = 0 THEN		10500	0072
BEGIN SVX (2 * JQ) + 0 J %		10600	0073
WRITE (TAPE6, FL7000, LIST7)		10700	0075
END J %		10800	0079
SVYCALC [JL + 1] + SVYCALC [JL + 1] + DLT * SVX (2 * JQ -		10900	0079
1) J %		11000	0082
SVA (2 * JQ - 1, JL + 1) + DLT		11100	0084
SVA (2 * JQ, JL + 1) + - TZERO (JL + 1) * DLT		11200	0087
GO TO L12 J %		11300	0092
END J %		11400	0095
TEX1 + EXP (- SVX (2 * JQ) * TZERO [JL + 1])		11500	0095
XDT + SVX (2 * JQ) * DLT J %		11600	0098
FX + FNDEXP (- XDT) J %		11700	0100
JT1 + - FX * TEX1 J %		11800	0102
JT2 + JT1 / SVX (2 * JQ) J %		11900	0103
SVYCALC [JL + 1] + SVYCALC [JL + 1] + JT2 * SVX (2 * JQ - 1)		12000	0105
J %		12100	0109

SVA [2 * JQ = 1, JL + 1] + JT2)	12200	0110
SVA [2 * JQ, JL + 1] + SVX [2 * JQ = 1] * (TEX1 / SVX [2 * JQ]) * (DLT * (FX + 1) + FX * (TZERO [JL + 1] + 1 / SVX [2 * JQ])) / %	12300	0113
	12400	0118
	12500	0122
L121	12600	0124
END UNTIL (JQ + (JQ + 1)) > JMM	12700	0125
END UNTIL (JL + (JL + 1)) > (JB - 1)	12800	0126
JF + 0 / %	12900	0130
JI + 1 / %	13000	0131
DO	13100	0131
BEGIN SVDF [JI] + SVY [JI] = SVYCALC [JI]	13200	0131
JF + JF + (SVDF [JI] / SVSIGMA [JI]) * 2	13300	0134
END UNTIL (JI + (JI + 1)) > JB / %	13400	0135
JJ + 1 / %	13500	0139
DO	13600	0140
BEGIN SVG [JJ] + 0 / %	13700	0140
JI + 1 / %	13800	0141
DO	13900	0142
BEGIN SVG [JJ] + SVG [JJ] + (SVDF [JI] / SVSIGMA [JI] * 2) * SVA [JJ, JI]	14000	0142
	14100	0144
END UNTIL (JI + (JI + 1)) > JB	14200	0145
SVG [JJ] + = 2 * SVG [JJ]	14300	0149
END UNTIL (JJ + (JJ + 1)) > JM / %	14400	0150
GO TO DUMMY / %	14500	0153
L190: READ (TAPE7, FL2, JB, JMODE)	14600	0154
FOR I + 1 STEP 1 UNTIL JB DO READ (TAPE7, FL1, LIST1)	14700	0167
CLOSE (TAPE7, RELEASE) / %	14800	0174
GO TO SWG01 [JMODE] / %	14900	0176
L220: JI + 2 / %	15000	0178
DO	15100	0178
BEGIN SVX [JI] + 0.69314718 / SVX [JI]	15200	0178
END UNTIL (JI + (JI + 2)) > JM / %	15300	0179
GO TO L8 / %	15400	0183
L250: GO TO SWG02 [JMODE] / %	15500	0186
L260: JI + 2 / %	15600	0188
DO	15700	0188
BEGIN SVX [JI] + 0.69314718 / SVX [JI]	15800	0188
END UNTIL (JI + (JI + 2)) > JM / %	15900	0189
WRITE (TAPE6, FL4000, LIST3) / %	16000	0193
L290: WRITE (TAPE6, FL5000) / %	16100	0196
JCHISQ + 0 / %	16200	0200
JI + 1 / %	16300	0201
DO	16400	0202

BEGIN JCHI + SVDF (JI) / SVSIGMA (JI)	16500	0202
JCHISQ + JCHISQ + JCHI * 2	16600	0203
WRITE (TAPE6, FL6000, LIST4)	16700	0205
END UNTIL (JI + (JI + 1)) > JB	16800	0209
GO TO DUMMY	16900	0211
DUMMY:	17000	0213
END	17100	0213
0005 IS 0220 LONG, NEXT SEG 0002		
PROCEDURE SRREADY	17200	0072
BEGIN REAL ARRAY SVQGS (0 : 1), SVQGSF (0 : 1)	17300	0072
START OF SEGMENT ***** 0007		
INTEGER JI	17400	0004
REAL JTP1	17500	0004
COMMENT THE FOLLOWING SUBROUTINES ARE REQUIRED:	17600	0004
SRMATMPY, SRFCN	17700	0004
FORMAT FL1 (/ " UNDERSHOT")	17800	0004
START OF SEGMENT ***** 0008		
0008 IS 0006 LONG, NEXT SEG 0007		
LABEL DUMMY, L200, L201, L223, L227, L229	17900	0004
SWITCH SWGD1 + L200, L201	18000	0004
GO TO SWGD1 (JL)	18100	0009
L200: JI + 1	18200	0012
L201: SRMATMPY (JN, JN, SVH, SVG, SVS)	18300	0012
JI + 1	18400	0016
DO	18500	0017
BEGIN SVS (JI) + = SVS (JI)	18600	0017
END UNTIL (JI + (JI + 1)) > JN	18700	0018
JM + 1	18800	0021
SVQGS (1) + 0	18900	0022
JI + 1	19000	0023
DO	19100	0024
BEGIN SVQGS (1) + SVQGS (1) + SVS (JI) * SVG (JI)	19200	0024
END UNTIL (JI + (JI + 1)) > JN	19300	0025
JGS + SVQGS (1)	19400	0029
IF (JGS + JE) > 0 THEN GO TO L227	19500	0030
JTP1 + = 2 * (JF / JGS)	19600	0032
JEL + MIN (2, JTP1)	19700	0034
JSL + = JGS	19800	0035
JI + 1	19900	0036
DO	20000	0037
BEGIN SVXP (JI) + SVX (JI) + JEL * SVS (JI)	20100	0037
END UNTIL (JI + (JI + 1)) > JN	20200	0038
JM1 + 2	20300	0047
SRFCN (JN, SVGP, JFP, SVXP, JM1)	20400	0043

JM = 1 ; *	20500	0045
SVQGGSP [1] = 0 ; *	20600	0046
J1 = 1 ; *	20700	0047
DO	20800	0048
BEGIN SVQGGSP [1] = SVQGGSP [1] + SVS [J1] * SVGP [J1]	20900	0048
END UNTIL (J1 + (J1 + 1)) > JM ; *	21000	0050
JGSP = SVQGGSP [1] ; *	21100	0053
IF JGSP ≥ 0 THEN GO TO L229 ; *	21200	0054
IF (JFP ≥ JF) THEN GO TO L229 ; *	21300	0056
WRITE (TAPE4, FL1) ; *	21400	0057
JFB = JFP ; *	21500	0060
J1 = 1 ; *	21600	0061
DO	21700	0062
BEGIN SVGB [J1] = SVGP [J1] ; *	21800	0062
SVT [J1] = SVXP [J1]	21900	0063
END UNTIL (J1 + (J1 + 1)) > JM ; *	22000	0064
IF (JEL ≥ 2) THEN GO TO L223 ; *	22100	0067
JL = 3 ; *	22200	0068
GO TO DUMMY ; *	22300	0069
L223: JDELTA = 2 * JDELTA ; *	22400	0070
JTU = 1 / JSL ; *	22500	0071
JL = 2 ; *	22600	0072
GO TO DUMMY ; *	22700	0073
L227: JL = 1 ; *	22800	0073
GO TO DUMMY ; *	22900	0074
L229: JL = 4 ; *	23000	0075
GO TO DUMMY ; *	23100	0076
DUMMY:	23200	0077
END ; *	23300	0078
0007 IS 0032 LONG, NEXT SEG 0002		
PROCEDURE SRAIM ; *	23400	0072
BEGIN REAL ARRAY SVQGT1 (0 : 1), SVQGT1 (0 : 1);	23500	0072
START OF SEGMENT ***** 0009		
INTEGER J1 ; *	23600	0004
REAL JZ, JTI, JTP1 ; *	23700	0004
COMMENT THE FOLLOWING SUBROUTINES ARE REQUIRED:	23800	0004
SRMATMPY, SRFCN ; *	23900	0004
FORMAT FL1 (/ " RICOCHET") ; *	24000	0004
START OF SEGMENT ***** 0010		
0010 IS 0006 LONG, NEXT SEG 0009		
LABEL DUMMY, L312, L317, L335 ; *	24100	0004
JZ = JGS + JGSP + 3 * (JF = JFP) / JEL	24200	0004
JTU = JGS / JZ ; *	24300	0007



JTI = JGSP / JZ ; %	24400	0008
JQ = SQRT (1 - JTD * JTI) ; %	24500	0009
JQ = ABS (JQ * JZ) ; %	24600	0012
JA = (JGSP + JQ - JZ) / (JGSP + JGS + 2 * JQ)	24700	0013
JTU = (JEL * (JGSP + JZ + 2 * JQ) * JA + 2) / 3	24800	0017
JFU = JFP - JTU ; %	24900	0021
SRMATMPY (JN, JN, SVH, SVGP, SVT)	25000	0022
JTP1 = JGSP / JSL ; %	25100	0026
JI = 1 ; %	25200	0027
DO	25300	0028
BEGIN SVT [JI] = SVT [JI] + JTP1 * SVS [JI]	25400	0028
END UNTIL (JI + (JI + 1)) > JN ; %	25500	0030
JM = 1 ; %	25600	0033
SVQGT [1] = 0 ; %	25700	0034
JI = 1 ; %	25800	0035
DO	25900	0036
BEGIN SVQGT [1] = SVQGT [1] + SVT [JI] * SVGP [JI]	26000	0036
END UNTIL (JI + (JI + 1)) > JN ; %	26100	0038
JGTP = SVQGT [1] ; %	26200	0041
IF (2 * JTU + JGTP) < 0 THEN GO TO L317	26300	0042
L312: JTP1 = 1 - JA ; %	26400	0044
JI = 1 ; %	26500	0046
DO	26600	0047
BEGIN SVT [JI] = JA * SVX [JI] + JTP1 * SVXP [JI]	26700	0047
END UNTIL (JI + (JI + 1)) > JN ; %	26800	0049
JL = 1 ; %	26900	0052
GO TO DUMMY ; %	27000	0053
L317: IF (JF + JGTP / 2) < 0 THEN GO TO L312	27100	0053
JI = 1 ; %	27200	0056
DO	27300	0057
BEGIN SVT [JI] = SVT [JI] + SVXP [JI]	27400	0057
END UNTIL (JI + (JI + 1)) > JN ; %	27500	0058
JM1 = 2 ; %	27600	0061
SRFCN (JN, SVGB, JFB, SVT, JM1)	27700	0062
IF (JFB ≥ JFO) THEN GO TO L312 ; %	27800	0065
WRITE (TAPE6, FL1) ; %	27900	0066
JI = 1 ; %	28000	0069
DO	28100	0070
BEGIN SVS [JI] = SVT [JI] + SVXP [JI]	28200	0070
END UNTIL (JI + (JI + 1)) > JN ; %	28300	0071
JM = 1 ; %	28400	0075
SVQGT [1] = 0 ; %	28500	0075
JI = 1 ; %	28600	0077
DO	28700	0077

BEGIN SVQGYT [1] + SVQGYT [1] + SVS [JI] * SVGB [JI]	28800	0077
END UNTIL (JI + (JI + 1)) > JN / %	28900	0079
JGTT + SVQGYT [1] / %	29000	0083
JGIT + JGTT = JGTP / %	29100	0084
IF JGTT < 0 THEN GO TO L335 / %	29200	0085
JGSS + JGTT / %	29300	0086
JSL + = JGTP / %	29400	0087
JEL + 1 / %	29500	0088
JL + 2 / %	29600	0089
GO TO DUMMY / %	29700	0089
L335: JL + 3 / %	29800	0090
GO TO DUMMY / %	29900	0091
DUMMY:	30000	0092
END / %	30100	0093
	0009 IS 0098 LONG, NEXT SEG 0002	
PROCEDURE SRFINE / %	30200	0072
BEGIN REAL ARRAY SVQGSB [0 : 1] / %	30300	0072
	START OF SEGMENT ***** 0011	
INTEGER JI / %	30400	0002
REAL JTP1, JTP2 / %	30500	0002
COMMENT THE FOLLOWING SUBROUTINES ARE REQUIRED:	30600	0002
SRFCN / %	30700	0002
FORMAT FL1 (/ " MOVE LEFT"), FL2 (/ " MOVE RIGHT")	30800	0002
	START OF SEGMENT ***** 0012	
	0012 IS 0012 LONG, NEXT SEG 0011	
LABEL DUMMY, L413, L418, L426, L428	30900	0002
JM1 + 2 / %	31000	0002
SRFCN (JN, SVGB, JFB, SVT, JM1)	31100	0002
JM + 1 / %	31200	0005
SVQGSB [1] + 0 / %	31300	0006
J1 + 1 / %	31400	0007
DO	31500	0008
BEGIN SVQGSB [1] + SVQGSB [1] + SVS [JI] * SVGB [JI]	31600	0008
END UNTIL (JI + (JI + 1)) > JN / %	31700	0010
JGSB + SVQGSB [1] / %	31800	0013
JTP1 + MIN (JFB, JFP) / %	31900	0014
IF (JTP1 < JFB - JE) THEN GO TO L418	32000	0016
JTP1 + JA / (1 - JA) / %	32100	0017
JTP2 + (1 - JA) / JA / %	32200	0019
JTU + JGSB * (JTP1 - JTP2) / %	32300	0021
IF (ABS (JT0) < J0) THEN GO TO L413	32400	0023
JGSS + 2 * J0 / %	32500	0024
JL + 1 / %	32600	0025
GO TO DUMMY / %	32700	0026

L413: JGSS + JTO + 2 * JO ) %	32800	0027
JI + 1 ) %	32900	0028
DO	33000	0029
BEGIN SVG (JI) + (SVGB (JI) = SVG (JI)) * JTP1 + (SVGP (JI) =	33100	0029
SVGB (JI)) * JTP2	33200	0032
END UNTIL (JI + (JI + 1)) > JN ) %	33300	0033
JL + 2 ) %	33400	0036
GO TO DUMMY ) %	33500	0037
L416: IF (JF ≥ JFP) THEN GO TO L428)	33600	0037
WRITE (TAPE6, FL1) ) %	33700	0039
JEL + (1 - JA) * JEL ) %	33800	0042
JFP + JFB ) %	33900	0044
JGSP + JGSB ) %	34000	0045
JI + 1 ) %	34100	0046
DO	34200	0046
BEGIN SVXP (JI) + SVT (JI) ) %	34300	0046
SVGP (JI) + SVGB (JI)	34400	0048
END UNTIL (JI + (JI + 1)) > JN ) %	34500	0049
L426: JL + 3 ) %	34600	0052
GO TO DUMMY ) %	34700	0052
L428: WRITE (TAPE6, FL2) ) %	34800	0053
JEL + JEL * JA ) %	34900	0057
JF + JFB ) %	35000	0058
JGS + JGSB ) %	35100	0059
JI + 1 ) %	35200	0060
DO	35300	0061
BEGIN SVX (JI) + SVT (JI) ) %	35400	0061
SVG (JI) + SVGB (JI)	35500	0062
END UNTIL (JI + (JI + 1)) > JN ) %	35600	0063
GO TO L426 ) %	35700	0066
DUMMY:	35800	0066
END ) %	35900	0067
0011 IS 0071 LONG, NEXT SEG 0002		
PROCEDURE SRDRESS ) %	36000	0072
BEGIN REAL ARRAY SVQTO (0 : 1) ) %	36100	0072
START OF SEGMENT ***** 0013		
INTEGER DX1 ) %	36200	0002
INTEGER JI, JJ ) %	36300	0002
REAL JTP1 ) %	36400	0002
COMMENT THE FOLLOWING SUBROUTINES ARE REQUIRED:	36500	0002
SRMATMPY ) %	36600	0002
FORMAT FL1 (/ " IT ", I4, " STEP ", I4, " F=", E14. 6, " GS="	36700	0002
START OF SEGMENT ***** 0014		



JI + 1 ; %	41100	0126
DO	41200	0127
BEGIN SVG (JI) + SVGB (JI) ; %	41300	0127
SVX (JI) + SVT (JI)	41400	0129
END UNTIL (JI + (JI + 1)) > JN ; %	41500	0129
WRITE (TAPE6, FL1, LIST1) ; %	41600	0132
IF NOT SENS# [1] THEN GO TO L517;	41700	0136
WRITE (TAPE6, FL2, LIST2) ; %	41800	0137
WRITE (TAPE6, FL3, LIST3) ; %	41900	0141
L517: WRITE (TAPE6, FL4) ; %	42000	0145
JIT + JIT + 1 ; %	42100	0148
JL + 1 ; %	42200	0149
GO TO DUMMY ; %	42300	0150
L524: WRITE (TAPE6, FL5) ; %	42400	0151
L525: JTP1 + JEL * JSL / JGSS ; %	42500	0154
JDELTA + JDELTA * JTP1 ; %	42600	0156
JTU + (JTP1 - 1) / JSL ; %	42700	0158
GO TO L510 ; %	42800	0159
WRITE (TAPE6, FL6) ; %	42900	0160
WRITE (TAPE6, FL7) ; %	43000	0163
JI + 1 ; %	43100	0167
DO	43200	0168
BEGIN WRITE (TAPE6, FL8, LIST4)	43300	0168
END UNTIL (JI + (JI + 1)) > JN ; %	43400	0171
WRITE (TAPE6, FL9, LIST5) ; %	43500	0174
WRITE (TAPE6, FL2, LIST2) ; %	43600	0177
WRITE (TAPE6, FL10, LIST6) ; %	43700	0181
IF NOT SENS# [2] THEN GO TO L543;	43800	0185
WRITE (PUNCH, FL11, LIST2) ; %	43900	0186
JI + 1 ; %	44000	0190
DO	44100	0190
BEGIN WRITE (PUNCH, FL11, LIST7)	44200	0190
END UNTIL (JI + (JI + 1)) > JN ; %	44300	0194
WRITE (PUNCH, FL11, LIST8) ; %	44400	0196
L543: JL + 2 ; %	44500	0200
GO TO DUMMY ; %	44600	0201
DUMMY:	44700	0202
END ; %	44800	0203
0013 IS 0209 LONG, NEXT SEG 0002		
PROCEDURE SRRAND (JRAND) ; %	44900	0072
REAL JRAND ; %	45000	0072
BEGIN REAL JARG2 ; %	45100	0072
START OF SEGMENT ***** 0015		
LABEL DUMMY ; %	45200	0000

JANG2 + 5881 * 5881 ) %	45300	0000
JRAND + 31 * ((JRANO) MOD (JANG2))	45400	0001
COMMENT THE RANDOM NUMBER HAS SOME VALUE BETWEEN ZERO AND 5881 SQUAR	45500	0003
ED ) %	45600	0003
COMMENT MINUS 1. THIS IS LEHMERS PROCEDURE, REF TODD PAGE 181	45700	0003
GO TO DUMMY ) %	45800	0003
DUMMY:	45900	0005
END ) %	46000	0005
	0015 IS 0007 LONG, NEXT SEG 0002	
PROCEDURE SRSTUFF ) %	46100	0072
BEGIN REAL ARRAY SVQTP1 (0 : 11) ) %	46200	0072
	START OF SEGMENT ***** 0016	
INTEGER JI ) %	46300	0002
REAL JDIV, JTP1 ) %	46400	0002
COMMENT THE FOLLOWING SUBROUTINES ARE REQUIRED:	46500	0002
SRRAND, SRMATHPY ) %	46600	0002
FORMAT FL1 (/ " RANDOM STEP ", I4, " GS=", E14, 6)	46700	0002
	START OF SEGMENT ***** 0017	
	0017 IS 0010 LONG, NEXT SEG 0016	
LIST LIST1 (JMS, JGS) ) %	46800	0002
LABEL DUMMY, L617 ) %	46900	0010
JK + JK - 1 ) %	47000	0010
IF JK < 0 THEN GO TO L617 ) %	47100	0011
JMS + JMS + 1 ) %	47200	0012
WRITE (TAPE6, FL1, LIST1) ) %	47300	0013
JRAND + 1 ) %	47400	0017
JI + 1 ) %	47500	0018
DO	47600	0019
BEGIN SRRAND (JRANO) ) %	47700	0019
JDIV + (5881 * 5881) - 1 ) %	47800	0019
SVT [JI] + (JRANO / JDIV) - 0.5	47900	0021
END UNTIL (JI + (JI + 1)) > JN ) %	48000	0022
SRMATHPY (JN, JN, SVH, SVT, SVS)	48100	0026
JN + 1 ) %	48200	0029
SVQTP1 [1] + 0 ) %	48300	0030
JI + 1 ) %	48400	0031
DO	48500	0032
BEGIN SVQTP1 [1] + SVQTP1 [1] + SVS [JI] * SVT [JI]	48600	0032
END UNTIL (JI + (JI + 1)) > JN ) %	48700	0034
JTP1 + SVQTP1 [1] ) %	48800	0037
JTP1 + SQRT (JTP1) ) %	48900	0038
JP + SQRT (JF / 5) ) %	49000	0039
JEL + JP / JTP1 ) %	49100	0041
JI + 1 ) %	49200	0042
DO	49300	0043

Statement	Address	Label
BEGIN SVX (JI) + SVX (JI) + JEL * SVS (JI)	49400	0043
END UNTIL (JI + (JI + 1)) > JN J %	49500	0045
JM1 + 2 J %	49600	0048
JL + 1 J %	49700	0049
GO TO DUMMY J %	49800	0050
L617: JL + 2 J %	49900	0053
JMS + 0 J %	50000	0053
GO TO DUMMY J %	50100	0054
DUMMY:	50200	0055
END J %	50300	0055
0016 IS 0059 LONG, NEXT SEG 0002		
PROCEDURE MAIVPRO J %	50400	0072
BEGIN INTEGER DX1 J %	50500	0072
START OF SEGMENT ***** 0018		
INTEGER JNC, JI, JJ, JJI J %	50600	0000
REAL JFAC, TO, T1, PROC, INOUT J %	50700	0000
COMMENT THE FOLLOWING SUBROUTINES ARE REQUIRED:	50800	0000
SRFCN, SRREADY, SRAIN, SRFIRE, SRORESS, SRSTUFF	50900	0000
FORMAT FL1 (	51000	0000
START OF SEGMENT ***** 0019		
" IDENTIFICATION TITLE "		0000
, " " FL2 (3 I6, F6, 1), FL3 (6 E12, 4), FL5 (	51200	0000
" VARIABLE METRIC MINIMIZATION"), FL6 (/ " N=", I2, " K=", I2,	51300	0000
" E=", E14, 6, " P=", E14, 6, " DELTA=", E14, 6), FL7 (/	51400	0000
" X=", 8 E14, 6 / (/ " " 8 E14, 6)), FL8 (/ " H"), FL9 (/ " "	51500	0000
, 8 E14, 6 / (/ " " 8 E14, 6)), FL10 (/ " IT ", I4, " STEP ",	51600	0000
I4, " F=", E14, 6), FL4 (/ " - - - - - - - -"), FL10 (/	51700	0000
" FINAL VALUES"), FL11 (/ " ERROR MATRIX"), FL20 (/	51800	0000
"PROCESSOR TIME = ", F6, 2, "SECONDS I/O TIME = ", F6, 2),	51900	0000
FL13 (/ " F=", E14, 6, " GS=", E14, 6), FL12 (/ " G=", 8 E14, 6	52000	0000
/ (/ " " 8 E14, 6)) J %	52100	0000
0019 IS 0146 LONG, NEXT SEG 0018		
LIST LIST1 (JN, JK, JNC, JFAC) J %	52200	0000
LIST LIST2 (FOR DX1 + 1 STEP 1 UNTIL JN DO SVX (DX1))	52300	0010
LIST LIST3 (FOR DX1 + JI STEP 1 UNTIL JN DO SVH (DX1, JI))	52400	0020
LIST LIST4 (JDELTA, JE, JP) J %	52500	0031
LIST LIST5 (FOR DX1 + 1 STEP 1 UNTIL JN DO SVC (JJ, DX1))	52600	0040
LIST LIST6 (JN, JK, JE, JP, JDELTA)	52700	0051
LIST LIST7 (FOR DX1 + 1 STEP 1 UNTIL JN DO SVH (DX1, JI))	52800	0062
LIST LIST8 (JIT, JMS, JF) J %	52900	0073
LIST LIST9 (JF, JGS) J %	53000	0082
LIST LIST10 (FOR DX1 + 1 STEP 1 UNTIL JN DO SVG (DX1))	53100	0090
LIST LIST20 (PROC, INOUT) J %	53200	0100
LABEL L101, L1064, L1065, L109, L1165, L1201, L1209, L121, L124,	53300	0108

L126, L129, L132, L133, L135, L137, L159, L139, L1393, L1395,	53400	0108
L142, L157, L162, LEND ; %	53500	0108
SWITCH SWG01 + L139, L159, L137, L126;	53600	0108
SWITCH SWG02 + L129, L135, L137;	53700	0114
SWITCH SWG03 + L135, L132, L126;	53800	0119
SWITCH SWG04 + L124, L162 ; %	53900	0124
SWITCH SWG05 + L1165, L142 ; %	54000	0129
L101: JMS + 0 ; %	54100	0134
T1 + TIME (3) ; %	54200	0135
T0 + TIME (2) ; %	54300	0137
READ (TAPE7, FL1) [L1] ; %	54400	0138
READ (TAPE7, FL2, LIST1) [L1] ; %	54500	0143
READ (TAPE7, FL3, LIST2) [L1] ; %	54600	0148
JI + 1 ; %	54700	0153
DO	54800	0153
BEGIN JJ + JI ; %	54900	0153
DO	55000	0154
BEGIN SVH [JJ, JI] + 0	55100	0154
END UNTIL (JJ + (JJ + 1)) > JN	55200	0155
END UNTIL (JI + (JI + 1)) > JN ; %	55300	0157
JI + 1 ; %	55400	0161
DO	55500	0161
BEGIN IF JFAC ≤ 0 THEN GO TO L1064;	55600	0161
SVH [JI, JI] + JFAC ; %	55700	0163
GO TO L1065 ; %	55800	0165
L1064: READ (TAPE7, FL3, LIST3);	55900	0169
L1065:	56000	0173
END UNTIL (JI + (JI + 1)) > JN ; %	56100	0173
JI + 1 ; %	56200	0175
DO	56300	0176
BEGIN JJ + JI ; %	56400	0176
DO	56500	0176
BEGIN SVH [JI, JJ] + SVH [JJ, JI]	56600	0176
END UNTIL (JJ + (JJ + 1)) > JN	56700	0179
END UNTIL (JI + (JI + 1)) > JN ; %	56800	0181
READ (TAPE7, FL3, LIST4) ; %	56900	0184
IF JNC ≤ 0 THEN GO TO L109 ; %	57000	0188
JJ + 1 ; %	57100	0189
DO	57200	0190
BEGIN READ (TAPE7, FL3, LIST5)	57300	0190
END UNTIL (JJ + (JJ + 1)) > JNC;	57400	0193
L109: WRITE (TAPE6, FL5) ; %	57500	0196
WRITE (TAPE6, FL1) ; %	57600	0200
WRITE (TAPE6, FL6, LIST6) ; %	57700	0204



WRITE (TAPE6, FL7, LIST2) ; %	57800	0207
WRITE (TAPE6, FL8) ; %	57900	0211
JI + 1 ; %	58000	0215
DO	58100	0215
BEGIN WRITE (TAPE6, FL9, LIST7)	58200	0215
END UNTIL (JI + (JI + 1)) > JN ; %	58300	0219
JM1 + 1 ; %	58400	0221
L1165: JF + 0 ; %	58500	0222
SRFCN (JN, SVG, JF, SVX, JM1) ; %	58600	0223
IF JF ≤ 0 THEN GO TO L1393 ; %	58700	0226
JL + 1 ; %	58800	0227
JIT + 0 ; %	58900	0228
WRITE (TAPE6, FL14, LIST8) ; %	59000	0229
WRITE (TAPE6, FL7, LIST2) ; %	59100	0233
WRITE (TAPE6, FL4) ; %	59200	0236
L1201: IF JNC ≤ 0 THEN GO TO L121;	59300	0240
JJ1 + 1 ; %	59400	0242
DO	59500	0243
BEGIN JI + 1 ; %	59600	0243
DO	59700	0243
BEGIN SVCTEM [JI] + SVC [JJ1, JI];	59800	0243
SVT [JI] + 0	59900	0246
END UNTIL (JI + (JI + 1)) > JN;	60000	0246
JI + 1 ; %	60100	0249
DO	60200	0250
BEGIN JJ + 1 ; %	60300	0250
DO	60400	0251
BEGIN SVT [JI] + SVT [JI] + SVH [JJ, JI] * SVCTEM [JJ]	60500	0251
END UNTIL (JJ + (JJ + 1)) > JN	60600	0253
END UNTIL (JI + (JI + 1)) > JN;	60700	0256
JTD + 0 ; %	60800	0259
JI + 1 ; %	60900	0260
DO	61000	0260
BEGIN JTD + JTD + SVCTEM [JI] * SVT [JI]	61100	0260
END UNTIL (JI + (JI + 1)) > JN;	61200	0261
IF (JTD ≤ JE) THEN GO TO L1209;	61300	0265
JI + 1 ; %	61400	0266
DO	61500	0267
BEGIN JJ + 1 ; %	61600	0267
DO	61700	0268
BEGIN SVH [JJ, JI] + SVH [JJ, JI] = SVT [JI] * SVT [JJ] /	61800	0268
JTD	61900	0271
END UNTIL (JJ + (JJ + 1)) > JN	62000	0271
END UNTIL (JI + (JI + 1)) > JN;	62100	0274
L1209:	62200	0277

END UNTIL (JJ1 + (JJ1 + 1)) > JNC;	62300	0281
L121: SRREADY ; %	62400	0283
GO TO SWG01 [JL] ; %	62500	0284
L124: JL + 2 ; %	62600	0286
GO TO L1201 ; %	62700	0287
L126: SRAIM ; %	62800	0288
GO TO SWG02 [JL] ; %	62900	0289
L129: SRFIRE ; %	63000	0291
GO TO SWG03 [JL] ; %	63100	0292
L132: JL + 1 ; %	63200	0294
L133: SRDRESS ; %	63300	0295
GO TO SWG04 [JL] ; %	63400	0296
L135: JL + 2 ; %	63500	0298
GO TO L133 ; %	63600	0299
L137: JL + 3 ; %	63700	0300
GO TO L133 ; %	63800	0301
L159: JL + 4 ; %	63900	0302
GO TO L133 ; %	64000	0303
L139: IF SENSW [1] THEN GO TO L1395;	64100	0304
L1393: WRITE (TAPE6, FL7, LIST2);	64200	0306
L1395: SRSTUFF ; %	64300	0310
GO TO SWG05 [JL] ; %	64400	0311
L142: WRITE (TAPE6, FL10) ; %	64500	0313
WRITE (TAPE6, FL11) ; %	64600	0317
J1 + 1 ; %	64700	0321
DO	64800	0321
BEGIN WRITE (TAPE6, FL9, LIST7)	64900	0321
END UNTIL (J1 + (J1 + 1)) > JN ; %	65000	0325
WRITE (TAPE6, FL13, LIST9) ; %	65100	0327
WRITE (TAPE6, FL7, LIST2) ; %	65200	0331
WRITE (TAPE6, FL12, LIST10) ; %	65300	0335
JM1 + 3 ; %	65400	0339
SRFCN (JN, SVG, JF, SVX, JM1) ; %	65500	0339
PRUC + (TIME (2) - TD) / 60 ; %	65600	0342
INOUT + (TIME (3) - T1) / 60 ; %	65700	0344
IF NOT SENSW [2] THEN GO TO L157;	65800	0347
WRITE (PUNCH, FL3, LIST2) ; %	65900	0348
J1 + 1 ; %	66000	0351
DO	66100	0352
BEGIN WRITE (PUNCH, FL3, LIST3)	66200	0352
END UNTIL (J1 + (J1 + 1)) > JN ; %	66300	0356
WRITE (PUNCH, FL3, LIST4) ; %	66400	0358
L157: WRITE (TAPE6, FL20, LIST20);	66500	0362
GO TO LEND ; %	66600	0366

```

L102: WRITE (TAPE6, FL20, LIST20)
GO TO LEND / *
LEND:
END / *

```

```

COMMENT INITIALIZING BLOCK / *
XPR + Q + K + 0 / *
SENSM [1] + TRUE / *
SENSM [2] + TRUE / *
SENSM [3] + FALSE / *
SENSM [4] + FALSE / *
SENSM [5] + FALSE / *
SENSM [6] + FALSE / *
SENSL [1] + FALSE / *
SENSL [2] + FALSE / *
SENSL [3] + FALSE / *
SENSL [4] + FALSE / *
MAINPRD / *
L1: END.

```

```

66700 0362
66800 0371
66900 0372
67000 0373
0018 IS 0380 LONG, NEXT SEQ 0002
67100 0072
67200 0072
67300 0073
67400 0075
67500 0076
67600 0077
67700 0078
67800 0080
67900 0081
68000 0082
68100 0083
68200 0085
68300 0086
68400 0086

```

## APPENDIX F

## PROCEDURE RSLTS

Following the analysis by least squares fitting for the parameters which best describe the flux decay data obtained after a Georgia Tech Research Reactor rod drop, it is desirable to adjust the resulting parameters so that they may be independent of the power history before the experiment and the details of shutdown. This is also necessary if one desires to compare them with small-sample data reported in the literature. This adjustment is necessary due to:

1. non-saturation of delayed neutron precursors
2. post-rod-drop sub-critical multiplication of neutrons resulting in additional fissions after shutdown
3. effective zero-time correction.

The non-saturation of precursors results in a simple absence of delayed neutron producers, hence a decrease in observed abundance. Additional fissions after shutdown produce analyzed periods which are longer than the true periods and result in changed relative group abundances as well. The zero-time correction was discussed in Appendix C. The correction terms which are applied in the B-5500 ALGOL Procedure RSLTS will now be outlined.

In the reactor which has been operated at some equilibrium level,  $n_0$ , without external source and with  $k_0 = 1$ , the reactor kinetics equations become:

$$\frac{dn}{dt} = \frac{k_{p_0} - 1}{\ell^*} n_0 + \sum_i \lambda_i C_{i_0} = 0 \quad (7)$$

$$\frac{dC_i}{dt} = \sum_i \frac{\beta_i^{\text{eff}} n_0}{\ell^*} - \lambda_i C_{i_0} = 0$$

where  $k_{p_0}$  is the prompt reproduction number.

From Equation 7,

$$n_0 = \frac{\ell^* \sum_i \lambda_i C_{i_0}}{1 - k_{p_0}} = \frac{\ell^* \sum_i \lambda_i C_{i_0}}{\sum_i \beta_i^{\text{eff}}}$$

Following a negative reactivity insertion,  $-\Delta k$ , such as occurs in a rod drop, there is a drop within several prompt neutron lifetimes to a lower neutron level determined by the new prompt reproduction number,  $k_{p_1}$ . Keepin<sup>23</sup> refers to this lower neutron level as "quasistatic" since it is nearly constant on a time scale encompassing many prompt neutron lifetimes. The level finally begins to be decreased by delayed neutron precursor decay, but just after the prompt drop the instantaneous value of  $dn/dt$  is approximately zero and the time zero precursor concentrations,  $C_{i_0}$ , are essentially unchanged. Thus

$$\frac{dn}{dt} \cong \frac{k_{p_1} - 1}{\ell^*} n_1 + \sum_i \lambda_i C_{i_0} = 0$$

$$n_1 \cong \frac{\ell^* \sum_i \lambda_i C_{i0}}{1 - k_{p0}}$$

$$\frac{n_1}{n_0} \cong \frac{1 - k_{p0}}{1 - k_{p1}} \cong \frac{\sum_i \beta_{i\text{eff}}}{\sum_i \beta_{i\text{eff}} + \Delta k} \quad (8)$$

Since

$$n(t)/n_0 = \sum_i a_i e^{-\lambda_i' t} \quad (9)$$

describes the decay in neutron level following a rod drop, with the zero-time for Equation 9 coinciding with time 0 (i.e. the time before the prompt drop) in Equation 8, then

$$\sum_i a_i = \frac{\sum_i \beta_{i\text{eff}}}{\sum_i \beta_{i\text{eff}} + \Delta k}$$

The summation is on  $i$  over the entire range of delayed neutron precursors. Therefore,

$$a_i = \frac{\beta_{i\text{eff}}}{\sum_i \beta_{i\text{eff}} + \Delta k} \quad (10)$$

assuming that each delayed neutron precursor group is at equilibrium and the zero-time is precise. In order to account for non-equilibrium, Equa-

tion 10 may be modified:

$$a_i = \frac{\beta_{i,\text{eff}}(1 - e^{-\lambda_i t})}{\sum_i \beta_{i,\text{eff}} + \Delta k} \quad (11)$$

where  $t$  is the time of operation at a steady power before the rod drop. This formulation assumes that the equilibrium fraction for the  $i^{\text{th}}$  precursor is adequately determined by the  $(1 - e^{-\lambda_i t})$  buildup term, which in fact ignores power history other than that at constant power immediately preceding the rod drop. In the execution of Procedure RSLTS, the equilibrium fraction is accounted for as described in Appendix B.

The application of RP-129 and RODROP permitted an assessment of the constructive zero-time of an instantaneous reactivity insertion equivalent to the actual insertion. These techniques are discussed in Appendix C. The difference between constructive zero-time and the zero-time used for curve fitting (the time the control blade hit its down-limit switch) should be applied to the abundance of each group for enhancement of the abundance value. This enhancement factor is  $e^{\lambda_i(t_d - t_o)}$ , where  $t_d$  is the assumed drop time and  $t_o$  is the constructive zero-time. Thus, the final value of effective delayed neutron relative abundance may be expressed as

$$R_i = \frac{a'_i e^{\lambda_i(t_d - t_o)} / Q_i}{\sum_i a'_i e^{\lambda_i(t_d - t_o)} / Q_i} \quad (12)$$

The analyzed decay constants,  $\lambda'_i$ , which appear in Equation 9 are smaller than the  $\lambda_i$  in Equation 11 since the power level decays more slowly due to precursors generated after the rod drop. The fractional decrease in  $\lambda_i$  is directly related to the  $i^{\text{th}}$  group fraction of the normalized power level after the prompt drop.

$$\frac{\lambda_i - \lambda'_i}{\lambda_i} = \frac{\beta_{i\text{eff}}}{\sum_i \beta_{i\text{eff}} + \Delta k}$$

Then

$$\lambda_i = \lambda'_i / \left(1 - \frac{\beta_{i\text{eff}}}{\sum_i \beta_{i\text{eff}} + \Delta k}\right) \quad (13)$$

Since

$$\frac{\beta_{i\text{eff}}}{\sum_i \beta_{i\text{eff}} + \Delta k} = \frac{a'_i e^{\lambda_i(t_d - t_0)}}{Q_i}$$

Equation 13 would not appear capable of explicit solution for  $\lambda_i$ . An iterative procedure might have been employed in which the first  $\lambda_i$  used to determine the value of  $Q_i$  required in Equation 12 was  $\lambda'_i$ . This is a good first guess since a single rod drop of  $\Delta k = 0.075$  produces a maximum value of

$$\frac{\beta_{i\text{eff}}}{\sum_i \beta_{i\text{eff}} + \Delta k} \cong \frac{0.0035}{0.0075 + 0.075} \cong 0.043$$

and generally much smaller values. In practice, all four shim rods were



dropped and the value of  $\frac{\beta_{i,\text{eff}}}{\sum_i \beta_{i,\text{eff}} + \Delta k}$  was sufficiently small that the equilibrium fraction value could be determined by a single pass through Procedure BLDUP using  $\lambda'_i$ .

With the value of  $\frac{\beta_{i,\text{eff}}}{\sum_i \beta_{i,\text{eff}} + \Delta k}$  thus determined, the final value of  $\lambda_i$  was obtained directly from Equation 13.

COMMENT R S L T S J		0000
BEGIN FILE OUT TAPE6 1 (2, 15) J X		100 0000
	START OF SEGMENT *****	0002
FILE IN TAPE7 0 (2, 15) J X	200	0005
FILE OUT PUNCH 0 (2, 10) J X	300	0010
INTEGER ARRAY TYPE [0 : 1022], T [0 : 1022]	400	0015
REAL ARRAY SVH [0 : 40, 0 : 40], SVX [0 : 40], SVXP [0 : 40],	500	0019
EQFRAC [0 : 30], RELAB [0 : 30], BLEM [0 : 30], CONCR [0 : 40],	600	0025
PHI [0 : 1022], ENH [0 : 40], ENRDR [0 : 40]	700	0033
INTEGER I, J, C, NP, JT, IND, TD, NOINT, 0, KJ	800	0039
INTEGER CONIND, TPREV, TCON, Z, M, TSTART	900	0039
REAL BSUM, PHID, DTSTART, NZERO J X	1000	0039
PROCEDURE RLDP (IND, I, LAM, EQFRAC)	1100	0039
INTEGER IND, I J X	1200	0039
REAL ARRAY LAM [0], EQFRAC [0] J X	1300	0039
BEGIN REAL SUMINI, FAC1, FAC2, FAC3, FAC5, FAC6, FAC7, L, E	1400	0039
	START OF SEGMENT *****	0003
REAL ARRAY CZERO [0 : 30], CR [0 : 30], THA [0 : 30], TTMIN [0 : 30], CT [0 : 30] J X	1500	0000
LABEL L1, L8, L2, L3, L4, L5, L6, L7	1600	0006
FORMAT FL10 (I10), FL11 (I1, I6, R17, 2, I1, I6, R17, 2, I1, I6,	1700	0010
R17, 2), FL12 (I10, R12, 4), FL13 (I10, X10, E12, 4)	1800	0010
	START OF SEGMENT *****	0004
	1900	0010
	0004 IS 0027 LONG, NEXT SEG	0003
LIST LIST10 (NOINT) J X	2000	0010
LIST LIST11 (FOR K + 1 STEP 1 UNTIL NOINT DO (TYPE [K], T [K],	2100	0016
PHI [K]) J X	2200	0022
LIST LIST12 (TD, PHID) J X	2300	0029
LIST LIST13 (I, EQFRAC [I]) J X	2400	0037
TCON + 0.0 J X	2500	0045
TPREV + 0.0 J X	2600	0045
IF IND = 0 THEN GO TO L1 J X	2700	0046
FOR K + 1 STEP 1 UNTIL NP DO CZERO [K] + 0.0	2800	0047
READ (TAPE7, FL10, LIST10) J X	2900	0052
READ (TAPE7, FL11, LIST11) J X	3000	0056
READ (TAPE7, FL12, LIST12) J X	3100	0060
FOR K + 1 STEP 1 UNTIL NOINT DO T [K] + T [K] * 60	3200	0064
TD + TD * 60 J X	3300	0073
L1: T (NOINT + 1) + TD J X	3400	0074
PHI (NOINT + 1) + PHID J X	3500	0076
CR [I] + (PHID / LAM [I]) J X	3600	0078
THA [I] + 0.693 / LAM [I] J X	3700	0080
TTMIN [I] + TD * 6 * THA [I] J X	3800	0082
SUMINT + 0 J X	3900	0085
Z + NOINT J X	4000	0085

IF (TTMIN [I] ≤ TCON) THEN GO TO L4J	4100	0086
L2J IF (TTMIN [I] ≥ T [Z]) THEN GO TO L3J	4200	0088
Z + Z = 1 J %	4300	0089
GO TO L2 J %	4400	0091
L3J TSTART + T [Z] J %	4500	0093
GO TO L4 J %	4600	0094
L4J TSTART + TCON J %	4700	0094
Z + 1 J %	4800	0095
LAJ FOR M + Z STEP 1 UNTIL NUINT DO	4900	0096
BEGIN IF (TYPE [M] ≠ 0) THEN GO TO L6J	5000	0098
L5J FAC1 + T [M + 1] = T [M] J %	5100	0099
FAC2 + EXP (LAM [I] × (T [M + 1] - TD))J	5200	0102
FAC3 + EXP (LAM [I] × (T [M] - TD))J	5300	0105
FAC5 + (T [M + 1] × PHI [M] - T [M] × PHI [M + 1]) / FAC1J	5400	0108
FAC6 + FAC2 = FAC3 J %	5500	0113
FAC7 + (PHI [M + 1] - PHI [M]) / FAC1J	5600	0114
L + FAC5 × FAC6 / LAM [I] + FAC7 × ((T [M + 1] × FAC2 - T [M]	5700	0117
× FAC3) / LAM [I] = FAC6 / LAM [I] × LAM [I])J	5800	0120
SUMINT + SUMINT + L J %	5900	0125
GO TO L7 J %	6000	0126
L6J FAC1 + T [M + 1] = T [M] J %	6100	0127
FAC2 + EXP (LAM [I] × (T [M + 1] - TD))J	6200	0129
FAC3 + EXP (LAM [I] × (T [M] - TD))J	6300	0132
FAC6 + LN (PHI [M + 1] / PHI [M])J	6400	0135
E + FAC1 × PHI [M] × (1 / (FAC6 + LAM [I] × FAC1)) × ((PHI [M	6500	0138
+ 1] / PHI [M]) × FAC2 = FAC3J	6600	0141
SUMINT + SUMINT + E J %	6700	0144
L7J	6800	0146
END J %	6900	0146
CT [I] + CZERO [I] × EXP (- LAM [I] × (TSTART - TPREV)) + SUMINT	7000	0148
J %	7100	0151
EQFRAC [I] + CT [I] / CR [I] J %	7200	0152
LBJ WRITE (TAPE6, FL13, LIST13)J	7300	0155
END J %	7400	0158
	0003 IS 0167 LONG, NEXT SEG 0002	
PROCEDURE RSLTSJ	7500	0039
BEGIN LABEL L1, L4, LF1N J %	7600	0039
	START OF SEGMENT ***** 0005	
FORMAT ID1C	0000	
	START OF SEGMENT ***** 0006	
" IDENTIFICATION TITLE	" ,	0000
" "		0000
	0006 IS 0016 LONG, NEXT SEG 0005	

FORMAT FL1 (I2), FL2 (6 R12, 4), FL3 (/,	7700	0000
	START OF SEGMENT ***** 0007	
GROUP APRIME ENHANCEMENT REL ABUND ERROR ESTIMATE OR	7800	0000
IGINAL LAMBDA CORRECTED LAMBDA ERROR ESTIMATE"		0000
) FL4 (/ /, X2, I2, X1, R11, 4, X1, R12, 5, X2, E12, 5, X2,	7900	0000
E12, 5, X7, E11, 4, X8, E11, 4, X7, E11, 4))	8000	0000
	0007 IS 0053 LONG, NEXT SEG 0005	
LIST LIST2 (FOR I + 1 STEP 1 UNTIL NP DO SVX [I])	8100	0000
LIST LIST3 (FOR I + J1 STEP 1 UNTIL NP DO SVH [I, J1])	8200	0010
LIST LIST4 (K, SVXP [I], ENH [I], RELAB [I], ERROR [I], SVXP [J]	8300	0021
, SVX [J], ENRON [J]) ; *	8400	0030
C + 0 ; *	8500	0038
IND + 1 ; *	8600	0038
BSUM + 0 ; *	8700	0039
READ(TAPE7, ID1)		0040
WRITE(TAPE6, ID1)		0044
READ (TAPE7, FL1, NP) ; *	8800	0047
HEAD (TAPE7, FL2, DTSTART, NZEND)	8900	0058
READ (TAPE7, FL2, LIST2) ; *	9000	0070
WRITE (TAPE6, FL2, LIST2) ; *	9100	0074
FOR J1 + 1 STEP 1 UNTIL NP DO HEAD (TAPE7, FL2, LIST3)	9200	0078
LIST C + C + 1 ; *	9300	0086
FOR I + 1 STEP 2 UNTIL (NP - 1) DO	9400	0088
BEGIN SVXP [I] + SVX [I] ; *	9500	0092
SVXP [I + 1] + SVX [I + 1]	9600	0094
END ; *	9700	0095
FOR I + 1 STEP 2 UNTIL (NP - 1) DO	9800	0098
BEGIN L4: C + C + 1 ; *	9900	0102
D + I + 1 ; *	10000	0104
BLOUP (IND, D, SVXP, EQFRAC) ; *	10100	0105
IND + 0 ; *	10200	0108
ENH [I] + EXP (SVX [I + 1] * DTSTART) / EQFRAC [I + 1]	10300	0108
BTEM [I] + SVXP [I] * ENH [I]	10400	0113
SVX [I] + BTEM [I] ; *	10500	0115
LFIN: C + 0 ; *	10600	0116
BSUM + BSUM + SVX [I]	10700	0117
END ; *	10800	0118
FOR I + 1 STEP 2 UNTIL (NP - 1) DO	10900	0119
BEGIN RELAB [I] + SVX [I] / BSUM	11000	0124
ENRON [I] + SQRT (SVH [I, I]) * ENH [I] / BSUM	11100	0126
ENRON [I + 1] + SQRT (SVH [I + 1, I + 1])	11200	0130
SVX [I + 1] + SVXP [I + 1] / (1 - BTEM [I] / NZERO)	11300	0134
END ; *	11400	0137

```

WRITE (TAPE6, FL3) J *
FOR K = 1 STEP 1 UNTIL (NP / 2) DO
  BEGIN J = 2 * K J *
    I + J = 1 J *
    WRITE (TAPE6, FL4, LIST4)
  END J *
END J *

RSLTS   END. *
```

```

11500  0139
11600  0142
11700  0146
11800  0148
11900  0149
12000  0152
12100  0153
0005 IS 0156 LONG, NEXT SEG 0002
12200  0039
```

## APPENDIX G

## SCHEMATIC DIAGRAMS OF ELECTRONIC UNITS

The following pages in this appendix are devoted to schematic diagrams which describe the electronic circuits developed in the course of this work. These designs, while they have been influenced and in some cases specified by the author of this thesis, are not his own. They are the designs of Mr. J. C. Gundlach of Reactor Controls, Inc. and Messrs. R. E. Meek and T. L. Erb of the Georgia Tech Nuclear Research Center.

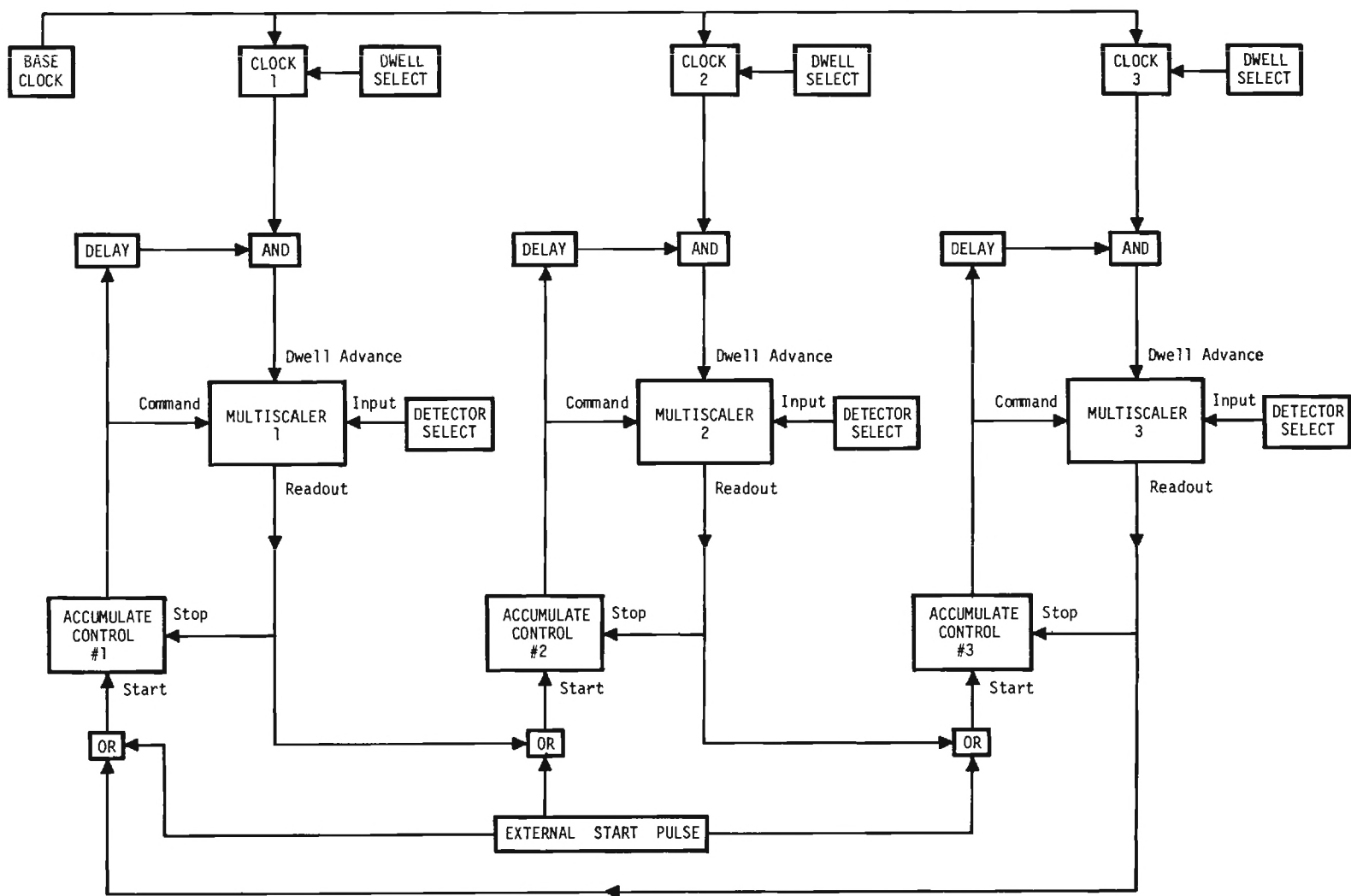
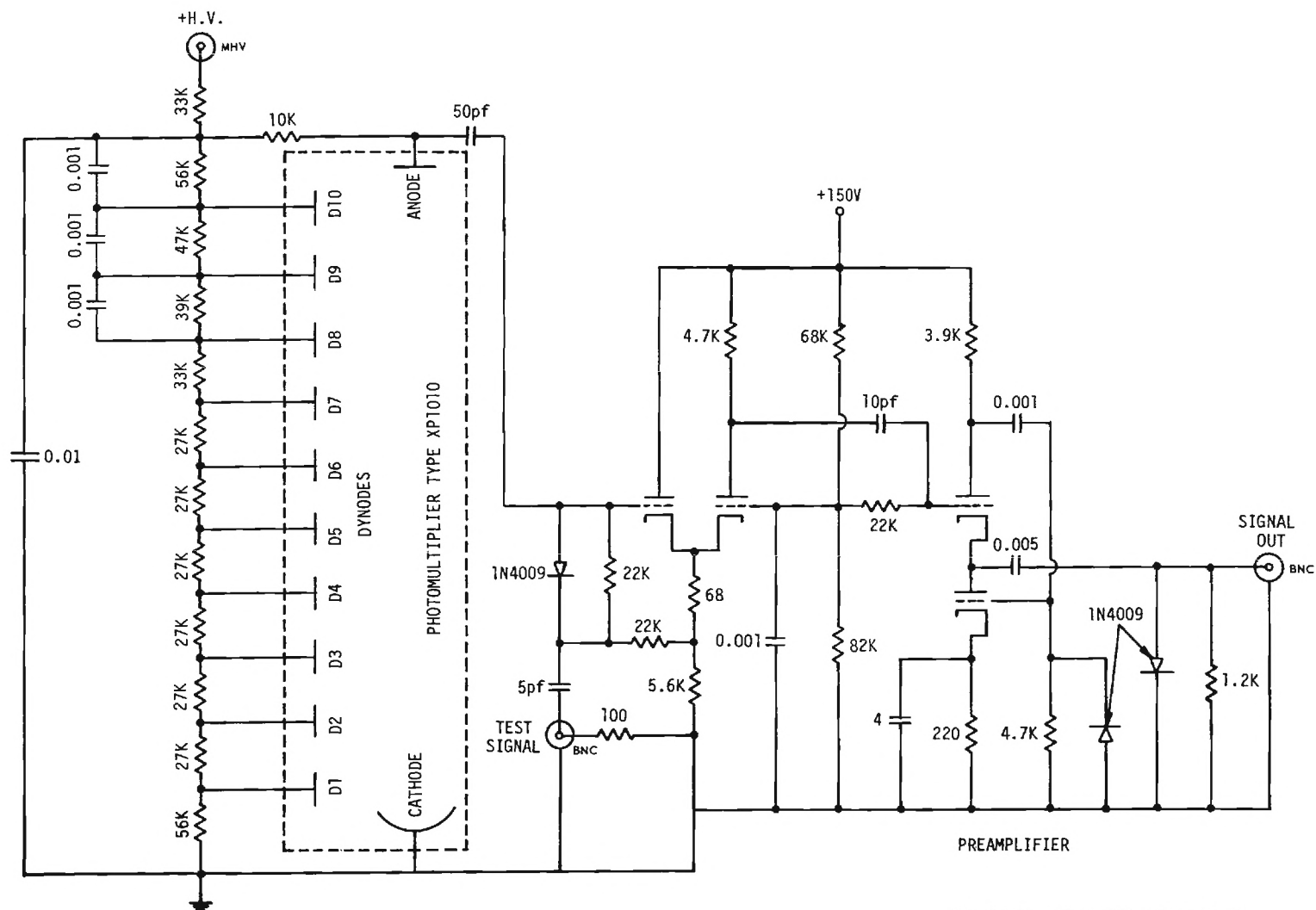


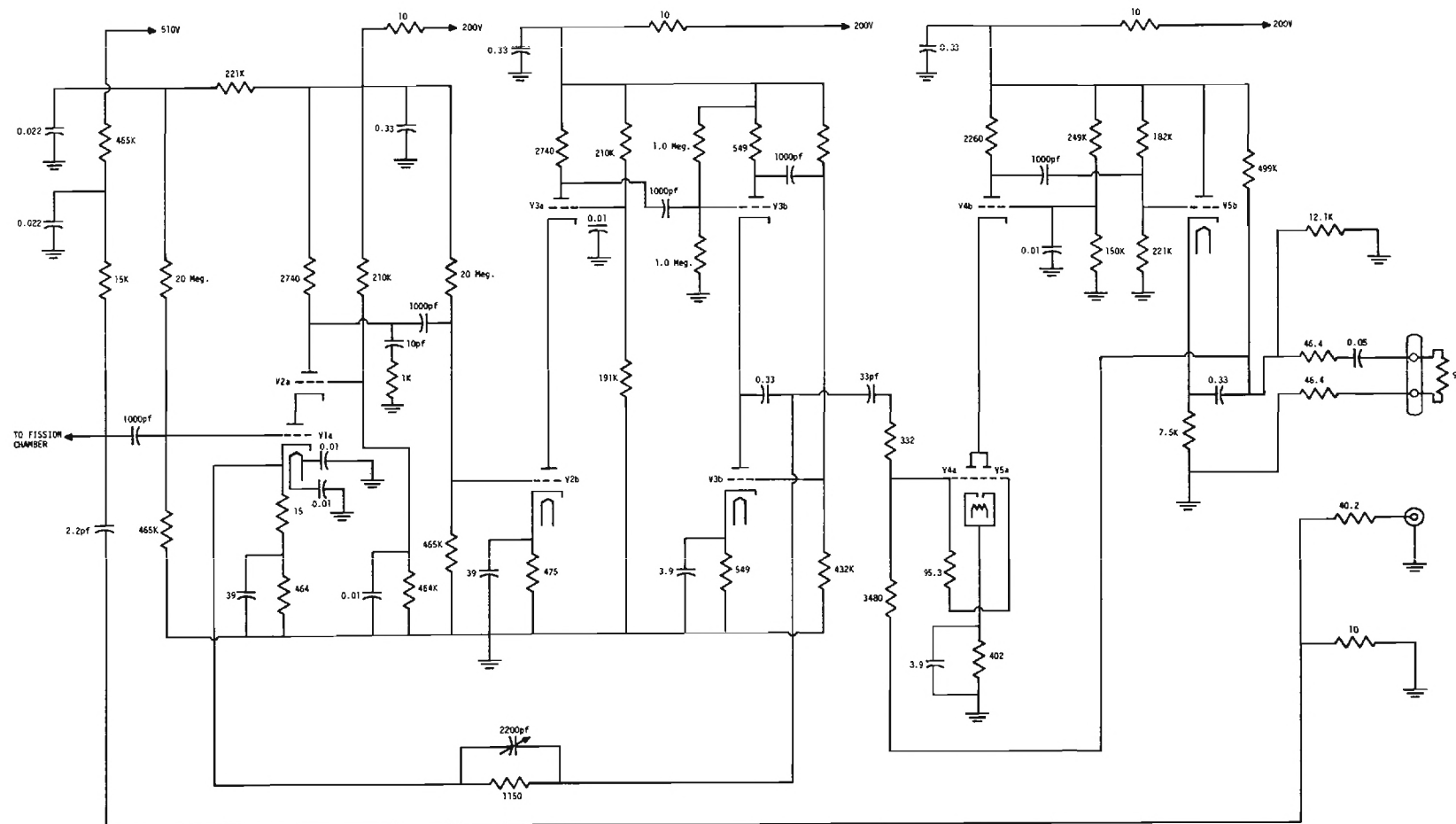
Figure 29. Schematic Block Diagram of Multiscaler Sequencing Logic



ALL TUBES: Type 7586 (Nuvistor)

Figure 30. Schematic Diagram of Scintillation Detector High Voltage Divider and Preamplifier





(Copyright Reactor Controls, Inc.)

NOTE: All Tubes are type 6922

Figure 31. Schematic Diagram of Fission Chamber Preamplifier

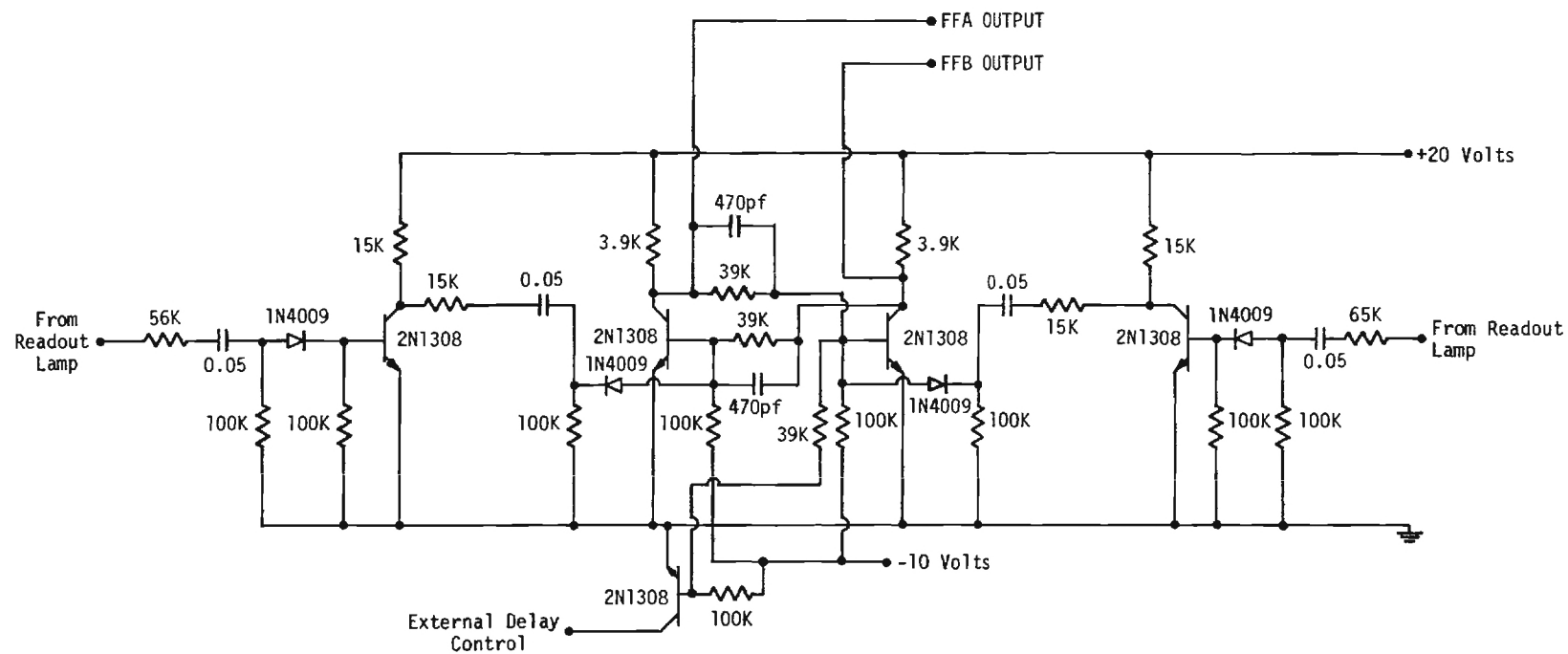


Figure 32. Schematic Diagram of Analyzer and Clock Control Circuit

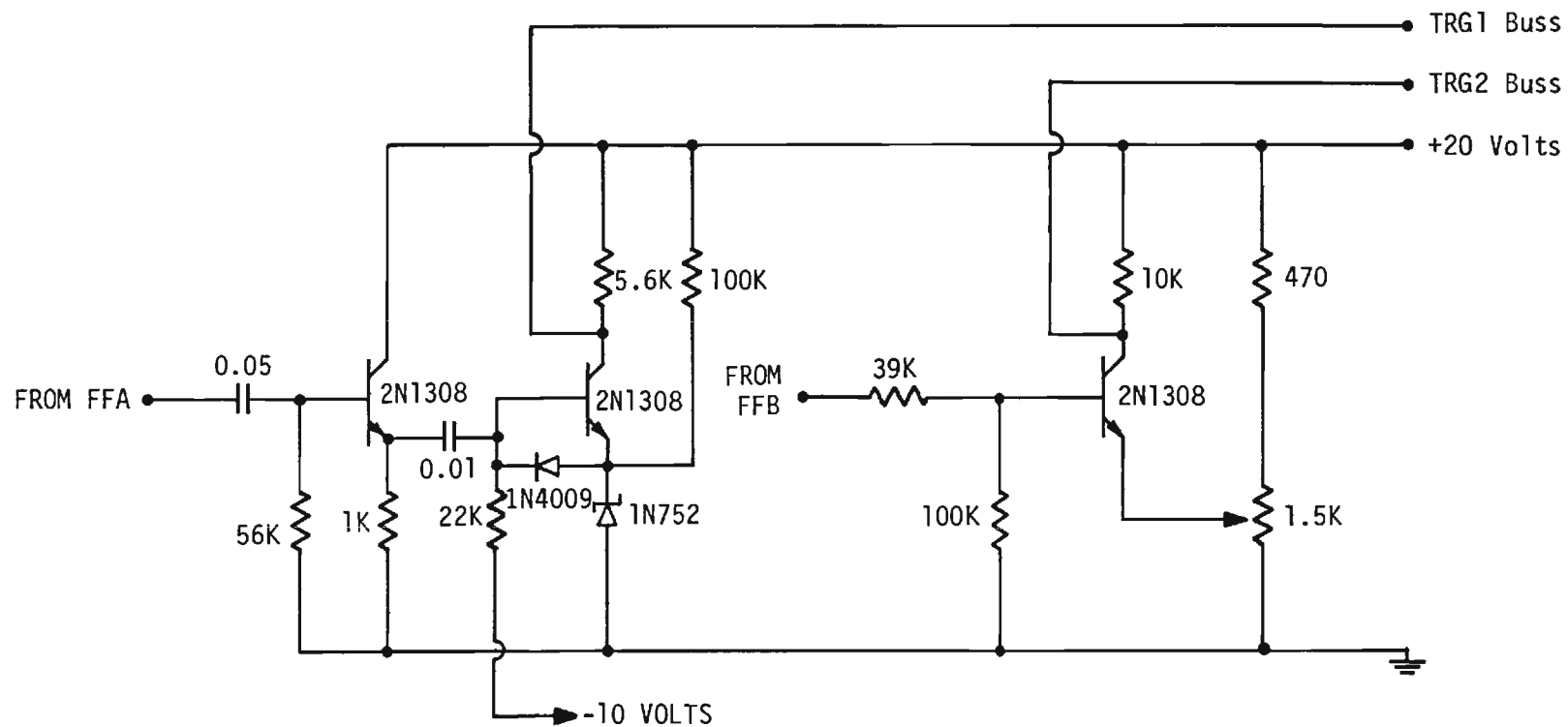


Figure 33. Schematic Diagram of Decade Divider Trigger Section

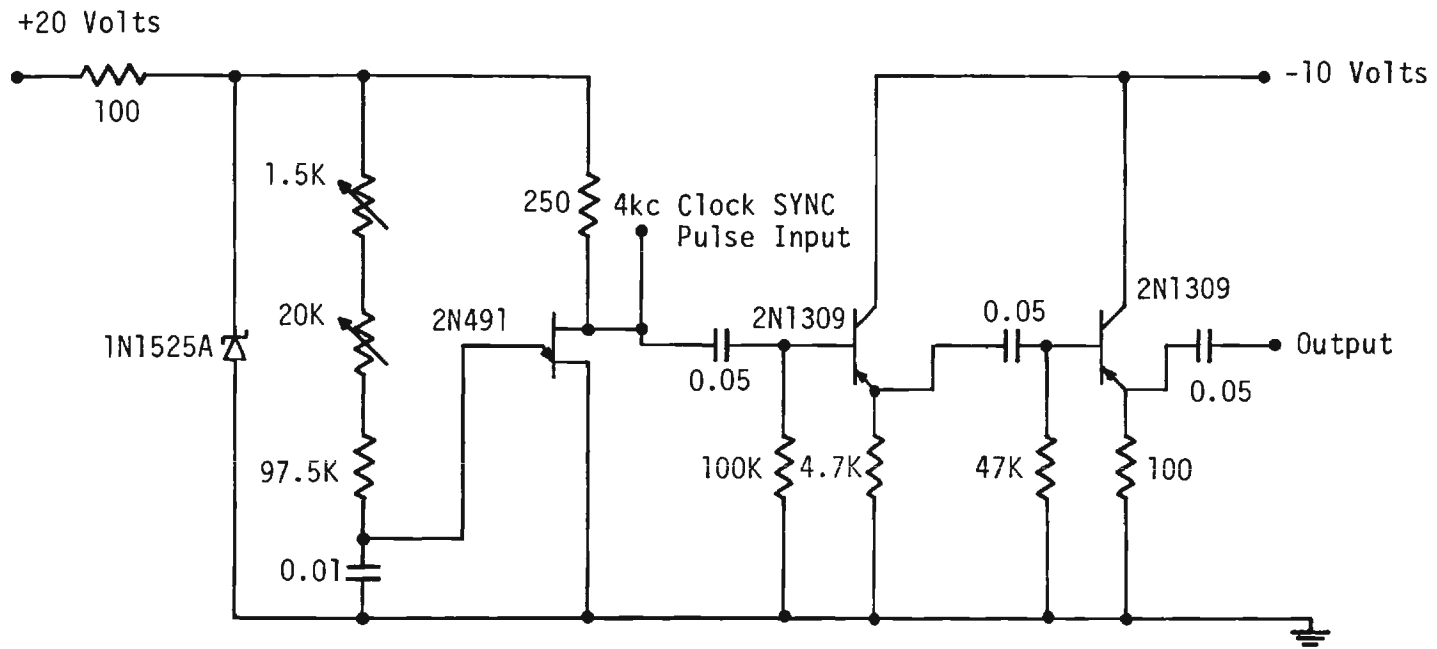


Figure 34. Schematic Diagram of 1 kc Oscillator

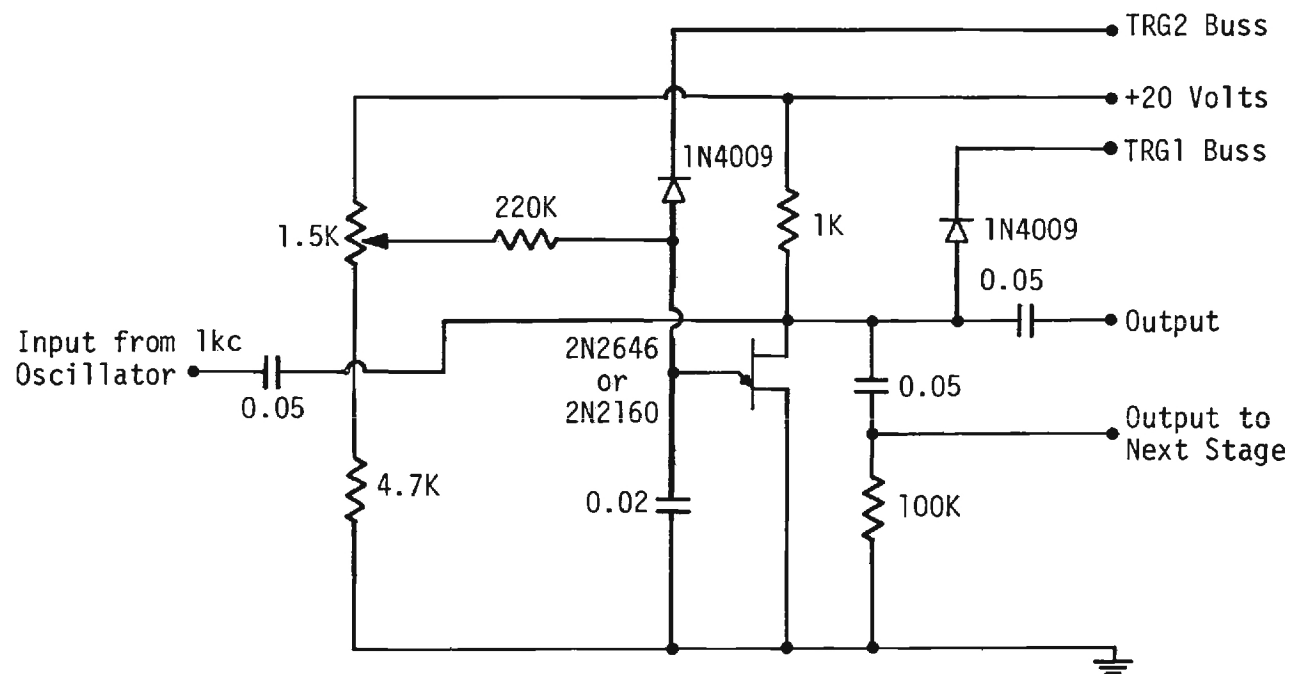
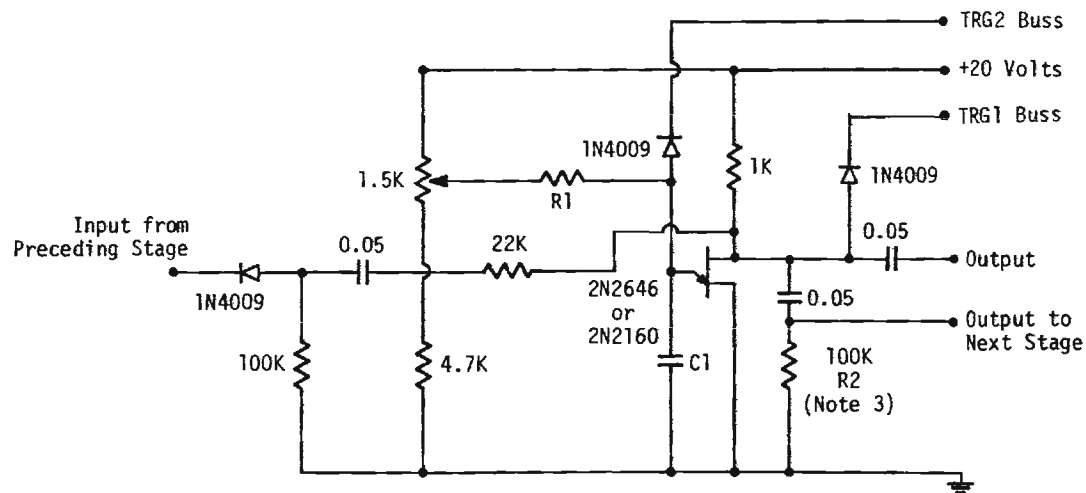


Figure 35. Schematic Diagram of Decade Divider First Section



#### NOTE

1. There are Four of these per Clock Unit.
2. The R1, C1, Combinations are:

STAGE	R1	C1
1	522K	0.25 $\mu$ fd
2	20K	60 $\mu$ fd
3	75K	60 $\mu$ fd
4	950K	60 $\mu$ fd

3. Resistor R2 is 150K in Stage 4.

Figure 36. Schematic Diagram of Decade Divider Intermediate Section

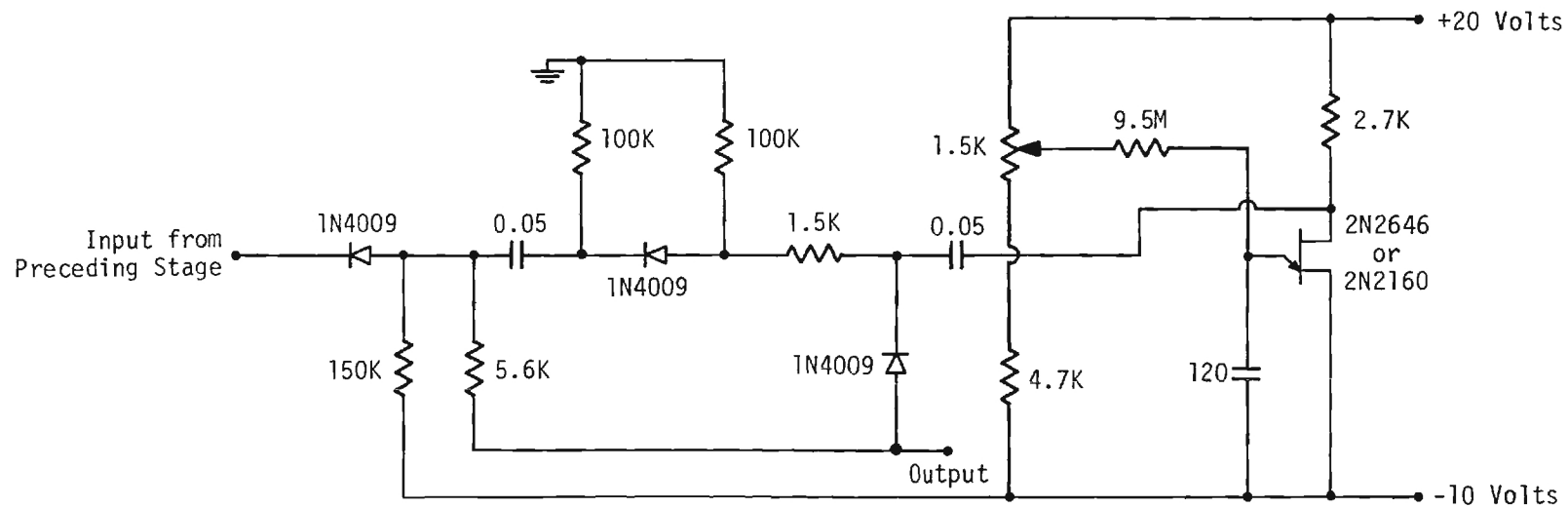


Figure 37. Schematic Diagram of Decade Divider Final Section

## BIBLIOGRAPHY

1. A. M. Weinberg and E. P. Wigner, The Physical Theory of Neutron Chain Reactors (The University of Chicago Press, Chicago, 1958), p. 115.
2. R. Roberts, R. Meyer, and P. Wang, Physical Review 55, 510 (1939).
3. S. Glasstone and M. C. Edlund, The Elements of Nuclear Reactor Theory (D. Van Nostrand Co., Inc., Princeton, 1952), chap. 4.
4. A. M. Weinberg and E. P. Wigner, The Physical Theory of Neutron Chain Reactors (The University of Chicago Press, Chicago, 1958), p. 154.
5. R. C. Mobley and R. A. Laubenstein, Phys. Rev. 80, 309 (1950).
6. G. R. Keepin, Physics of Nuclear Kinetics (Addison-Wesley Publishing Co., Inc., Reading, Mass., 1965), p. 142.
7. S. Glasstone and M. C. Edlund, The Elements of Nuclear Reactor Theory (D. Van Nostrand Co., Inc., Princeton, 1952), chap. 10.
8. C. E. Cohn and B. J. Toppel, Argonne National Laboratory Report ANL-6134 (1960).
9. D. J. Hughes, J. Dabbs, A. Cahn, and D. Hall, Phys. Rev. 73, 111 (1948).
10. S. Bernstein, W. M. Preston, G. Wolfe, and R. E. Slattery, Phys. Rev. 71, 573 (1947).
11. G. R. Keepin, Nucleonics 20, No. 8, 150 (1962).
12. G. R. Keepin, T. F. Wimett, and R. K. Zeigler, Phys. Rev. 107, 1044 (1957).
13. B. P. Maksimutenko, Journal of Experimental and Theoretical Physics (USSR) 35, 815 (1958).
14. W. Spatz, D. Hughes, and A. Cahn, Phys. Rev. 72, 163 (1947).
15. O. J. Hahn and R. C. Axtmann, Princeton University Report PNS-1 (Unpublished) (1962).
16. B. S. Finn, Nuclear Science and Engineering 7, 369 (1960).



## BIBLIOGRAPHY (Continued)

17. W. K. Ergen, Aircraft Nuclear Propulsion Report ANP-59 (1951).
18. R. Batchelor and H. R. McK. Hyder, *Journal of Nuclear Energy* 3, 7 (1956).
19. M. W. Johns and B. W. Sargent, *Canadian Journal of Physics* 32, 136 (1954).
20. P. R. Tunnicliffe, Atomic Energy of Canada Ltd. Report AECL-401 (1952).
21. Letter from R. W. Meier, Würenlingen, 1963.
22. G. R. Keepin, Progress in Nuclear Energy (Pergamon Press, London, 1956) Vol. I, p. 191.
23. G. R. Keepin, Physics of Nuclear Kinetics (Addison-Wesley Publishing Co., Inc., Reading, Mass., 1965) chap. 4.
24. H. S. Isbin, Nuclear Reactor Theory (Reinhold Publishing Corp., New York, 1963), p. 80.
25. R. Perez-Belles, J. D. Kington, and G. de Saussure, *Nucl. Sci. and Eng.* 12, 505 (1962).
26. T. J. Thompson, Private Communication, 1964.
27. "Final Safeguards Report for the Georgia Tech Research Reactor" (Unpublished)(1963).
28. R. Stedman, *Review of Scientific Instruments* 31, 1156 (1960).
29. U.S. Atomic Energy Commission, License No. R-97, "Technical Specifications for the Georgia Institute of Technology," Appendix A (1964).
30. C. E. Cohn and J. J. Kaganove, *Transactions of the American Nuclear Society* 5, 388, No. 2 (1962).
31. J. J. Kaganove, Argonne National Laboratory Report ANL-6132 (1960).
32. C. E. Cohn, Private Communication, 1964.
33. W. C. Davidon, Argonne National Laboratory Report ANL-5990 (Rev.) (1959).
34. R. Fletcher and M. J. D. Powell, *The Computer Journal* 7, 163 (1964).
35. R. V. Meghreblan and D. K. Holmes, Reactor Analysis (McGraw-Hill Book Company, Inc., New York, 1960), p. 614.

## BIBLIOGRAPHY (Concluded)

36. S. Glasstone and M. C. Edlund, The Elements of Nuclear Reactor Theory (D. Van Nostrand Co., Inc., Princeton, 1952), p. 333.
37. W. W. Graham and D. S. Harmer, "Georgia Institute of Technology Technical Report No. NE-1" (Unpublished)(1963).

## VITA

Walter Waverly Graham, III was born on April 30, 1933 in Nashville, Tennessee. He attended public schools there and in Annapolis, Maryland, and graduated from Hillsboro High School, Nashville in 1951. Between the years 1951 and 1955, Mr. Graham was a midshipman at the United States Naval Academy, serving as Brigade Commander and Editor-in-Chief of The Log Magazine. Commissioned an Ensign in 1955, he was assigned duty on USS Massey (DD778), Staff Commander Destroyer Flotilla Four, USS O'Hare (DDR889), and as a Combat Information Center Instructor at the Fleet Air Defense Training Center, Dam Neck, Virginia.

Mr. Graham left active duty in 1959 to attend graduate school at Vanderbilt University. He completed the Master of Science degree in Nuclear Engineering in 1960 and was employed by the General Atomic Division, General Dynamics Corporation, San Diego, California. At General Atomic, Mr. Graham was engaged in the design of the Peach Bottom High Temperature Gas-Cooled Reactor Fission Product Removal System. He is author of "TNT, A Program for Analyzing the Transient Performance of the Peach Bottom HTGR Fission Product Trapping System," GAMD-3168, and co-author of "The Removal of Radioactive Krypton and Xenon from a Flowing Helium Stream by Fixed-Bed Adsorption," GA-2395.

Mr. Graham is married to the former Ann Bennett of Nashville; they have two children, Kerry and Holly. He is a deacon in the Presbyterian Church, U.S. and holds the rank of Lieutenant Commander in the U.S. Naval Reserve. He is a member of the American Nuclear Society and Sigma Xi.